AD_____

Award Number DAMD17-98-1-8584

TITLE: Regulation of Androgen Responses in Prostate Cancer by BAG-1

PRINCIPAL INVESTIGATOR: John C. Reed, MD, Ph.D.

CONTRACTING ORGANIZATION: The Burnham Institute
La Jolla, California 92037

REPORT DATE: March 2001

TYPE OF REPORT: Final

PREPARED FOR: U.S. Army Medical Research and Materiel Command
Fort Detrick, Maryland 21702-5012

REPORT DOCUMENTATION PAGE

Form Approved
OMB No. 074-0188

1. AGENCY USE ONLY (Leave blank)	2. REPORT DATE	3. REPORT TYPE AND DATES COVERED
	March 2001	Final (1 Sept 98 - 28 Feb 01)

4. TITLE AND SUBTITLE
Regulation of Androgen Responses in Prostate Cancer by BAG1

5. FUNDING NUMBERS
DAMD17-98-1-8584

6. AUTHOR(S)
John C. Reed, MD, Ph.D.

7. PERFORMING ORGANIZATION NAME(S) AND ADDRESS(ES)
The Burnham Institute
La Jolla, California 92037

E-MAIL:
Jreed@burnham-inst.org

8. PERFORMING ORGANIZATION REPORT NUMBER

9. SPONSORING / MONITORING AGENCY NAME(S) AND ADDRESS(ES)
U.S. Army Medical Research and Materiel Command
Fort Detrick, Maryland 21702-5012

10. SPONSORING / MONITORING AGENCY REPORT NUMBER

11. SUPPLEMENTARY NOTES

12a. DISTRIBUTION / AVAILABILITY STATEMENT
Approved for public release; distribution unlimited

12b. DISTRIBUTION CODE

13. ABSTRACT ***(Maximum 200 Words)***

Androgen ablation therapy and anti-androgenic drugs represent the principal treatments for metastatic prostate cancer. However, nearly all tumors eventually relapse as hormone-refractory disease. A need therefore exists for better understanding of the mechanisms that allow prostate cancer cells to grow in an androgen - independent manner. This study focuses on BAG-1, a protein that is expressed in prostate cancers and which binds to androgen receptors, increasing their sensitivity to androgenic hormones. BAG-1 is a novel regulator of Hsp70 family molecular chaperones that was originally cloned in our laboratory. The activity of many steroid hormone receptors is known to be regulated by Hsp70 and Hsp90 family proteins. Recently, we have discovered that a previously unrecognized isoform of BAG-1, termed BAG-1L, can form complexes with androgen receptors (AR) and potentiate the actions of AR in prostate cancers, markedly lowering the concentrations of dihydrotestosterone needed for AR-mediated transactivation. In contrast, the shorter BAG-1 protein forms complexes with RAR family retinoid receptors, preventing retinoid-induced transactivation of target genes, abrogating cell growth suppression, and blocking apoptosis. Since BAG-1 and BAG-1L are commonly expressed in prostate cancers, we hypothesize that these proteins contribute to mechanisms of tumor resistance to anti-androgen and retinoid-based therapy. In this proposal, we describe experiments designed to further explore the biological roles and molecular mechanisms by which BAG-1 and BAG-1L regulate responses of prostate cancers to steroid hormones that control the proliferation, differentiation and survival of these malignancies.

14. SUBJECT TERMS

15. NUMBER OF PAGES
55

16. PRICE CODE

17. SECURITY CLASSIFICATION OF REPORT	18. SECURITY CLASSIFICATION OF THIS PAGE	19. SECURITY CLASSIFICATION OF ABSTRACT	20. LIMITATION OF ABSTRACT
Unclassified	Unclassified	Unclassified	Unlimited

FOREWORD

Opinions, interpretations, conclusions and recommendations are those of the author and are not necessarily endorsed by the U.S. Army.

_N/A_ Where copyrighted material is quoted, permission has been obtained to use such material.

_N/A_ Where material from documents designated for limited distribution is quoted, permission has been obtained to use the material.

_N/A_ Citations of commercial organizations and trade names in this report do not constitute an official Department of Army endorsement or approval of the products or services of these organizations.

_√_ In conducting research using animals, the investigator(s) adhered to the "Guide for the Care and Use of Laboratory Animals," prepared by the Committee on Care and use of Laboratory Animals of the Institute of Laboratory Resources, national Research Council (NIH Publication No. 86-23, Revised 1985).

_√_ For the protection of human subjects, the investigator(s) adhered to policies of applicable Federal Law 45 CFR 46.

_√_ In conducting research utilizing recombinant DNA technology, the investigator(s) adhered to current guidelines promulgated by the National Institutes of Health.

_√_ In the conduct of research utilizing recombinant DNA, the investigator(s) adhered to the NIH Guidelines for Research Involving Recombinant DNA Molecules.

_N/A_ In the conduct of research involving hazardous organisms, the investigator(s) adhered to the CDC-NIH Guide for Biosafety in Microbiological and Biomedical Laboratories.

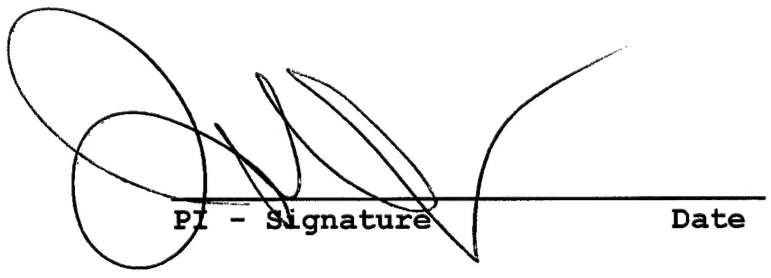

PI - Signature Date

Final Report
DAMD17-98-1-8584

John C. Reed, MD, Ph.D.

Regulation of Androgen Responses in Prostate Cancer by BAG-1

September 1, 1998 – February 28, 2001

TABLE OF CONTENTS PAGE

INTRODUCTION

Prostate cancer is an androgen-driven disease. In the absence of testosterone or related androgens which can serve as ligands for the androgen receptor, the secretory epithelial cells of the prostate undergo rapid programmed cell death (1). Current treatment for metastatic adenocarcinoma of the prostate is predicated on the cell death inducing effects of anti-androgens and hormone ablative measures which reduce endogenous production of androgens. However, nearly all hormone-dependent prostate cancers eventually relapse as fatal hormone-independent disease (2).

Multiple, still largely unidentified mechanisms may account for the complete independence or reduced dependence of prostate cancers on androgens (reviewed in (3-5). AR gene deletion and sequestration of AR in the cytoplasm have been described in some hormone-independent tumors, implying that genetic alterations associated with tumor progression can abrogate the necessity for AR in some cases. However, many tumors may rely on other strategies which allow cancer cells to grow in low concentrations of androgens, including AR gene amplification or over-expression (6, 7) and AR mutations which permit trans-activation of target genes with little or no requirement for steroid hormones (1, 2). Since most hormone-insensitive prostate cancers still retain a wild-type AR, presumably alterations in the factors that control the levels of AR and its function play a major role in resistance to anti-androgen and hormone ablative therapies. Thus, a need exists to understand more about the molecular mechanisms that govern the activity of ARs.

Upon binding steroid ligands, the AR undergoes a conformational change, translocates to the nucleus and binds to specific DNA sequences located near or in promoter regions of target genes. After binding DNA, the receptor interacts with components of the basal transcription machinery and sometimes sequence-specific transcription factors, resulting in positive or negative effects on gene transcription (3, 4). A number of proteins have been identified which associate with hormone-receptor complexes, including several heat shock family proteins and various types of transcription co-activators (reviewed in (5, 6). However, many details remain unclear as to the molecular mechanisms by which these proteins modulate the activities of steroid hormone receptors and even less is known about whether alterations in their expression or function might contribute to the deregulation of steroid hormone responses in prostate cancer.

In this proposal, we describe experiments designed to explore the biological significance and molecular mechanisms by which AR is regulated by BAG-1 family proteins. BAG-1 is a novel Hsp70-family binding protein cloned in our laboratory. We have discovered that an isoform of this protein, BAG-1L, forms complexes with AR and potentiates the activity of this steroid hormone receptor, allowing it to transactive target genes with 100-1,000 x lower concentrations of dihydrotestosterone. We have also determined that BAG-1 and BAG-1L are expressed in most prostate cancers. Our goals have been to define the overall significance of BAG-1 family proteins on AR responses in prostate

cancers and to delineate the mechanisms by which these Hsp70-binding proteins control the function of AR and other steroid hormone receptors of relevance to prostate cancer cell growth, differentiation, and survival. These studies may reveal new strategies for improving androgen ablation therapy and attacking hormone-refractory metastatic prostate cancer.

BODY

OBJECTIVES

The original funded objectives of the project were to:

1. Determine the expression and location of BAG-1 and BAG-1L in primary and metastatic prostate cancer.

2. Study consequences of ablation of BAG-1 and BAG-1L expression in prostate cancer cell lines.

3. Examine in vivo effects of BAG-1 and BAG-1L on the androgen-dependence of the normal prostate gland.

PROGRESS

Objective #1. Determine the expression and location of BAG-1 and BAG-1L in primary and metastatic prostate cancer.

This aim has been accomplished. We generated monoclonal antibodies which recognize the BAG-1 and the BAG-1L proteins. We determined that BAG-1 is cytosolic while BAG-1L is nuclear. Using these monoclonal antibodies, we have used immunohistochemical methods and archival paraffin-embedded prostate cancer specimens to evaluate the expression of the nuclear (BAG-1L) and cytosolic (BAG-1) proteins in over 700 cases of prostate cancer. Comparisons were made with BAG-1 immunostaining results in normal prostate and benign prostatic hypertrophy. Tissue microarray technology was exploited for much of this analysis, permitting us to analyze large numbers of tumor specimens.

BAG-1 immunostaining was generally present in $\leq 30\%$ of normal prostate epithelial cells, with 51/54 normal specimens having $\leq$ 30% BAG-1 immunopositive epithelial cells. By comparison, most (91%) prostate cancers contained elevated percentages of BAG-1 immunopositive cells, with 657 of 722 specimens (91%) having elevated percentages ($\geq$ 40%) of BAG-positive tumor cells. No correlations of BAG-1 immunostaining data with Gleason grade or clinical stage were observed. The percentages of BAG-1 immunopositive cells were also not significantly different when comparing primary verses metastatic disease. However, in men treated with radical prostatectomy (n = 160), log-rank analysis demonstrated an association between BAG-1 immunostaining data and recurrence-free survival ($p = 0.009$), with higher percentages of BAG-1 immunopositive cells associated with longer recurrence-free survival (median survival 4.6 versus 2.4 years). Further analysis of these data is underway, as we seek additional correlations of BAG-1 immunostaining data with clinical endpoints.

From these observations, two conclusions can be reached. First, tumor-specific increases in BAG-1 levels commonly occur in prostate cancers. Second,

compared to tumors that do not over-express BAG-1, the expression of BAG-1 may be associated with longer survival. Interestingly, a similar association of BAG-1 expression with longer survival has been observed by our group for breast cancer (13). We suspect there data are an indication that tumors with higher levels of BAG-1 may remain hormone-dependent, and thus are more effectively treated but this is only a speculation. A manuscript describing these findings are in preparation.

Kaplan-Meier estimate for recurrence free survival (RFS) in men treated by radical prostatectomy

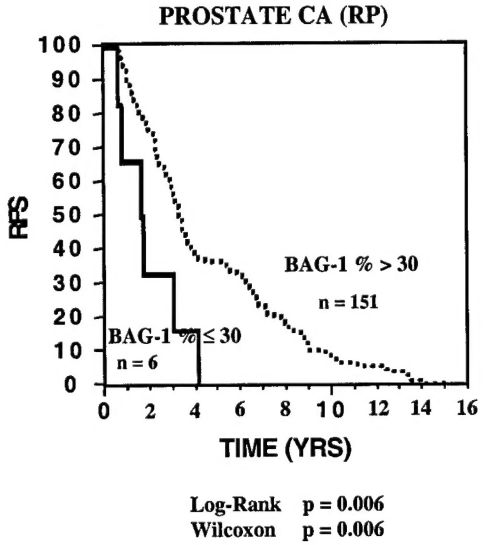

Figure 1. **Association of elevated BAG-1 immunostaining with longer RFS in prostate cancers.** A prostate tissue microarray was constructed as described previously. The scoring of immunostaining results for all tumors was based on the percentage of immunopositive cells (0-100%). Data were dichotomized at 30%, based on comparisons with 54 normal prostate specimens, suggesting that 30% is within normal limits (WNL). The prostate cancer specimens were obtained from the archives of the Institutes for Pathology, University of Basel (Basel, Switzerland), the Cantonal Institute for Pathology (Liestal, Switzerland) and the Tampere University Hospital (Tampere, Finland). Tissue samples included 137 primary tumors with stage $T1_{a/b}$ according to International Union Against Cancer criteria (International Union Against Cancer (UICC) (Classification of Malignant Tumors, 5th ed. Berlin. Wiley-Liss, 1997), incidentally discovered after transurethral resection for presumed BPH, and 117 primary tumors treated by radical prostatectomy, including 38 specimens with clinical stage T1-T2 and 79 locally advanced tumors (clinical stage T3) (17). Statistical analysis was performed by log-rank and Wilcoxon methods.

Objective #2. Study consequences of ablation of BAG-1 and BAG-1L expression in prostate cancer cell lines.

To interfere with BAG-1 and BAG-1L function in prostate cancers, we expressed mutants of BAG-1 or BAG-1L which lack the C-terminal domain

required for Hsc70-binding, so-called ΔC mutants. Our initial efforts focused on assessing the impact of these trans-dominant inhibitory mutants of BAG-1 and BAG-1L on function of the Androgen Receptor (AR). These studies revealed that BAG-1L(ΔC) suppresses the function of the AR, preventing it from transactivating reporter genes in transient transfection reporter gene assays.

An initial description of this work has been published by our group (14), and recently we have extended the analysis to other cell lines, and included additional structure-function studies of BAG-1L, thus confirming and solidifying these impressions (15, 16). Copies of the relevant publications are provided in the attached appendix. An example of an experiment is presented in Figure 1, where various concentrations of a plasmid encoding BAG-1L(ΔC) were compared with another plasmid producing a BAG-1L mutant missing it N-terminal 50 aminoacids, BAG-1L(ΔN). The BAG-1L(ΔC) protein interfered with AR-induced activation of a reporter gene plasmids, whereas the BAG-1L(ΔN) protein did not.

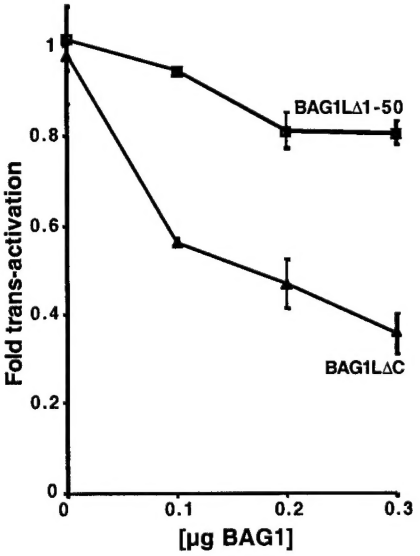

Figure 2. <u>BAG-1L(ΔC) functions as a trans-dominant inhibitor which interferes with AR function</u>. COS-7 cells were transfected with 0.04μg of pSG5-AR, 0.5μg of pLCI, 0.06μg of pCMV-βGal, 0.03μg of pcDNA3-Bag-1L and increasing amount of pcDNA3-Bag-1LΔ1-50 or pcDNA3-Bag-1LΔC. Total DNA was maintained at 1.4μg by the addition of empty plasmid. 30 hrs after transfection, cells were stimulated with 1nM R1881. Cell extracts were prepared and assayed for CAT and β-galactosidase activity at 40 hrs after transfection. Data are expressed as in Figure 1 (mean ± S.D., n=2). We are now attempting to generate stable transfectants in prostate cancer cell lines so that we may complete this Objective.

In addition to assessing the impact on AR of interfering with BAG-1 function, we also extended our studies to include the Vitamin D Receptor (VDR). This steroid receptor also plays an important role in prostate cancer. Natural and synthetic ligands for VDR have been reported to suppress prostate cancer growth in vitro and in animal models, raising hopes that this approach might be used in the treatment of this disease. We found that BAG-1L forms complexes with VDR in a ligand-dependent manner, and that it enhances transcriptional activity of VDR (18). In PC3 prostate cancer cells stably transfected with BAG-1L expression plasmids, growth inhibition induced by natural and synthetic ligands of VDR was improved, suggesting that patients whose tumor contain higher levels of BAG-1L might be candidates for Vitamin D-based therapies. A publication describing these results is provided in the attached appendix.

Objective #3. Examine in vivo effects of BAG-1 and BAG-1L on the androgen-dependence of the normal prostate gland.

Efforts to generate transgenic mice expressing BAG-1 or BAG-1L under the control of a probasin promoter are underway. Constructs were prepared and were tested by transfection in prostate cancer cell lines in vitro before progressing to transgenic mouse production. Mouse lines are currently under evaluation.

PUBLICATIONS

1. Froesch, B. A., Takayama, S., and Reed, J. C. BAG-1L protein enhances androgen receptor function., *J Biol Chem. 273:* 11660-11666, 1998.
2. Takayama, S., Krajewski, S., Krajewska, M., Kitada, S., Zapata, J. M., Kochel, K., Knee, D., Scudiero, D., Tudor, G., Miller, G. J., Miyashita, T., Yamada, M., and Reed, J. C. Expression and location of Hsp70/Hsc-binding anti-apoptotic protein BAG-1 and its variants in normal tissues and tumor cell lines, *Cancer Res. 58:* 3116-3131, 1998.
3. Knee, D. A., Froesch, B. A., Nuber, U., Takayama, S., and Reed, J. C. Structure-function analysis of Bag1 proteins: Effects on androgen receptor transcriptional activity, *J Biol Chem. 276:* 12718-12724, 2001.
4. Guzey, M., Takayama, S., and Reed, J. C. BAG1L enhances trans-activation function of the vitamin D receptor., *J Biol Chem. 275:* 40749-40756, 2000.
5. Briknarova, K., Takayama, S., Brive, L., Havert, M. L., Knee, D. A., Velasco, J., Homma, S., Cabezas, E., Stuart, J., Hoytt, D. W., Satterthwait, A. C., Llinas, M., Reed, J. C., and Ely, K. R. Structural analysis of interactions between BAG1 co-chaperone and Hsc70 heat shock protein, *Nature Struct Biol. 8:* 359-352, 2001.

CONCLUSIONS

Understanding the molecular basis for progression of prostate cancers to hormone-refractory disease is critical for designing new therapeutic strategies for the treatment of advanced prostate cancer. We have discovered a protein, BAG-1L, that binds the androgen receptor (AR) and enhances its resistance to anti-androgenic agents. Our findings accomplished with funding from this grant indicate that BAG-1 expression is abnormally elevated in the vast majority of prostate cancers. Future studies of the impact of BAG-1 overexpression and BAG-1 inhibition in the prostate glands of transgenic mice will reveal the overall significance of BAG-1 for regulation of androgen-responses in normal and malignant prostate tissue, and will help contribute to new strategies for overcoming hormone-resistant prostate cancer.

REFERENCES

1. Kyprianou, N. and Isaacs, J. T. Activation of programmed cell death in the rat ventral prostate after castration, *Endocrinology. 122:* 552-562, 1988.
2. Crawford, E. D., Eisenberger, M. A., McLeod, D. C., Spaulding, J., Benson, R., Dorr, F. A., Blumenstein, B. A., Davis, M. A., and Goodman, P. J. A control randomized trial of Leuprolide with and without flutamide in prostatic cancer, *N Engl J Med. 321:* 419-424, 1989.
3. Marcelli, M., Tilley, W. D., Zoppi, S., Griffin, J. E., Wilson, J. D., and McPhaul, M. J. Molecular basis of androgen resistance, *J Endocrinol Invest. 15:* 149-159, 1992.
4. McPhaul, M. J., Marcelli, M., Zoppi, S., Griffin, J. E., and Wilson, J. D. Genetic basis of endocrine disease. 4. The spectrum of mutations in the androgen receptor gene that causes androgen resistance, *J Clin Endocrinol Metab. 76:* 17-23, 1993.
5. Coetzee, G. A. and Ross, R. K. Prostate cancer and the androgen receptor, *J Natl Cancer Inst. 86:* 872-873, 1994.
6. Koivisto, P., Kononen, J., Palmberg, C., Tammela, T., Hyyt2inen, E., Isola, J., Trapman, J., Cleutjens, K., Noordzij, A., Visakorpi, T., and Kallioniemi, O.-P. Androgen receptor gene amplification: a possible molecular mechanism for androgen deprivation therapy failure in prostate cancer, *Cancer Res. 57:* 314-319, 1997.
7. Visakorpi, T., Hyytinen, E., Koivisto, P., Tanner, M., Keinanen, R., Palmberg, C., Palotie, A., Tammela, T., Isola, J., and Kallioniemi, O. P. In vivo amplification of the androgen receptor gene and progression of human prostate cancer, *Nature Genet. 9:* 401-406, 1995.
8. McPhaul, M. J., Marcelli, M., Tilley, W. D., Griffin, J. E., and Wilson, J. D. Androgen resistance caused by mutations in the androgen receptor gene, *FASEB J. 5:* 2910-2915, 1991.
9. Tsai, M. J., , and O'Malley, B. W. Molecular mechanisms of action of steroid/thyroid receptor superfamily members, *Annu Rev Biochem. 63:* 451-486, 1994.
10. Anzick, S., Kononen, J., Walker, R., Azorsa, D., Tanner, M., Guan, X., Sauter, G., Kallioniemi, O., Trent, J., and Meltzer, P. AIB1, a steroid receptor coactivator amplified in breast and ovarian cancer, *Science. 277:* 965-968, 1997.
11. Pratt, W. B. and Welsh, M. J. Chaperone functions of the heat shock proteins associated with steroid receptors, *J Cell Biol. 5:* 83-93, 1994.
12. Shibata, H., Spencer, T. E., Onate, S. A., Jenster, G., Tsai, S. Y., Tsai, M. J., and O'Malley, B. W. Role of co-activators and co-repressors in the mechanism of steroid/thyroid receptor action, *Recent Prog Horm Res. 52:* 141-164, 1997.

13. Turner, B.C., Krajewski, S., Krajewska, M., Takayama, S., Gumbs, A.A., Rebbeck, T.A., Carter, D., Haffty, B.G., and Reed, J.C. Bag-1: A novel biomarker predicting long term survival in early-stage breast cancer, *J Clin Oncol.* 19:992-1000, 2001.
14. Froesch, B.A., Takayama, S., and Reed, J.C. BAG-1L protein enhances androgen receptor function, *J Biol Chem.* 273: 11660-11666, 1998.
15. Briknarová, K., Takayama, S., Brive, L., Harvert, M.L., Knee, D.A., Velasco, J., Homma, S., Cabezas, E., Stuart, J., Hoytt, D.W., Satterthwait, A.C., Llinas, M., Reed, J.C., and Ely, K.R. Structural analysis of interactions between BAG-1 co-chaperone and Hsc70 heat shock protein. *Nature Struct Biol.* 8:349-352, 2001.
16. Knee, D.A., Froesch, B.A., Nuber, U., Takayama, S., and Reed, J.C. Structure-function analysis of Bag-1 proteins effects on androgen receptor transcriptional activity, *J Biol Chem.* 276:12718-24, 2001.
17. Kononen, J., Bubendorf, L., Kallioniemi, A., Barlund, M., Schraml, P., Leighton, S., Torhorst, J., Mihatsch, M.J., Sauter, G., and Kallioniemi, O.P. Tissue microarrays for high-throughput molecular profiling of tumor specimens, *Nature Med.* 4:844-847, 1998.
18. Guzey, M., Takayama, S., and Reed, J.C. Bag-1L enhances trans-activation function of the vitamin D receptor, *J Biol Chem.* 275:40749-56, 2000.

THE JOURNAL OF BIOLOGICAL CHEMISTRY

Vol. 273, No. 19, Issue of May 8, pp. 11660–11666, 1998
Printed in U.S.A.

BAG-1L Protein Enhances Androgen Receptor Function*

(Received for publication, November 26, 1997, and in revised form, February 20, 1998)

Barbara A. Froesch, Shinichi Takayama, and John C. Reed‡

From the Burnham Institute, La Jolla, California 92037

BAG-1 is a regulator of heat shock protein (Hsp) 70/Hsc70 family proteins that interacts with steroid hormone receptors. The recently identified BAG-1 long (BAG-1L) protein, an isoform of BAG-1 that arises from translation initiation at a noncanonical CUG codon, was co-immunoprecipitated with androgen receptors (AR) from LNCaP prostate cancer cells and other cell lysates, whereas the shorter originally identified BAG-1 and BAG-1M (RAP 46) proteins were not. BAG-1L, but not BAG-1 or BAG-1M (RAP46), also markedly enhanced the ability of AR to transactivate reporter gene plasmids containing an androgen response element (ARE) in PC3 prostate cancer and other cell lines. A C-terminal region deletion mutant of BAG-1L failed to co-immunoprecipitate with AR and functioned as a trans-dominant inhibitor of BAG-1L, impairing AR-induced transactivation of ARE-containing reporter plasmids. In addition, BAG-1L significantly reduced the concentrations of 5α-dihydrotestosterone (DHT) required for AR activity but did not induce ligand-independent transactivation. BAG-1L also markedly improved the ability of AR to transactivate reporter genes when cells were cultured with DHT in combination with the anti-androgen cyproterone acetate. The effects of BAG-1L on AR could not be explained by detectable alterations in the DHT-induced translocation of AR from cytosol to nucleus, nor by BAG-1L-induced increases in the amounts of AR protein. These findings implicate BAG-1L in the regulation of AR function and may have relevance to mechanisms of prostate cancer resistance to hormone-ablative and anti-androgen therapy.

Prostate cancer is the most common malignancy in the United States and the second leading cause of cancer-related death among men (1). The normal prostate gland contains a two-layer epithelium composed of a population of small round stem cells called basal cells, which line the basement membrane, and a population of larger differentiated epithelial cells called secretory cells, which secrete a variety of proteins and other substances into the lumen of the gland (2, 3). Although both basal and secretory cells contain androgen receptors (AR)[1] (4, 5), only the luminal secretory epithelial cells are dependent on steroid hormone for their function, growth, and survival (4). In the absence of testosterone or related androgens, which can serve as ligands for AR, the secretory cells undergo rapid programmed cell death (6). Current treatment for metastatic adenocarcinoma of the prostate is predicated on the cell death-inducing effects of anti-androgens and hormone-ablative measures, which reduce endogenous production of androgens. However, nearly all hormone-dependent prostate cancers eventually relapse as fatal hormone-independent disease (7).

Multiple, still largely unidentified mechanisms may account for the complete independence or reduced dependence of prostate cancers on androgens (reviewed in Refs. 8–10). AR gene deletion or sequestration of the AR from the nucleus to the cytoplasm have been described in some hormone-independent tumors, implying that genetic alterations associated with tumor progression can abrogate the necessity for AR in some cases. However, many tumors may rely on other strategies that allow cancer cells to grow in low concentrations of androgens, including AR gene amplification or overexpression (11, 12) and AR mutations that permit transactivation of target genes with little or no requirement for steroid hormones (9, 13). Since most hormone-insensitive prostate cancers still retain a wild-type AR, presumably alterations in the factors that control the levels of AR and its function appear to play a major role in resistance to anti-androgen and hormone-ablative therapies. Thus, a need exists to understand more about the molecular mechanisms that govern the activity of AR.

Steroid hormones mediate their effects by binding to specific intracellular receptors that act as hormone-dependent transcription factors. Upon binding steroid ligands, the AR undergo a conformational change, translocate to the nucleus, and bind to specific DNA sequences located near or in promoter regions of target genes. After binding DNA, the receptor interacts with components of the basal transcription machinery and sometimes sequence-specific transcription factors, resulting in positive or negative effects on gene transcription (14, 15). A number of proteins have been identified that associate with the inactive or hormone-bound hormone-receptor complexes, including several heat shock family proteins and various types of transcription co-activators (reviewed in Refs. 16 and 17). However, many details remain unclear as to the molecular mechanisms by which these proteins modulate the activities of steroid hormone receptors, and even less is known about whether alterations in their expression or function might contribute to the deregulation of steroid hormone responses in cancers.

Recently, an isoform of the human BAG-1 protein (known as RAP46 (see below)) (18, 19) has been reported to bind several steroid hormone receptors *in vitro*, including AR (19). It is unknown, however, what effect if any, BAG-1 has on the functions of these steroid-dependent transcription factors. Interestingly, BAG-1 and its alternative isoform RAP46 were recently shown to bind tightly to heat shock protein (Hsp) 70/Hsc70 family proteins and modulate their chaperone activity *in vitro* (20–22). In this regard, BAG-1 appears to function analogously to bacterial GrpE, stimulating the exchange of ADP for ATP on

* This work was supported by NCI, National Institutes of Health, Grant CA-67329, the Swiss Science National Foundation, and Cancer Research Switzerland Grant BIL KFS 19891995. The costs of publication of this article were defrayed in part by the payment of page charges. This article must therefore be hereby marked "*advertisement*" in accordance with 18 U.S.C. Section 1734 solely to indicate this fact.

‡ To whom correspondence should be addressed: Scientific Director, The Burnham Institute, 10901 N. Torrey Pines Rd., La Jolla, CA 92037. Tel.: 619-646-3140; Fax: 619-646-3194; E-mail: jreed@burnham-inst.org.

[1] The abbreviations used are: AR, androgen receptor(s); ARE, androgen response element; DHT, 5α-dihydrotestosterone; CAT, chloramphenicol acetyltransferase; Hsp, heat shock protein; PAGE, polyacrylamide gel electrophoresis; FCS, fetal calf serum; CPA, cyproterone acetate; PBS, phosphate-buffered saline; CMV, cytomegalovirus.

Hsc70 (22). It seems plausible therefore that BAG-1 could alter the bioactivity of AR and other steroid hormone receptors, given that many steroid hormone receptors are constitutively bound to heat shock proteins and that their hormone binding affinity and DNA binding activity can be increased in the presence of Hsp90 and Hsp70, respectively, under some circumstances (23–25).

The human and murine BAG-1 proteins are predicted to be amino acids 230 and 219 base pairs in length, respectively, based on cDNA cloning (18, 19, 26, 27). However, recently longer isoforms of the human and mouse BAG-1 proteins have been identified that can arise by translation initiation from noncanonical CUG codons located upstream and in frame with the originally described BAG-1 open reading frames (27, 28). This longer isoform of BAG-1 contains a basic motif resembling nuclear localization sequences and preferentially targets to nuclei. The human BAG-1 and BAG-1 long (BAG-1L) proteins migrate as ~36-kDa and 57–58-kDa proteins, respectively in SDS-PAGE experiments. In addition, a less abundant isoform of BAG-1 that migrates at ~46–53 kDa has been described and termed either BAG-1M or RAP46. The BAG-1M (RAP46) protein arises from translation initiation at an AUG codon located upstream of the usual start site in the BAG-1 mRNA (27).[2] BAG-1M (RAP46) is produced in human, but not mouse, cells.[2]

Like BAG-1, the BAG-1L and BAG-1M proteins also bind to Hsp70 and Hsc70.[2] BAG-1 is ubiquitously expressed, whereas BAG-1L is found preferentially in steroid hormone-dependent tissues such as testis, ovary, breast, and prostate.[2] Although little is known about the expression of BAG-1 and BAG-1L in cancers, both proteins were detected by immunoblotting in 9 of 9 prostate cancer cell lines tested.[2] In this report, we present evidence that the BAG-1L protein may play an important role in the AR signaling pathway, in that it can form complexes with AR and enhance the androgen-dependent transactivation function of this steroid hormone receptor.

MATERIALS AND METHODS

Plasmids—The plasmids pcDNA3-hu-BAG-1L and pcDNA3-hu-BAG-1 were generated as described previously (26).[2] Translation of the longer form (BAG-1L) was forced by mutation of the noncanonical in frame first CTG codon of the cDNA to ATG.[2] pcDNA3-BAG-1/BAG-1M lacks the upstream CTG-containing region of the cDNA and encodes both the originally described ~36-kDa form of BAG-1 and ~the 46–53-kDa BAG-1M (RAP46) proteins. The plasmid pcDNA3-hu-BAG-1L (ΔC) (lacking the last 47 amino acids of the human BAG-1 protein) was generated by polymerase chain reaction using pcDNA3-BAG-1L as a template and the *Eco*RI-containing forward primer 5′-GGGAATTCAGTGCGGGCATGGCTC-3′ together with the *Xho*I containing reverse primer 5′-CCCTCGAGTTATGGCAGGATCAGTGTGTG-3′. After digestion of the polymerase chain reaction product at the *Eco*RI and *Xho*I sites, the resulting ~0.8-kilobase pair fragments were subcloned into *Eco*RI/*Xho*I-digested pcDNA3. pSG5-AR contains the cDNA for the wild-type AR (29). The reporter pLCI plasmid contains the full-length mouse mammary tumor virus long terminal repeat sequence linked with the chloramphenicol acetyltransferase (CAT) gene (29, 30). pCMV-p53wt expression vector, MYH101–81 containing the p53 response element and the TATA box from the *BAX* promoter, and pUCSV3-CAT containing a SV40 early region promoter have been described (31, 32).

Cell Culture—The human prostate cancer cell lines LN-CaP and PC3, the transformed human embryonal kidney 293, and the monkey kidney COS7 cell lines were obtained from the American Type Culture Collection (Rockville, MD). The ALVA31 human prostate cancer cell line was generously provided by Dr. G. Miller (University of Colorado, Denver, CO). Cells were maintained in a humidified atmosphere with 5% CO_2 in RPMI 1640 or Dulbecco's modified Eagle's medium (293 and COS7) supplemented with 10% FCS, 3 mM glutamine, 100 units/ml penicillin, and 100 mg/ml streptomycin (Life Technologies, Inc.). Two days prior to experiments, cells were transferred into CT-FCS to reduce background levels of steroids. 5α-Dihydro-testosterone (DHT) (Sigma) and cyproterone acetate (CPA) (Sigma) were dissolved in dimethyl sulfoxide and added to the cultures at a minimum dilutions of 0.0001% (v/v). Control cells received an equivalent amount of solvent only.

Transfections and Enzyme Assays—COS7, PC3, and 293T cells at 60% confluency were transfected by a standard calcium phosphate precipitate method (33). The medium was replaced with fresh charcoal-treated fetal calf serum/Dulbecco's modified Eagle's medium 1 h before transfection. The total amount of plasmid DNA used was normalized to 2.5 μg/well and 8 μg/plate for transfection in 12-well and 6-cm^2 plates, respectively, by the addition of empty plasmid. For reporter gene assays, 0.2 μg of a β-galactosidase expression plasmid pCMV-βgal was co-transfected with the CAT reporter gene to normalize the transfection efficiency. Cells were exposed to the precipitate for 5 h at 37 °C. For COS7 and PC3 cells, a glycerol shock was applied. Cells were exposed to 15% glycerol in HBS buffer (25 mM HEPES pH 7.05, 0.75 mM Na_2HPO_4, 140 mM NaCl) for 4 min. The glycerol was removed by washing three times with PBS and replacement with fresh charcoal-treated fetal calf serum medium. For 293 cells, the medium was replaced without applying a shock.

ALVA31 cells were transfected by a lipofection method. Briefly, 1.3 μg of DNA was diluted into 50 μl of Opti-MEM medium (Life Technologies) and combined with 3.3 μl of Lipofectamine (Life Technologies) in 50 μl of Opti-MEM. After incubation for 20 min, 0.35 ml of Opti-MEM was added, and the mixtures were overlaid onto monolayers of cells. After culturing at 37 °C and 5% CO_2 for 6 h, 0.45 ml of Opti-MEM containing 20% charcoal-stripped fetal bovine serum was added to the cultures.

At 32–36 h after transfection, cells were stimulated with 0.001–10 nM DHT or 0.1 nM R1881 (ALVA31). Cell extracts were prepared 48 h after transfection. For reporter gene experiments, cells lysates were made as described in Ref. 34 and assayed for CAT and β-galactosidase activity. All transfection experiments were carried out in triplicate, repeated at least three times, and normalized for β-galactosidase activity.

Cell Extracts and Subcellular Fractionation—For gene expression experiments, cells were washed two times in PBS and lysed in radioimmune precipitation buffer (35) containing protease inhibitors (1 mM phenylmethylsulfonyl fluoride, 0.28 trypsin inhibitory units/ml aprotinin, 50 μg/ml leupeptin, 1 μM benzamidine, 0.7 μg/ml pepstatin). For protein localization experiments, nuclear and nonnuclear fractions were prepared according to the method of Schreiber *et al.* (36). Briefly, cells were collected and washed two times with ice-cold PBS. Cell pellets were resuspended in buffer A (10 mM HEPES, pH 7.9, 10 mM KCl, 0.1 mM EDTA, 0.1 mM EGTA, 2.5 mM dithiothreitol, protease inhibitors) and left on ice for 15 min prior to the addition of Nonidet P-40 to 0.6% (v/v) final concentration. After centrifugation, supernatants (cytoplasmic fractions) were collected, and the nuclear pellets were washed twice in the same buffer. Pellets were finally resuspended in buffer B (20 mM HEPES, pH 7.9, 400 mM NaCl, 25% glycerol, 0.1 mM EDTA, 0.1 mM EGTA, 2.5 mM dithiothreitol, protease inhibitors) and vigorously shaken for 10 min, and the postnuclear supernatants were cleared by centrifugation. Fractions were normalized based on the bicinchoninic acid method (Pierce) prior to SDS-PAGE/immunoblot assay.

Immunoblotting—Aliquots containing 25 μg of protein were subjected to SDS-PAGE using 10% gels, followed by electrotransfer to Immobilon-P transfer membranes (Millipore Corp., Bedford, MA). Immunodetection was accomplished using 1:1000 (v/v) of anti-BAG-1 monoclonal antibody ascites (26, 37)[2] or polyclonal rabbit AR antiserum (Clone AR N20, Santa Cruz Biotechnology, Inc., Santa Barbara, CA), followed by horseradish peroxidase-conjugated secondary antibody (Amersham Pharmacia Biotech). Detection was performed using an enhanced chemiluminescence detection method (ECL; Amersham Pharmacia Biotech) or the Vector SG substrate (Vector Laboratories, Burlingame, CA).

Co-immunoprecipitations—LN-CaP cells (2×10^7) were collected at 70% confluency and lysed in HKMEN buffer (10 mM HEPES, pH 7.2, 142 mM KCl, 5 mM $MgCl_2$, 2 mM EGTA, 0.2% Nonidet P-40, protease inhibitors). Cell lysates were passaged several times through a 30½-gauge needle to disrupt the nuclei. Altnernatively, COS7 cells were transiently transfected with AR and BAG-1 expression plasmids, washed several times in PBS, and treated with 1 mM dimethyl-3,3′-dithiobispropionimadate (Pierce) in PBS for 30 min on ice. After extensive washing in ice-cold PBS, cells were lysed in radioimmune precipitation buffer containing protease inhibitors. Immunoprecipitations were performed in HKMEN either using the IgG_1 anti-BAG-1 monoclonal KS6C8 (26)[2] or a polyclonal rabbit AR antiserum (clone AR PA1–110 ABR, Inc.) conjugated to protein G-agarose (Zymed, San Fran-

[2] S. Takayama, S. Krajewski, M. Krajewska, S. Kitada, J. Zapata, K. Kochel, D. Knee, D. Scudiero, G. Tudor, G. J. Miller, M. Yamada, T. Miyashita, and J. Reed, submitted for publication.

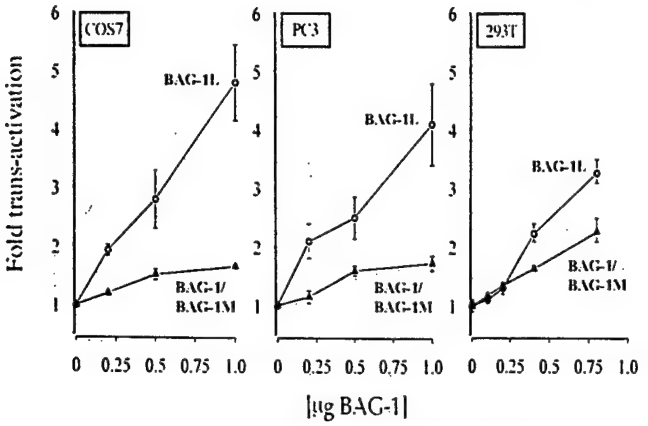

FIG. 1. **Effect of BAG-1 on the AR-mediated transactivation of an ARE-containing reporter gene.** The AR-encoding plasmid pSG5-AR (0.4 μg), was co-transfected by a standard calcium phosphate precipitate method into PC3 prostate cancer cells, COS7 monkey kidney cells, and 293T human embryonic kidney cells with 0.5 μg of pLCI reporter plasmid, 0.2 μg of pCMV-βgal and increasing amounts of BAG-1 expression plasmids as indicated. The total amount of plasmid DNA used was normalized to 2.5 μg/well by the addition of empty plasmid. Thirty-two hours after transfection, cells were stimulated with 5 nM DHT. Cell extracts were prepared and assayed for CAT and β-galactosidase activity at 48 h. Data were normalized using β-galactosidase, and results are expressed as -fold transactivation relative to DHT-stimulated cells transfected with AR expression vector in combination with pcDNA3 control plasmids. All transfection experiments were carried out in triplicate wells and repeated at least three times. The BAG-1 expression plasmid pcDNA3-BAG-1/BAG-1M produces approximately equivalent amounts of the BAG-1 and BAG-1M (RAP46) proteins.

cisco, CA). Control immunoprecipitations were performed using IgG_1 or rabbit preimmune serum. Immune complexes were analyzed by SDS-PAGE/immunoblot assay using anti-BAG-1 monoclonal antibody with an enhanced chemiluminescence detection method.

RESULTS

BAG-1L Enhances AR-mediated Transactivation of an Androgen Response Element (ARE)-containing Reporter Gene—The human BAG-1M (RAP46) protein had been shown to bind to AR *in vitro* (19). We therefore asked whether BAG-1 family proteins can influence the transcriptional activity of this steroid hormone receptor. For these experiments, three different cell lines were transiently co-transfected with plasmids encoding various BAG-1 isoforms and AR, together with a ARE-containing CAT reporter plasmid. The cells were then cultured in the presence or absence of DHT. In the presence of hormone, BAG-1 family proteins increased the transcriptional activity of AR in a concentration-dependent manner, with the plasmid producing the BAG-1L protein displaying far more effect than the plasmid encoding for both BAG-1 and BAG-1M (Fig. 1). The extent of BAG-1L-mediated up-regulation of AR-induced transactivation varied among cell lines, with COS7 and PC3 demonstrating as much as ~ 5-fold increases when transfected with BAG-1L but 293T cells exhibiting only a modest effect. Immunoblot analysis confirmed the production of the BAG-1, BAG-1M, BAG-1L, and AR proteins in the transfected cells and demonstrated production of similar amounts of BAG-1 and BAG-1M compared with BAG-1L (see below for examples). Thus, differences in the relative amounts of BAG-1, BAG-1M, and BAG-1L proteins produced could not account for the greater potency of BAG-1L.

The transcription-potentiating effect of BAG-1L was dependent on the addition of androgen to cultures. As shown in Fig. 2, AR-mediated transactivation of the ARE-CAT reporter plasmid remained at background levels when cells were co-transfected with plasmids encoding BAG-1 family proteins but cultured in

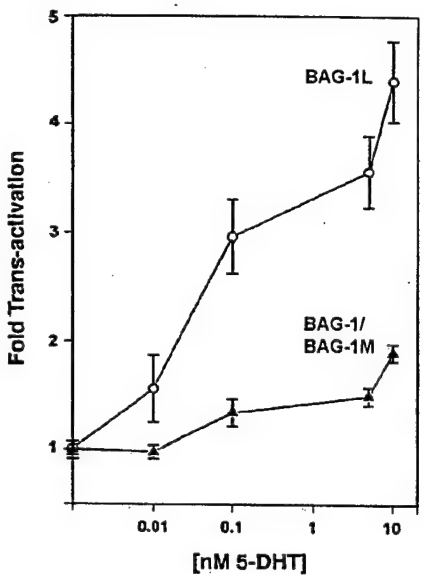

FIG. 2. **BAG-1L enhances DHT-induced transactivation by AR.** PC3 cells were transfected as described for Fig. 1, except that the concentration of pcDNA3-BAG-1/BAG-1M or pcDNA3-BAG-1L expression plasmids was held constant at 0.8 μg. Thirty-two hours after transfection, cells were stimulated with 0.001–10 nM DHT. Cell extracts were prepared and assayed for CAT and β-galactosidase activity at 48 h after transfection. Data are expressed as in Fig. 3 (mean ± S.D.; $n = 3$).

the absence of DHT. However, cells transfected with the BAG-1L-producing plasmid displayed greater sensitivity to androgen compared with control transfected cells or cell over-expressing BAG-1/BAG-1M. The BAG-1L-mediated increases in AR-induced transactivation of the ARE-CAT reporter gene were detected at concentrations as low as 0.01 nM DHT and were substantially higher than control cells or BAG-1/BAG-1M-expressing cells over a broad range of hormone concentrations (0.01- 10 nM). The effects of BAG-1L were dependent on AR, since co-transfections lacking the AR-encoding plasmid failed to result in ARE-CAT plasmid reporter gene transactivation above background levels (not shown).

To further examine the specificity of BAG-1L-mediated enhancement of AR transcriptional activity, the effects of BAG-1L on expression of other reporter genes were evaluated. The tumor suppressor p53 was chosen because, by analogy to steroid receptors, p53 is often associated with Hsp90 and Hsp70 in the cytoplasm and must translocate from cytosol to nucleus to exert its transcriptional regulatory action (38). Co-transfection of BAG-1L-encoding expression plasmid into PC3 cells with a p53-producing vector and a p53-RE-CAT reporter gene demonstrated that BAG-1L does not influence p53-mediated transactivation (Fig. 3). Similarly, BAG-1L had no effect on the constitutive expression of either a SV40 early region promoter-driven CAT or the CMV immediate early region *lacZ* reporter gene plasmid used for normalizing transfection efficiencies (Fig. 3 and data not shown). These viral promoter/enhancers contain Sp1 binding sites, thus suggesting that BAG-1L does not nonspecifically modulate this family of transcription factors.

BAG-1L Decreases the Response of AR to Anti-androgen CPA—The observation that BAG-1L increased the sensitivity of AR to its ligand DHT (Fig. 2) prompted us to explore the effects of BAG-1L on the suppression of AR transactivity by the anti-androgen cyproterone acetate. For these experiments, AR and ARE-CAT were transfected into COS7 cells with either pcDNA3 control DNA or an equivalent amount of pcDNA3-BAG-1L. The cells were treated ~1.5 days later with 1 nM DHT alone or in combination with various concentrations of CPA.

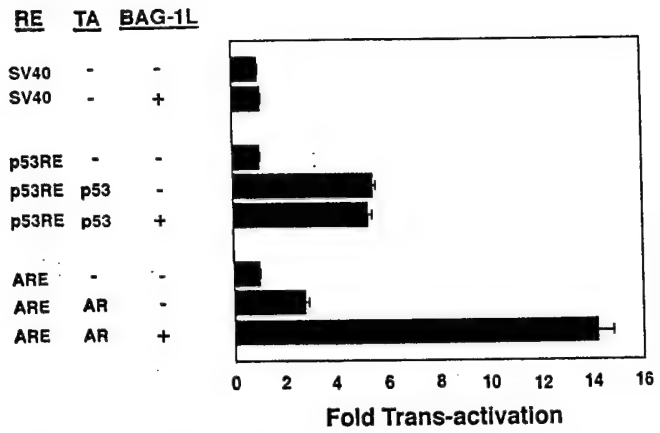

FIG. 3. **BAG-1L specifically enhances AR-mediated transactivation.** PC3 cells were co-transfected by a standard calcium phosphate precipitate method with 0.4 μg of pSG5-AR, pCMV-p53wt, or empty plasmid DNA and 0.5 μg of pLCI, MYH-101–81, or pUCSV3-CAT, respectively. A β-galactosidase expression plasmid (0.2 μg) was co-transfected to normalize for transfection efficiency. Thirty-two hours after transfection, cells were stimulated with 5 nM DHT. Cell extracts were prepared at 48 h and assayed for CAT and β-galactosidase activity. Results are expressed as -fold transactivation activity relative to cells transfected with the reporter gene alone (mean ± S.D.; $n = 3$). *TA*, transactivator; *RE*, response element.

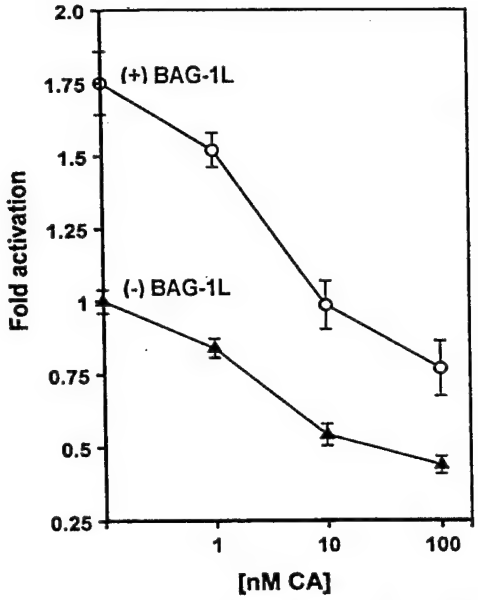

FIG. 4. **BAG-1L reduces inhibitory effects of the anti-androgen CPA on AR-mediated transactivation.** COS7 cells were transfected as described in Fig. 1 except that the concentration of pcDNA3-control or pcDNA3-BAG-1L expression plasmids was held constant at 0.3 μg. Approximately 1.5 days after transfection, cells were treated with 1 nM DHT and various concentrations of CPA as indicated. Cell extracts were prepared and assayed for CAT and β-galactosidase activity as described in Fig. 1, and the normalized data were expressed as a -fold transactivation relative to pcDNA-3 control-transfected cells, which received DHT without CPA.

Relative CAT activity was then measured 12–14 h later. As shown in Fig. 4, CPA reduced in a concentration-dependent manner the DHT-induced transactivation of the ARE-CAT reporter gene plasmid in both control and BAG-1L-transfected COS7 cells. However, because AR-mediated reporter gene transactivation started at higher levels in BAG-1L transfectants, approximately 2 log higher concentrations of CPA androgens were generally required to reduce reporter gene activity to levels comparable with control-transfected cells (Fig. 4).

In Vivo Binding of BAG-1L to the AR—Although BAG-1M (RAP46) has been reported to bind AR *in vitro*, the interaction of these proteins has not been demonstrated previously in cells. Co-immunoprecipitation assays were therefore performed using lysates prepared from untransfected LN-CaP cells, which constitutively express high levels of the BAG-1, BAG-1M, BAG-1L, and AR proteins (39).[2] A polyclonal anti-AR antiserum or a preimmune control serum was employed for immunoprecipitations, and the resulting immune complexes were subjected to SDS-PAGE/immunoblot analysis using the anti-BAG-1 monoclonal antibody KS6C8. As a control, BAG-1 proteins were also immunoprecipitated using the same anti-BAG-1 monoclonal antibody. Alternatively, an IgG_1 control antibody was employed to confirm specificity.

As shown in Fig. 5, the BAG-1L protein was readily detected in association with anti-AR immune complexes (*lane 5*). In contrast, the BAG-1 and BAG-1M proteins did not co-immunoprecipitate with AR but were found in anti-BAG-1 immune complexes, confirming their presence in LN-CaP cells under these conditions. The specificity of these results was confirmed by the absence of BAG-1 family and AR proteins in immune complexes prepared using IgG_1 control monoclonal antibody or the preimmune control serum. Although BAG-1L could be detected in AR-containing immune complexes, the reciprocal experiment involving the use of anti-BAG-1 antibody in attempts to co-immunoprecipitate AR proved unsuccessful. Additional experiments suggested that this was due to antibody-induced disruption of BAG-1L interactions with AR (data not shown). Attempts to determine whether BAG-1L can associate with AR in the absence of steroid hormone have been hampered by the rapid turnover of unliganded AR, resulting in lower levels of

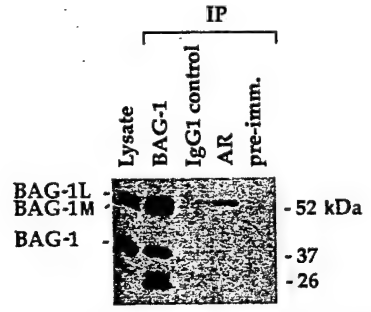

FIG. 5. **Co-immunoprecipitation of BAG-1L protein with AR.** Lysates were prepared from the human prostate cell line LN-CaP grown in the presence of DHT. Immunoprecipitations were performed using the IgG_1 anti-BAG-1 monoclonal KS6C8, an anti-AR polyclonal antiserum, an IgG_1 control antibody, or a preimmune control serum. Immune complexes were analyzed by SDS-PAGE/immunoblot assay using anti-BAG-1 monoclonal KS6C8. Lysate from cells (one-tenth input) were also run directly in the gel as a control.

AR and making quantitative comparisons difficult. However, thus far, we have detected association of BAG-1L with AR only when androgens have been present.

The C-terminal Hsc70-binding Domain of BAG-1L Is Required for Interactions with AR—Previously, we showed that the last 47 amino acids of the BAG-1 protein are required for binding to the ATPase domain of Hsc70 (20). We therefore compared a mutant of BAG-1L lacking this carboxyl-terminal domain, BAG-1L (ΔC), with the wild-type BAG-1L protein. Association with AR was examined after treatment with the reversible chemical cross-linker dimethyl-3,3′-dithiobispropionimadate in total cell lysates derived from transiently transfected COS7 cells. As shown in Fig. 6*A*, anti-AR immunoprecipitates contained BAG-1L protein, as determined by immunoblot analysis using anti-BAG-1 antibody. In contrast, the BAG-1L (ΔC) protein was not detected in anti-AR immune complexes. The BAG-1 and BAG-1M isoforms of BAG-1 also did

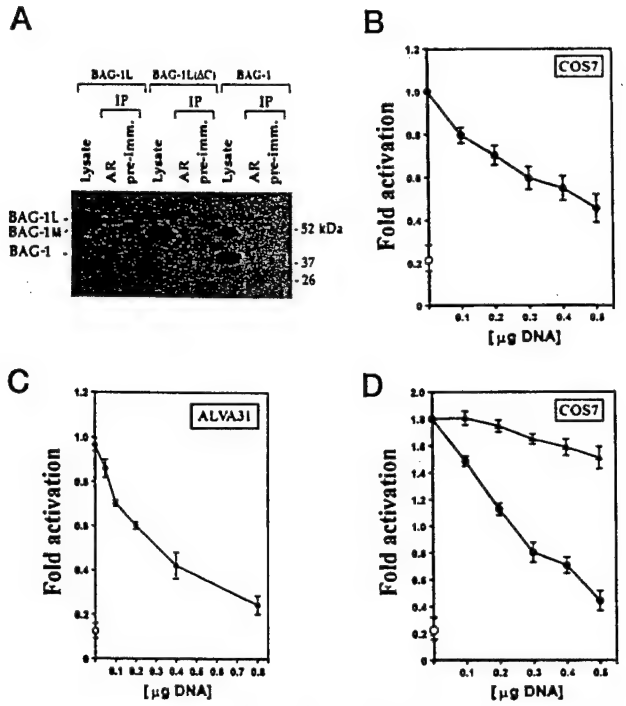

FIG. 6. **The BAG-1L (ΔC) mutant protein fails to interact with AR and functions as a trans-dominant inhibitor of the wild-type BAG-1L protein.** *A*, COS7 cells were transiently transfected with equivalent amounts of AR and one of the following BAG-1 expression plasmids: pcDNA3-BAG-1L, pcDNA3-BAG-1L (ΔC), or pcDNA3-BAG-1/BAG-1M (produces approximately equivalent amounts of BAG-1 and BAG-1M proteins). Two days later, cells were treated with the reversible chemical cross-linker dimethyl-3,3′-dithiobispropionimadate (1 mM in PBS) for 30 min, washed several times in ice-cold PBS and lysed in radioimmune precipitation buffer. Immunoprecipitations were performed as described in Fig. 5 using the anti-AR polyclonal antiserum or a preimmune control serum, followed by immunoblotting using the anti-BAG-1 monoclonal KS-6C8 and an ECL-based detection method. The positions of the BAG-1L, BAG-1M, and BAG-1 protein are indicated. In *B* and *C*, COS7 or ALVA31 cells were transiently co-transfected as described with 0.4 or 0.2 μg of pSG5-AR, 0.5 or 0.3 μg of the murine mammary tumor virus CAT reporter plasmid pLCI, and 0.2 or 0.1 μg of pCMV-βgal, respectively, and various amounts of pcDNA3-BAG-1 (ΔC) (dark circles) or an equivalent amount of pcDNA3 control plasmid (total DNA normalized by the addition of pcDNA3 control plasmid). In *D*, COS7 cells were transfected as in *B*, except 0.3 μg of pcDNA3-BAG-1L was included in all transfections, and pcDNA3-BAG-1L (ΔC) was compared with pcDNA3-BAG-1/BAG-1M, which produces approximately equivalent amounts of the wild-type BAG-1 and BAG-1M proteins (*solid triangles*). The total amount of plasmid DNA used was normalized to 2.5 μg/well by the addition of pcDNA-3 control plasmid. Approximately 1.5 days after transfection, cells were stimulated with (*B* and *D*) 1 nM DHT or 0.1 nM R1881 (*C*). Cells that did not receive androgen are indicated by *open circles*. Cell extracts were prepared and assayed for CAT and β-galactosidase activity at ~48 h. Data were normalized using β-galactosidase, and results are expressed as -fold transactivation relative to DHT-stimulated cells transfected with AR expression vector in combination with pcDNA3 control plasmids. All transfection experiments were carried out in triplicate wells and repeated at least three times (mean ± S.D.; $n = 3$).

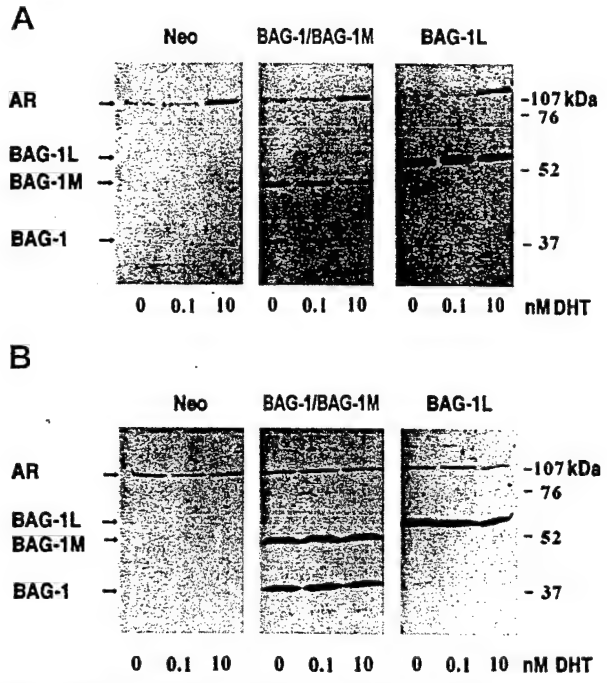

FIG. 7. **Effect of BAG-1 on the cytoplasmic/nuclear ratio of the AR.** COS7 cells were transiently co-transfected with 3 μg of pSG5-AR and 5 μg of either pcDNA3 (*Neo*), pcDNA3-BAG-1/BAG-1M, or pcDNA3-BAG-1L expression plasmids by a standard calcium phosphate method. Thirty-two hours after transfection, cells were stimulated with 0, 0.1, or 10 nM DHT. Nuclear (*A*) and nonnuclear (*B*) fractions were prepared 2 days after transfection. Nuclear and cytoplasmic extracts (35 μg of total protein) were subjected to SDS-PAGE/immunoblot assay and probed with antibodies to BAG-1 and AR.

not co-immunoprecipitate with AR (Fig. 6*A*; *lanes 7–9*). Successful production of the BAG-1L, BAG-1L (ΔC), BAG-1, and BAG-1M proteins was confirmed by immunoblot analysis of whole cell lysates derived from transfected COS7 cells (Fig. 6*A*). We conclude therefore that the C-terminal domain of BAG-1L is required for complex formation with AR.

To explore the functional consequences of removing the C-terminal domain from BAG-1L, co-transfection reporter gene assays were performed, assaying AR-mediated transactivation of an ARE-CAT in reporter gene plasmid. When co-transfected with AR, the BAG-1L (ΔC)-encoding plasmid suppressed in a concentration-dependent fashion the DHT-induced transactivation of ARE-CAT in COS7 cells (Fig. 6*B*) and in ALVA31 human prostate cancer cells (Fig. 6*C*). Both COS7 and ALVA31 express BAG-1L endogeneously, as determined by immunoblotting.[2] In addition, when varying amounts of BAG-1L (ΔC)-encoding plasmid were co-transfected with a fixed amount of wild-type BAG-1L and AR plasmid DNA, again the BAG-1L (ΔC) plasmid suppressed hormone-induced transactivation of the ARE-CAT reporter plasmid by up to 70% (Fig. 6*D*), suggesting that BAG-1L (ΔC) functions as a trans-dominant inhibitor of the wild-type BAG-1L protein. In contrast, under the same conditions, a plasmid encoding the BAG-1 and BAG-1M isoforms only slightly decreased AR transcriptional activity when co-expressed with BAG-1L. Immunoblot analysis verified that BAG-1L (ΔC) did not impair the production of either the BAG-1L or AR proteins (not shown).

Effects of BAG-1L on the Subcellular Localization of the AR—To investigate the mechanisms underlying the stimulatory effect of BAG-1L on AR transcriptional activity, we ascertained the effects of BAG-1L overexpression on DHT-induced nuclear translocation and stabilization of this steroid hormone receptor. COS7 monkey kidney cells were transiently transfected with plasmids encoding BAG-1/BAG-1M, BAG-1L, and AR at the same concentrations used for reporter gene assays. The cells were then stimulated with 0, 0.1, or 10 nM DHT, and the relative amounts of AR protein in the cytosol and nucleus were determined by immunoblot analysis of nuclear and nonnuclear fractions. As shown in Fig. 7, translocation of AR to the nucleus was induced in a concentration-dependent manner by DHT but was unaffected by overexpression of either BAG-1/BAG-1M or BAG-1L. At these same concentrations of DHT, however, BAG-1L promoted marked increases in AR-dependent transactivation of ARE-CAT (see above). Note also that the total levels of AR were not different when comparing cells that had been transfected with BAG-1L, BAG-1/BAG-1M, or Neo control plasmids (Fig. 7). DHT also did not appear to alter the relative proportions of the

BAG-1, BAG-1M, and BAG-1L proteins present within the nuclear and nonnuclear compartments.

DISCUSSION

The data presented here provide the first evidence that a recently identified longer isoform of the human BAG-1 protein (BAG-1L) can modulate the function of a steroid hormone receptor. In particular, we found that the BAG-1L protein can be co-immunoprecipitated with AR and significantly enhances AR-induced transactivation of a reporter gene, whereas the shorter BAG-1 and BAG-1M isoforms of the protein did not. Thus, despite evidence that the human BAG-1M (RAP46) protein can bind to AR and several other steroid hormone receptors *in vitro* (19), only the long form appears to physiologically interact with AR in cells and to regulate its function.

One factor that could contribute to the preferential binding of BAG-1L to AR in cells is that this longer isoform of BAG-1 contains a nucleoplasmin-like nuclear localization sequence within the NH_2-unique domain, which is missing from the shorter BAG-1 and BAG-1M (RAP46) protein.[2] In previous studies, we observed that BAG-1L targets preferentially but not exclusively to nucleus when transfected in COS7 and other cell lines, whereas BAG-1 and BAG-1M had a greater tendency to reside in the cytosol.[2] This is also true for the LN-CaP cells used in this study for co-immunoprecipitations, which contain all three isoforms of BAG-1, *i.e.* BAG-1, BAG-1M, and BAG-1L (data not shown). Since in the presence of androgen the AR resides almost exclusively in the nucleus (40), it is conceivable that under these conditions AR interacts with nuclear and not cytoplasmic proteins. Thus, the higher nuclear levels of BAG-1L compared with BAG-1 and BAG-1M may be largely responsible for its physical and functional interactions with AR protein complexes in cells.

Alternatively, another explanation for the observation that BAG-1L but not BAG-1 or BAG-1M (RAP46) was detected in association with AR in cells could be that the unique N-terminal region of the BAG-1L protein is required for binding to AR under physiological conditions. In this regard, it should be noted that the interaction of the BAG-1M (RAP46) protein with AR and other steroid hormone receptors has only been demonstrated *in vitro* and only then after treatment of steroid hormone receptor complexes with high salt at elevated temperature or with urea-containing solutions, conditions that could cause protein unfolding. In contrast, conformations of BAG-1 that are competent to bind AR complexes *in vivo* may only be achieved when the N-terminal unique region of BAG-1L is present. The N-terminal unique domain within BAG-1L could also directly bind to AR. However, clearly the N-terminal domain of BAG-1L is insufficient for AR binding, since deletion of the C-terminal last 47 amino acids abolished interactions BAG-1L with AR in cells. The failure of the BAG-1L (ΔC) protein to form complexes with AR was not due to altered subcellular localization of this protein compared with wild-type BAG-1L (data not presented).

The mechanism by which BAG-1L enhances the function of the AR remains to be determined. Clearly, the ability of BAG-1 proteins to bind to and modulate the function of Hsp70/Hsc70 family molecular chaperones by increasing ADP/ATP exchange and facilitating peptide release may provide some clues. As shown here, a carboxyl deletion mutant of BAG-1L lacking the last 47 amino acids, which are required for Hsc70 binding (20), was unable to form complexes with AR. This observation therefore suggests that Hsc70 bridges BAG-1L to AR, as has been proposed for its interactions with many other proteins (21). It is known that at least three members of the Hsp family, namely Hsp90, Hsp70, and Hsp56, are associated with the inactive forms of several steroid hormone receptors in the cytoplasm and may be important for maintaining the stability of these proteins in the absence of ligand and inducing conformations that are competent to bind steroid hormone ligands. Hsp70 has also been detected in the nucleus in association with receptor-DNA complexes where it putatively increases DNA binding affinity (23, 25). Thus, BAG-1L may alter AR interactions with molecular chaperones in ways that modulate the conformation of this steroid hormone receptor and enhance its responses to steroid ligands, *e.g.* by stabilizing hormone binding, increasing the affinity of AR interactions with DNA target sequences, or facilitating association with coactivator proteins (39). BAG-1L, however, did not appear to detectably increase the proportion of AR that translocates into the nucleus after the addition of DHT or to cause elevations in AR protein levels as might occur if BAG-1L stimulated nuclear translocation or prolonged the half-life of this protein. Also, expression of BAG-1L did not appear to increase the amount of Hsc70 or Hsp70 that would be co-immunoprecipitated with AR (not shown). These mechanisms, therefore, seem not to be involved in the potentiation of AR function by BAG-1L.

Alternatively, BAG-1L could conceivably bind directly to AR and exert its potentiating effect on AR independently of Hsp70. An Hsp70-independent mechanism of action is suggested by at least two observations. First, androgen has been reported to induce dissociation of not only Hsp90, but also Hsc70 from AR in concert with translocation of hormone-bound receptor into the nucleus (39). Since BAG-1L forms complexes with AR in the presence of hormone, this observation implies that BAG-1L may be able to interact with and modulate AR function within the nucleus after dissociation of Hsc70. One notable caveat, however, is that Hsp70 reportedly remains associated with estrogen and progesterone receptors while bound to their target DNA elements in the nucleus (16, 23, 25). Thus, unlike Hsp90, the Hsc70 family molecular chaperones may not always dissociate from nuclear hormone receptors upon binding ligand. Indeed, we have been able to co-immunoprecipitate at least small amounts of Hsc70/Hsp70 with AR in cells cultured with androgens.[3] Second, a C-terminal deletion mutant of BAG-1L that fails to bind Hsc70 functioned as a trans-dominant inhibitor of BAG-1L and reduced AR-mediated transactivation, thus suggesting the possibility of a Hsc70-independent mechanism. Although the reason why the BAG-1L (ΔC) mutant protein interferes with AR function requires further exploration, at least two possibilities can be considered. First, the BAG-1L (ΔC) protein may form dysfunctional complexes with endogenous wild-type BAG-1L, abrogating its effects on AR. However, biophysical characterization of the BAG-1 protein strongly suggests it is a monomer, unlike the functionally similar GrpE protein of prokaryotes, which is known to be a dimer (41). Thus, trans-dominant inhibition of endogenous BAG-1L may not explain why the BAG-1L (ΔC) protein inhibits AR function. Second, if BAG-1L normally bridges AR to other proteins such as transcriptional co-activators (reviewed in Ref. 28) and if the N-terminal unique domain of BAG-1L is necessary for this function, then the BAG-1L (ΔC) protein could theoretically sequester a co-factor essential for AR-mediated transcriptional activation. In this case, the BAG-1L (ΔC) protein, which does not bind to AR, would presumably prevent this hypothetical co-factor from binding to endogenous wild-type BAG-1L·AR complexes.

The role of BAG-1L in the fetal development of male reproductive organs and in the pathogenesis of prostate cancer remains to be established. In contrast to most androgen-unresponsive tissues, testes and the normal prostate gland, as well

[3] B. A. Froesch, S. Takayama, and J. C. Reed, unpublished data.

as 9 of 9 prostate cancer lines thus far tested, have been shown to express BAG-1L, in addition to the shorter ubiquitously expressed BAG-1 protein (20). The observation that BAG-1L significantly reduced the net suppressive effects of an anti-androgen on AR-mediated transactivation raises the possibility that overexpression of BAG-1L could provide a selective growth advantage for some prostate cancers during hormone ablation therapy. Although much remains to be learned about the specific mechanisms involved, the observations that (i) BAG-1L markedly enhances androgen-dependent transactivation by AR, (ii) BAG-1L reduces the efficacy of anti-androgens with respect to their suppression of AR-reporter gene transactivation, and (iii) BAG-1L (ΔC) antagonizes AR-mediated transactivation all suggest that further studies of BAG-1 and BAG-1L expression and function in normal and malignant prostate and other androgen-responsive tissues are warranted.

Acknowledgments—We thank Dr. Chawnshang Chang for the AR and ARE-CAT plasmids, Drs. X.-K. Zhang and D. Knee for helpful discussions, and H. Gallant and T. Potter for manuscript preparation.

REFERENCES

1. Parker, S. L., Tong, T., Bolden, S., and Wingo, P. A. (1997) *CA-Cancer J. Clin.* **47**, 5–27
2. Bonkhoff, H., Stein, U., and Remberger, K. (1994) *Prostate* **24**, 114–118
3. Bonkhoff, H., Stein, U., and Remberger, K. (1994) *Hum. Pathol.* **25**, 42–46
4. Soeffing, W. J., and Timms, B. G. (1995) *J. Androl.* **16**, 197–208
5. Evans, G., and Chandler, J. (1987) *Prostate* **11**, 339–351
6. Kyprianou, N., and Isaacs, J. T. (1988) *Endocrinology* **122**, 552–562
7. Crawford, E. D., Eisenberger, M. A., McLeod, D. C., Spaulding, J., Benson, R., Dorr, F. A., Blumenstein, B. A., Davis, M. A., and Goodman, P. J. (1989) *N. Engl. J. Med.* **321**, 419–424
8. Marcelli, M., Tilley, W. D., Zoppi, S., Griffin, J. E., Wilson, J. D., and McPhaul, M. J. (1992) *J. Endocrinol. Invest.* **15**, 149–159
9. McPhaul, M. J., Marcelli, M., Zoppi, S., Griffin, J. E., and Wilson, J. D. (1993) *J. Clin. Endocrinol. Metab.* **76**, 17–23
10. Coetzee, G. A., and Ross, R. K. (1994) *J. Natl. Cancer Inst.* **86**, 872–873
11. Koivisto, P., Kononen, J., Palmberg, C., Tammela, T., Hyytinen, E., Isola, J., Trapman, J., Cleutjens, K., Noordzij, A., Visakorpi, T., and Kallioniemi, O.-P. (1997) *Cancer Res.* **57**, 314–319
12. Visakorpi, T., Hyytinen, E., Koivisto, P., Tanner, M., Keinanen, R., Palmberg, C., Palotie, A., Tammela, T., Isola, J., and Kallioniemi, O. P. (1995) *Nat. Genet.* **9**, 401–406
13. McPhaul, M. J., Marcelli, M., Tilley, W. D., Griffin, J. E., and Wilson, J. D. (1991) *FASEB J.* **5**, 2910–2915
14. Tsai, M. J., and O'Malley, B. W. (1994) *Annu. Rev. Biochem.* **63**, 451–486
15. Anzick, S., Kononen, J., Walker, R., Azorsa, D., Tanner, M., Guan, X., Sauter, G., Kallioniemi, O., Trent, J., and Meltzer, P. (1997) *Science* **277**, 965–968
16. Pratt, W. B., and Welsh, M. J. (1994) *Cell Biol.* **5**, 83–93
17. Shibata, H., Spencer, T. E., Onate, S. A., Jenster, G., Tsai, S. Y., Tsai, M. J., and O'Malley, B. W. (1997) *Recent Prog. Horm. Res.* **52**, 141–164
18. Takayama, S., Sato, T., Krajewski, S., Kochel, K., Irie, S., Millan, J. A., and Reed, J. C. (1995) *Cell* **80**, 279–284
19. Zeiner, M., and Gehring, U. (1995) *Proc. Natl. Acad. Sci. U. S. A.* **92**, 11465–11469
20. Takayama, S., Bimston, D. N., Matsuzawa, S., Freeman, B. C., Aime-Sempe, C., Xie, Z., Morimoto, R. J., and Reed, J. C. (1997) *EMBO J* **16**, 4887–4896
21. Zeiner, M., Gebauer, M., and Gehring, U. (1997) *EMBO J.* **16**, 5483–5490
22. Höhfeld, J., and Jentsch, S. (1997) *EMBO J.* **16**, 6209–6216
23. Landel, C. C., Kushner, P. J., and Greene, G. L. (1994) *Mol. Endocrinol.* **8**, 1407–1419
24. Fang, Y., Fliss, A. E., Robins, D. M., and Caplan, A. J. (1996) *J. Biol. Chem.* **271**, 28697–28702
25. Srinivasan, G., Patel, N. T., and Thompson, E. B. (1994) *Mol. Endocrinol.* **8**, 189–196
26. Takayama, S., Kochel, K., Irie, S., Inazawa, J., Abe, T., Sato, T., Druck, T., Huebner, K., and Reed, J. C. (1996) *Genomics* **35**, 494–498
27. Packham, G., Brimmell, M., and Cleveland, J. L. (1997) *Biochem. J.* **328**, 807–813
28. Glass, C. K., Rose, D. W., and Rosenfeld, M. G. (1997) *Curr. Opin. Cell Biol.* **9**, 222–232
29. Lee, H. J., Kokontis, J., Wang, K. C., and Chang, C. (1993) *Biochem. Biophys. Res. Commun.* **194**, 97–103
30. Mowszowicz, I., Lee, H. J., Chen, H. T., Mestayer, C., Portois, M. C., Cabrol, S., Mauvais-Jarvis, P., and Chang, C. (1993) *Mol. Endocrinol.* **7**, 861–869
31. Miyashita, T., and Reed, J. C. (1995) *Cell* **80**, 293–299
32. Miyashita, T., Harigai, M., Hanada, M., and Reed, J. C. (1994) *Cancer Res.* **54**, 3131–3135
33. Sambrook, J., Fritsch, E. F., and Maniatis, T. (1989) *Molecular Cloning: A Laboratory Manual*, 2nd Ed., Cold Spring Harbor Laboratory, Cold Spring Harbor, NY
34. Nielsen, D. A., Chang, T. C., and Shapiro, D. J. (1989) *Anal. Biochem.* **179**, 19–23
35. Reed, J. C., Meister, L., Tanaka, S., Cuddy, M., Yum, S., Geyer, C., and Pleasure, D. (1991) *Cancer Res.* **51**, 6529–6538
36. Schreiber, E., Matthias, P., Muller, M. M., and Schaffner, W. (1989) *Nucleic Acids Res.* **17**, 6418
37. Krajewski, S., Zapata, J. M., and Reed, J. C. (1996) *Anal. Biochem.* **236**, 221–228
38. Selkirk, J. K., Merrick, B. A., Stackhouse, B. L., and He, C. (1994) *Appl. Theor. Electrophor.* **4**, 11–18
39. Veldscholte, J., Berrevoets, C. A., and Mulder, E. (1994) *J. Steroid Biochem. Mol. Biol.* **49**, 341–346
40. Kemppainen, J. A., Lane, M. V., Sar, M., and Wilson, E. M. (1992) *J. Biol. Chem.* **267**, 968–974
41. Harrison, C. J., Hayer-Hartl, M., Di Liberto, M., Hartl, F.-U., and Kuriyan, J. (1997) *Science* **276**, 431–435

[CANCER RESEARCH 58. 3116–3131. July 15. 1998]

Expression and Location of Hsp70/Hsc-Binding Anti-Apoptotic Protein BAG-1 and Its Variants in Normal Tissues and Tumor Cell Lines[1]

Shinichi Takayama, Stanislaw Krajewski, Maryla Krajewska, Shinichi Kitada, Juan M. Zapata, Kristine Kochel, Deborah Knee, Dominic Scudiero, Gabriella Tudor, Gary J. Miller, Toshiyuki Miyashita, Masao Yamada, and John C. Reed[2]

The Burnham Institute, La Jolla, California 92037 [S. T., S. Kr., M. K., S. Ki., J. M. Z., K. K., D. K., J. C. R.]; Science Applications International Corporation Frederick, National Cancer Institute-Frederick Cancer Research & Development Center, Frederick, Maryland 21702 [D. S., G. T.]; University of Colorado Health Science Center, Department of Pathology, Denver, Colorado 80262 [G. J. M.]; and The National Children's Medical Research Center, Department of Genetics, Tokyo 154, Japan [T. M., M. Y.]

ABSTRACT

BAG-1 is a multifunctional protein that blocks apoptosis and interacts with several types of proteins, including Bcl-2 family proteins, the kinase Raf-1, certain tyrosine kinase growth factor receptors, and steroid hormone receptors, possibly by virtue of its ability to regulate the Hsp70/Hsc70 family of molecular chaperones. Two major forms of the human and mouse BAG-1 proteins were detected by immunoblotting. The longer human and mouse BAG-1 proteins (BAG-1L) appear to arise through translation initiation at noncanonical CTG codons located upstream of and in-frame with the usual ATG codon used for production of the originally described BAG-1 protein. Immunoblotting experiments using normal tissues revealed that BAG-1L is far more restricted in its expression and is present at lower levels than the more prevalent BAG-1 protein. Human but not mouse tissues also produce small amounts of an additional isoform of BAG-1 of intermediate size (BAG-1M) that probably arises through translation initiation at yet another site involving an ATG codon. All three isoforms of human BAG-1 (BAG-1, BAG-1M, and BAG-1L) retained the ability to bind Hsc70. Subcellular fractionation and immunofluorescence confocal microscopy studies indicated that BAG-1L often resides in the nucleus, consistent with the presence of a nuclear localization sequence in the NH_2-terminal unique domain of this protein. In immunohistochemical assays, BAG-1 immunoreactivity was detected in a wide variety of types of cells in normal adult tissues and was localized to either cytosol, nucleus, or both, depending on the particular type of cell. In some cases, cytosolic BAG-1 immunostaining was clearly associated with organelles resembling mitochondria, consistent with the reported interaction of BAG-1 with Bcl-2 and related proteins. Furthermore, experiments using a green fluorescence protein (GFP)-BAG-1 fusion protein demonstrated that overexpression of Bcl-2 in cultured cells can cause intracellular redistribution of GFP-BAG-1, producing a membranous pattern typical of Bcl-2 family proteins. The BAG-1 protein was found at high levels in several types of human tumor cell lines among the 67 tested, particularly leukemias, breast, prostate, and colon cancers. In contrast to normal tissues, which only rarely expressed BAG-1L, tumor cell lines commonly contained BAG-1L protein, including most prostate, breast, and leukemia cell lines, suggesting that a change in BAG-1 mRNA translation frequently accompanies malignant transformation.

INTRODUCTION

The BAG-1 protein was originally identified as a novel regulator of apoptosis by virtue of its ability to bind Bcl-2, a potent blocker of cell death (1). In gene transfer experiments using cultured cells, overexpression of BAG-1 can collaborate with Bcl-2 in suppressing apoptosis induced via CD95 (Fas/APO-1), the general kinase inhibitor staurosporine, withdrawal of survival factors from media, thymidine excess, and chemotherapeutic drugs (1–4). Overexpression of BAG-1 by itself has also been reported to inhibit or delay cell death caused by growth factor deprivation, heat shock, and p53, in at least some types of cells (1, 2, 5, 6).

Recently, BAG-1 has been reported to form complexes with several proteins, including the protein tyrosine kinase growth factor receptors for HGF[3] (scatter factor) and PDGF (7). The BAG-1 binding site in the cytosolic domain of the HGF-R appears to be required for the generation of signals by this receptor that promote cell survival. In addition, overexpression of BAG-1 has been shown to increase the metastatic potential of tumor cells *in vivo*.[4] This finding could be relevant either to the effects of BAG-1 on HGF-R, which increases cell motility (8), or to its general ability to prevent cell death, because epithelial cells undergo apoptosis when detached from extracellular matrix unless protected by anti-apoptosis proteins (9).

The expression of BAG-1 is up-regulated by some growth factors such as IL-2, IL-3, and prolactin, suggesting a role for this protein in growth factor receptor generated signals for cell survival or proliferation (2, 10). Moreover, gene transfer-mediated elevations in BAG-1 protein levels have been shown to prolong the survival of fibroblastic and hematopoietic cell lines when deprived of growth factors (1, 2) as well as neuronal cells deprived for neurotrophins (3). In an IL-3-dependent hemopoietic cell line, enforced expression of BAG-1 not only promoted cell survival but also allowed for factor-independent cell growth (2). Of potential relevance to this observation, BAG-1 can form complexes with the serine/threonine protein kinase Raf-1, causing elevations its enzymatic activity through a Ras-independent mechanism (11).

Although many details are presently lacking, the diversity of proteins with which BAG-1 interacts may be attributable to its ability to bind and modulate the activities of the 70-kDa family of molecular chaperones, including Hsp70 and Hsc70 (5). BAG-1 therefore may represent a novel component of the chaperone system that modulates interactions of Hsp70/Hsc70 with other proteins, inducing alterations in the conformations of these target proteins and thereby altering their biochemical and biological activities in cells. In this regard, BAG-1 appears to function analogous to GrpE, the bacterial ADP-ATP exchange protein that collaborates with DnaK, the bacterial equivalent of Hsp70 in prokaryotes (12). Indeed, the predicted human and murine BAG-1 proteins share 17 and 19% amino acid identity and 28 and 30% amino acid similarity with bacterial GrpE. The human and mouse

Received 8/7/97; accepted 5/18/98.

The costs of publication of this article were defrayed in part by the payment of page charges. This article must therefore be hereby marked *advertisement* in accordance with 18 U.S.C. Section 1734 solely to indicate this fact.

[1] This work was supported by Grant CA67329 from the NIH/National Cancer Institute. J. M. Z. was a recipient of a fellowship from the Fulbright/Spaniard Ministry of Education and Science and is presently supported by funds provided by the Breast Cancer Fund of the State of California through the Breast Cancer Research Program of the University of California (#3FB-0093). D. K. is a recipient of a fellowship from the Susan B. Komen Foundation, as well as a Wellcome Travel Grant.

[2] To whom requests for reprints should be addressed, at The Burnham Institute, 10901 North Torrey Pines Road, La Jolla, CA 92037. Phone: (619) 646-3140; Fax: (619) 646-3194; E-mail: jreed@burnham-inst.org.

[3] The abbreviations used are: HGF, hepatocyte growth factor; HGF-R, HGF receptor; IL, interleukin; GST, glutathione *S*-transferase; ORF, open reading frame; PDGF, platelet-derived growth factor; PDGF-R, PDGF receptor; KLH, keyhole limpet hemocyanin; PMSF, phenylmethylsulfonyl fluoride; NLS, nuclear localization sequence; bFGF, basic fibroblast growth factor; ER, estrogen receptor.

[4] A. Yawata, M. Adachi, H. Okuda, Y. Naishiro, A. Takamura, S. Takayama, J. C. Reed, and K. Imai. Prolonged cell survival enhances peritoneal dissemination of gastric cancer cells, Oncogene, in press.

BAG-1 proteins also contain a ubiquitin-like domain near their NH_2-terminal, although the functional significance of this region of BAG-1 is presently unknown (1, 13).

Recently, alternative forms of the BAG-1 protein have been reported to arise through translation initiation at different sites within the BAG-1 mRNA (14). One of these isoforms of BAG-1, which has been termed RAP46, has been shown to bind several steroid hormone receptors (15). Although the functional significance of these interactions are still being defined, the findings suggest a role of some isoforms of the BAG-1 protein in regulating nuclear proteins, in addition to cytosolic proteins.

Given the capacity of BAG-1 to promote cell survival and its penchant for augmenting the bioactivities of several proteins known to be important for tumorigenesis (*e.g.*, Bcl-2, Raf-1, HGF-R, and PDGF-R), BAG-1 can be regarded as a candidate proto-oncogene that we hypothesize may become overexpressed in certain types of tumors. To provide information about the regulation of BAG-1 protein production, therefore, we generated monoclonal antibodies against the human BAG-1 protein and used them for assessing the expression of this protein in normal human tissues and a panel of 67 human tumor lines.

MATERIALS AND METHODS

Monoclonal Antibody Preparation. Bcl-2 transgenic mice (line B6; Ref. 10) were immunized without adjuvants at 4–6 weeks of age using s.c. and i.p. injections of purified GST-BAG-1 protein encoding the last 170 amino acids of the human BAG-1 protein (500 μg of total protein). Animals were boosted four times at 1–2-week intervals with ~400 μg of GST-BAG-1 protein, and spleens were harvested 3 days after the last immunization. Splenocytes were fused with SP/02 cells, and hybridoma selections were performed in 96-well plates, as described (11). Primary screening of hybridomas was accomplished by ELISA, using GST-BAG-1 protein. Of ~1100 hybridomas screened, 51 were positive. Of these, 28 were found to react with GST-BAG-1 but not GST control protein in a secondary ELISA screen. Ten hybridomas, which reacted specifically with BAG-1 protein on immunoblots, were obtained and isotyped (eight IgG1; two IgG2b). Four of these also immunoprecipitated BAG-1 protein and were used for this study: clones KS-6C8, KS-5A6, KS-10B6, and KS-13A10. Ascites was produced in pristane-primed Balb/c mice.

Antiserum Preparation. Polyclonal antisera 1680 and 1735 were generated using a GST-mouse-BAG-1 (8-219) fusion protein (1) and a synthetic peptide NH_2-CNERYDLLVTPQQNSEPVVQD-amide representing amino-acids 26-45 of the mouse BAG-1 protein, respectively. The peptide was synthesized with an NH_2-terminal cysteine to facilitate conjugation to maleimide-activated carrier proteins KLH and OVA (Pierce, Inc.) as described previously (16). New Zealand White female rabbits were injected s.c. with either 0.25 ml of GST-BAG-1 (0.5 mg/ml) or a combination of 0.25 ml each of KLH-peptide (1 mg/ml), and OVA-peptide (1 mg/ml) mixed in an equal volume of Freund's complete adjuvant (dose divided over 10 injection sites) and then boosted three times at weekly intervals, followed by another four to eight times at monthly intervals with 0.25 mg of either GST-BAG-1 or 0.25 mg each of KLH-peptide and OVA-peptide immunogens in Freund's incomplete adjuvant before collecting blood and obtaining immune serum. The generation and characterization of a rabbit anti-mouse BAG-1 antiserum targeted against amino acids 204-219 have been described (1).

Immunoblotting. For most experiments, cells were lysed in RIPA buffer (16) containing both protease inhibitors (1 mM PMSF, 0.28 TIU/ml aprotinin, 50 μg/ml leupeptin, 1 mM benzamidine, and 0.7 μg/ml pepstatin) and phosphatase inhibitors (5 mM NaF, 2 mM sodium orthovanadate, 10 mM sodium β-glycerophosphate, 2 mM sodium pyrophosphate, 50 mM *p*-nitrophenylphosphate, and 1 μM microcystin LR). Aliquots containing 50 μg of total protein were subjected to SDS-PAGE using 12% gels, followed by electro-transfer to nitrocellulose (0.45 μm) filters. Immunodetection was accomplished using 1:1000 (v/v) dilutions of monoclonal antibody ascites or rabbit antisera, followed by appropriate secondary antibodies and ECL-based detection as described (17). For correlations with the NCI 60 tumor cell line database, data on X-ray films were quantified by scanning densitometry using the IS-1000 image analysis system (Alpha Innotech, Inc.). After collecting data for the entire panel of tumor cell lines on several immunoblot filters, residual lysates from two representative tumor lines per blot were re-analyzed together in the same blot along with a standard curve created by using GST-hu-BAG-1 protein (1–20 ng/lane). The scanning densitometry results from the GST-BAG-1 standard-containing blot were used to normalize all data before estimating the ng of BAG-1 protein per 50 μg of total protein. Data from two independent GST-BAG-1 standard-containing blots were within 20% agreement.

Immunohistochemistry. Tissues for immunohistochemical analysis were derived either from human biopsy and autopsy material or normal adult Balb/c mice. Tissues were fixed in either neutral-buffered formalin, B5, Z-Fix (Anatech. Inc.), or Bouin's solution (Sigma Chemical Co., Inc.), embedded in paraffin, and sectioned (5 μm). For experiments with rabbit polyclonal antibodies directed against the mouse BAG-1 protein, an ABC/diaminobenzidine-based detection method was used, as described in detail (18–20). Typically, the dilution of anti-mBAG-1 polyclonal antiserum used was 1:500 or 1:1000 (v/v). For immunostaining of human tissues, the ascites form of anti-huBAG-1 murine monoclonal antibodies was diluted 1:200 (v/v) and detected using a streptavidin-based enhancement method [LSAB (+) kit (Dako, Inc., Santa Barbara, CA)]. Nuclei were counterstained with either hematoxylin or methyl green.

For all mouse tissues examined, the immunostaining procedure was performed in parallel using preimmune sera. In some cases, the antisera were preadsorbed with 5–10 μg/ml of the synthetic peptide immunogen, thus providing an additional control for immunospecificity. When using the anti-human BAG-1 monoclonal antibodies, an irrelevant mouse IgG1 monoclonal (Dako) was used as a specificity control for all experiments. Occasionally, preadsorption of monoclonal antibodies with GST-BAG-1 protein was also used to assess the specificity of immunostaining. The immunostaining results were arbitrarily scored according to intensity as: 0, negative; 1^+, weak; 2^+, moderate; and 3^+, strong to very strong. Results presented for each tissue were based on consensus from immunohistochemical analysis of multiple slides.

Laser Scanning and Fluorescence Confocal Microscopy. Some of the same immunostained paraffin sections counterstained with methylgreen and used for conventional light microscopy were examined by laser scanning microscopy. For these studies, a Zeiss conventional light microscope equipped with a argon-ion laser (488-nm emission) (LSM-10) was utilized in differential interference contrast mode, essentially as described (21). Plan-apochrome ×40 dry and ×63 oil objective lenses were used. Black and white images were derived through electronic processing methods, which enhance the positive reaction signals by contrast normalization using a scaling density. Final images were printed using Adobe Photoshop software and a laser printer.

For studies involving GFP, fluorescence images were obtained using a confocal laser scanning microscope (model GB-200; Olympus, Tokyo, Japan) equipped with a triple-line Kr/Ar laser with excitation at 488 nm and detection at 500 to 530 nm bandpass.

cDNA Cloning. The human BAG-1 cDNA clones used for these studies have been described (13). The mouse BAG-1 cDNA clone SN245-9 (1) was used as a hybridization probe for screening a mouse λgt-10 kidney library, resulting in the cDNA clone SN285-13, which contains 114 bp of sequence upstream of the originally described ORF. Additional 5′ sequence data were obtained from a mouse EST clone AA15486 and from comparisons with a mouse genomic clone, which was obtained by screening a λ-FixII 129 SVJ library (Stratagene, Inc.).

Plasmid Constructions. The 1290-bp human BAG-1 cDNA pKK240 (14), which spans −390 to 880 bp relative to the AUG start codon, was subcloned into the *Eco*RI site of pcDNA3 (Invitrogen, Inc.), creating the plasmid pKK-241-1. To produce BAG-1M protein, a version of this pcDNA3-BAG-1 expression plasmid lacking most of the sequences upstream of the alternative AUG start codon at −132 bp relative to the usual BAG-1 ORF was prepared by digestion with *Sac*II and *Bam*HI, thus discarding a 256-bp fragment that was separated from the plasmid by agarose gel electrophoresis (*Sac*II is located immediately upstream of the ATG (*CCGCGG*ATGA) in the pKK240 BAG-1 cDNA; the *Bam*HI site resides within the multiple cloning site of pcDNA3). After gel purification of the residual plasmid band and blunting the ends using T4 DNA polymerase with deoxynucleotide triphosphates, the plasmid was recircularized using T4 DNA-ligase to create pSN670-2, which was transformed into XL-1 blue bacteria (Stratagene, Inc). Mutants of hu-BAG-1, in which the CTG codons at −345 and −297 were converted to ATG, were

prepared by PCR using pKK241-1 as a template and the mutagenic forward primers 5′-gggaattcAGTGCGGGC*ATG*GCTC-3′ or 5′-gggaattcGAGCGG*AT-G*GGTTCCCG-3′ together with the reverse primer 5′-GCGCTCGAGCTCG-GCCAGGGCAAAG-3′. After digestion of the *Eco*RI and *Xho*I sites in the forward and reverse primers, respectively, the resulting ~1.0-kbp fragments were subcloned into *Eco*RI/*Xho*I-digested pcDNA3, creating the plasmids pSN 815-2 and pSN 815-4.

For expression or *in vitro* translation of mouse BAG-1 proteins, the plasmid pRc/CMV-S33 (1), which encodes the murine 219-amino acid BAG-1 protein, was used. In addition, a longer BAG-1 cDNA (SN285-13) was subcloned into the *Eco*RI site of pSKII.

For expression of GST-huBAG-1 fusion proteins in bacteria, a partial BAG-1 cDNA (hs33-2) that had been obtained from a λgt-11 human breast library and that encodes the last 182 amino acids of the huBAG-1 protein (13) was subcloned in-frame with the GST-encoding sequences in pGEX-3X (Pharmacia, Inc.) using a PCR approach. Briefly, the hs33-2 cDNA was subcloned into the *Eco*RI site of pSK-II (Strategene, Inc.), and this plasmid was used as a template for PCR amplication with the *Bam*HI-containing forward primer 5′-GGGGATCCGTGAACCAGTTGTCCA-3′ and the reverse primer 5′-CTACACCTCACTCGGCCAGG-3′. The resulting PCR product was digested with *Bam*HI and *Bgl*II, gel-purified by gel electrophoresis in 1% Nusieve agarose, and subcloned into the *Bgl*II site of pSKII-hs33-2, which had been prepared by digestion with *Bgl*II and *Bam*HI, thus fusing the PCR product that encodes amino acids 52-171 of huBAG-1 with the distal portion of the huBAG-1 ORF encoding residues 172–230 and creating the plasmid pKK169. After confirming the correct nucleotide sequence, huBAG-1 was excised from pKK169 with *Bam*HI and *Eco*RI and subcloned into the corresponding sites in pGEX-3X, creating the plasmid pKK170. Additional GST-BAG-1 deletion mutants of pKK170 were also prepared using pKK169 and then subcloning into pGEX-3X, including: (*a*) pKK170-2, which encodes residues 132–221 of huBAG-1 (deletion of COOH-terminal 9 amino acids relative to pKK-170) by digestion of pKK169 with *Bam*HI and *Pst*I; (*b*) pKK173-1, which encodes that last 99 amino acids of huBAG-1 (132–230) by digestion of pKK169 with *Pvu*II and *Eco*RI; and (*c*) pKK-173-2, which encodes residues 52–131 (Δ COOH-terminal 99 amino acids relative to pKK170) by digestion of pKK169 with *Pvu*II and *Pst*I.

To generate a plasmid producing GFP-BAG-1, the mouse BAG-1 cDNA SN245-9 in pSKII (1) was amplified by the PCR using forward primer 5′-GGAATTCCAAGACCGAGGAGAT-3′ and reverse primer 5′-CGG-GATCCAGGGCCAAGTTTGTA-3′, which have *Eco*RI and *Bam*HI linkers, respectively. The amplified product was digested with *Eco*RI and *Bam*HI, gel-purified, and subcloned into pEGFP-C1 (Clontech).

GST-Fusion Protein Production. The pKK170 plasmid encoding GST hBAG-1(52–230) was transformed into XL-1 blue *Escherichia coli* strain (Stratagene, Inc.). After overnight culture in LB with 50 μg/ml ampicillin, 2 ml of culture were transferred to 1 liter of Luria Burton-ampicillin media and grown at 37°C until the *A*600 reached ~1.0, then grown overnight at room temperature with 0.1 mM isopropyl-1-thio-β-D-galactopyranoside. Cells were then recovered by centrifugation and resuspend in 10 ml of 1× PBS (pH 7.4) containing 1% Triton X-100 and 1 mM PMSF. After freeze-thawing once, the suspension was sonicated twice on ice using a 5-mm diameter probe (Heat Systems, Inc.) at medium intensity (level 5 of 10) for 2 min. After centrifugation at ~10,000 × *g* for 20 min at 4°C, the resulting supernatant was mixed with ~2 ml of glutathione-Sepharose beads (packed volume) and rotated at 4°C for 2 h in a capped 15-ml polypropylene tube. After washing three times in the same PBS/Triton X-100 solution, 10 ml of elution buffer (10 mM glutathione and 10 mM Tris, pH 8.0) was added to the beads, and the supernatant containing GST-BAG-1 protein was recovered after 20 min at room temperature by centrifugation and dialyzed against PBS. Protein concentrations were estimated by Coomasie Blue staining of material in SDS-PAGE gels containing BSA standards.

Hsc70 Binding Assays. GST-Hsc70 (ATPase domain) and GST-CD40 (cytosolic domain) fusion proteins were produced and affinity-purified as described (5). Fusion proteins were then mixed at ~0.5–1.5 μg/μl of glutathione-Sepharose (packed volume) in binding buffer [10 mM HEPES (pH 7.5), 138 mM KCl, 2 mM EGTA, 5 mM $MgCl_2$, and 0.2% NP40 with 5% (w/v) BSA]. After washing the beads three times with the same solution to remove unbound GST fusion proteins, 5 μl of *in vitro* translation reactions in 95 μl of binding buffer were added to 15–20 μl of GST-beads, and the samples were nutated at 4°C for 2 h. Beads were washed three times in ice-cold binding buffer and resuspended in 20 μl of Laemmeli sample buffer, boiled, and analyzed by SDS-PAGE (12% gels). Gels were washed with ddH_2O and fixed in 10% acetic acid/25% isopropanol solution for 20 min, followed by 1.1 M sodium salicylate for 20 min, then dried and exposed to X-ray film.

***In vitro* Translations.** Proteins were translated *in vitro* in the presence or absence of [^{35}S]L-methionine (EASYTAG S.A.; ≈1,000 Ci/mmol; New England Nuclear, Inc.) using the TNT lysate kit and T7 RNA polymerase with 1 μg of pcDNA3 or pSKII-based plasmids in a total volume of 50 μl, according to the manufacturer's recommendations (Promega, Inc.).

RNA Blot Analysis. Total cellular RNA was prepared from 5 × 10^7 cells using an acidic-phenol/guanidine thiocyanate method (22, 23). RNA (10 μg/lane) was size-fractionated by gel electrophoresis in 1% agarose gels containing glyoxal and then transferred to nylon membranes (Zetaprobe; BioRad, Inc.) by a semidry downward capillary method using alkaline transfer buffer (22), followed by UV cross-linking (2400 joules; Stratalinker; Stratagene, Inc.). Blots were prehybridized in 1% SDS, 1 M NaCl, and 10% dextran sulfate, at 60°C for 1 h, followed by hybridization in the same solution containing 100 μg/ml of denatured, sheared, salmon sperm DNA and ~2 ng/ml of ^{32}P-labeled probe, which was prepared by a random priming method (Boehringer-Mannheim, Inc.) using a gel-purified mouse BAG-1 cDNA SN245-9 (1). Blots were washed twice in 2× SSC (24) at ambient temperature for 5 min and then twice in 2× SSC with 1% SDS at 60°C for 30 min, and then finally in 0.1× SSC at room temperature for 10–60 min, before exposure to X-ray film (Kodak, Inc.) using intensifying screens at −80°C.

Subcellular Fractionations. Nuclear and nonnuclear fractions were prepared according to the method of Hennighausen and Lubom (24). Briefly, ~1–5 × 10^7 cells were washed twice in ice-cold PBS and resuspended on ice in 0.5 ml of homogenization buffer [10 mM HEPES (pH 7.2), 10 mM KCl, 1.5 mM $MgCl_2$, 0.4% NP40, 0.3 M sucrose, 0.1 mM EGTA, 0.5 mM DTT, 0.5 mM PMSF, 2.5 mM benzamidine, 10 μg/ml aprotinin, and 5 μg/ml leupeptin]. After disrupting cells with 10–20 strokes of a Dounce homogenizer using a B pestle and verifying complete lysis by phase-contrast microscopy, 0.1-ml aliquots of the lysate were centrifuged at 350 × *g* for 5 min at 4°C in a swinging-bucket rotor to pellet nuclei. The nuclei were then washed twice in the same buffer and finally resuspended in RIPA buffer (16). The postnuclear supernatant was cleared by centrifugation at 16,000 × *g* for 2–3 min before storing at −80°C. Fractions were normalized for either cell-equivalents or total protein content based on the bicinchoninic acid method (Pierce, Inc.) before SDS-PAGE/immunoblot assay.

Cell Transfections. Rat-1 fibroblasts were transfected by a calcium phosphate DNA precipitation method at ~70% confluence in 10-cm diameter dishes. The culture medium (10 ml of DMEM with 10% fetal bovine serum) was changed 4 h before transfection with 10 μg of plasmid DNA that had been resuspended in 438 μl of ddH_2O, supplemented with 62 μl of 2 M $CaCl_2$/10 mM HEPES (pH 5.8), and then added dropwise to 500 μl of 2× HBSS [40 mM HEPES (pH 7.05), 275 mM NaCl, 10 mM KCl, 1.4 mM Na_2HPO_4, and 12 mM glucose]. The DNA-calcium-phosphate precipitate was removed after 8–12 h and replaced with fresh medium.

HeLa cells were seeded at 7 × 10^5 per 60-mm plate on the day before transfections. Cells were transfected with a total of 3 μg of DNA (pEGFP-mBAG-1 in combination with either pRc/CMV or pRc/CMV/Bcl-2 at a 1:2 molar ratio) using 15 μg of lipofectin (Life Technologies, Inc.) and 3 ml of OPTI-MEM I (Life Technologies, Inc.). After 6 h, the cells were recovered by trypsinization and seeded into glass-bottomed culture dishes (MatTek Corp., Ashland, MA) and returned to culture in DMEM/10% serum medium for 2 days.

RESULTS

Production and Characterization of BAG-1 Monoclonal Antibodies: Identification of Several BAG-1 Isoforms in Human Tissues. Immunoblot analysis was undertaken using whole-cell lysates derived from a variety of human tissues using anti-huBAG-1 monoclonal antibodies. Detailed comparisons of three independent anti-human BAG-1 monoclonal antibodies (KS-6C8, KS-10B6, and KS-5A6) demonstrated essentially identical patterns of reactivity with proteins in these tissue lysates, although data are shown here only for the KS-6C8 antibody

(Fig. 1). The epitope on BAG-1 detected by KS-6C8 was mapped to residues 132–221, whereas KS-5A6 and KS-10B6 bound to residues 52–131, based on immunoblot analysis of a panel of GST-BAG-1 fusion proteins (see "Materials and Methods").

All three anti-BAG-1 antibodies detected several proteins in certain tissues, in addition to the anticipated ~36 kDa BAG-1 protein originally predicted from cDNA cloning. Ovary and testis, for example, contained a ~56–57 kDa isoform of BAG-1, as well as small amounts of an additional ~52–53 kDa protein (Fig. 1). Many tumor cell lines also contained these ~52–53 and ~56–57 kDa BAG-1 bands, in addition to the expected ~36 kDa BAG-1 protein (see below). Lysates derived from peripheral blood mononuclear cells and tonsils uniquely contained still other anti-BAG-1 immunoreactive bands of ~37–38 kDa, which may represent phosphorylated forms of the major ~36 kDa BAG-1 protein.[5] Note that in contrast to the larger ~52–57 kDa and ~37–38 kDa forms of BAG-1, the predicted ~36 kDa BAG-1 protein was ubiquitously present throughout most human tissues, although liver, colon, breast, and uterine myometrium contained comparatively little of this protein.

Immunoblot analysis of murine tissues similarly revealed widespread expression of a ~30 kDa protein corresponding to BAG-1 (Fig. 1*B*), indicating that this is by far the most abundant isoform of the protein *in vivo*. However, several mouse tumor cell lines contained a ~50 kDa anti-BAG-1 immunoreactive band, in addition to the ~30 kDa originally described isoform of BAG-1. Of note, the pattern of anti-BAG-1 immunoreactive bands was less complex in murine compared with human tissues (discussed below).

In contrast to the variety of BAG-1 proteins seen in tissues, BAG-1 mRNAs were homogeneous with only one species identified by Northern blotting. A survey of several tissues derived from mice, for example, revealed the presence of a single transcript of ~1.8 kbp (Fig. 2*A*). Note that all tissues tested contained BAG-1 mRNA, although liver had the least relative amounts of BAG-1 mRNA, which required longer exposures to clearly visualize. Human cell lines also contained a single BAG-1 mRNA of ≈1.9 kbp (Fig. 2*B* and data not shown).

BAG-1 Isoforms Arise by Alternative Translation Initiation Site Usage within a Common BAG-1 mRNA. The presence of ~52–57 kDa bands reacting with three different anti-BAG-1 monoclonal antibodies suggested the presence of isoforms of this protein that arise by alternative mRNA splicing. However, exhaustive efforts to clone cDNAs encoding alternative forms of human and mouse BAG-1 proved fruitless. Inspection of the longest human and murine BAG-1 cDNAs cloned previously in our laboratory revealed an absence of stop codons upstream of the predicted ORFs encoding the most prevalent isoform of the human and mouse BAG-1 proteins, estimated to be 230 and 219 amino acids in length, respectively. Moreover, an additional upstream and in-frame ATG codon was found in the human BAG-1 mRNA, which would extend the ORF by 44 amino acids, leading to production of a 274-amino acid protein (Fig. 3). Recently, it has been suggested that this longer isoform of the human BAG-1 protein is identical to RAP46, a protein that binds steroid hormone receptors (15, 16). However, an analogous ATG codon was not found in the murine BAG-1 cDNAs (Fig. 3), implying that additional mechanisms must exist for generating longer isoforms of the BAG-1 protein.

Although no in-frame ATG codons are found in murine BAG-1 cDNAs, three upstream and in-frame CTG codons are present at positions −408, −360, and −336 bp relative to the ATG start codon of the originally described ORF. Similarly, the region 5′ of the human BAG-1 ORF contains analogous CTG codons at positions −345, −297, and −273. CTG codons are occasionally used as an alternative to ATG for translation initiation in eukaryotic mRNAs (25, 26). Among these upstream, in-frame CUG codons, however, only the most 5′ CUGs in the predicted human and mouse BAG-1 mRNAs are within an optimal context for translation initiation, with purines at −3 and a guanosine (G) at +4 relative to the CUG (where the C is +1; Refs. 25 and 26). Genomic cloning confirmed the absence of introns between the previously described ORF and this 5′ region in the mouse *BAG-1* gene (not shown).

To explore the possibility that the murine BAG-1 cDNA containing this 5′-untranslated region where the CTG codons reside could encode both the usual 219-amino acid BAG-1 protein plus a longer protein that might account for the ~50 kDa form of mouse BAG-1 seen by immunoblot analysis of murine tissues, a mouse BAG-1 cDNA containing this 5′-untranslated region was subcloned downstream of the T7 RNA polymerase in pSKII and *in vitro* transcribed and translated using reticulocyte lysates. Comparisons were made with a mouse BAG-1 cDNA that contained the usual ORF but which lacked this 5′

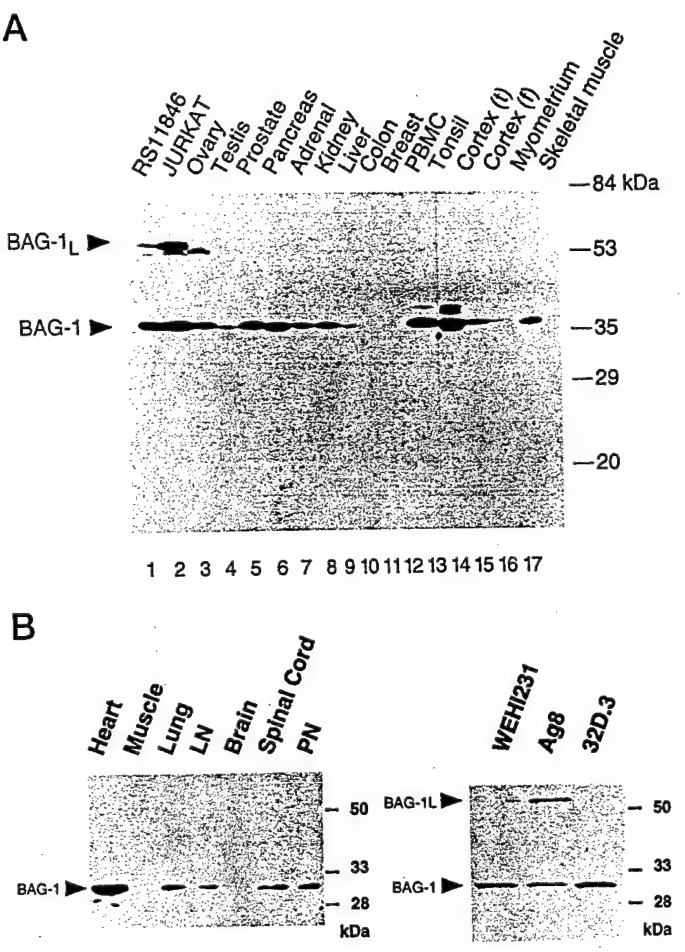

Fig. 1. Immunoblot analysis of BAG-1 proteins in tissues. In *A*, human tissue lysates were prepared and normalized for total protein content (50 μg/lane) before analysis by SDS-PAGE/immunoblot assay using the anti-human BAG-1 monoclonal antibody KS-6C8. Essentially identical results were obtained with two other independent monoclonal antibodies. *Arrowheads*, positions of the ~36-kDa BAG-1 and ~53–57-kDa higher molecular weight forms of BAG-1 proteins (*BAG-1L*). A ~38-kDa BAG-1 band seen in peripheral blood mononuclear cells (*PBMC*) and tonsil (*Lanes 13* and *14*) may represent a phosphorylated form BAG-1.[5] Both temporal (*t*) and frontal (*f*) brain cortex were analyzed (*Lanes 15* and *16*). Reprobing of the same blot with antibodies to other proteins such as tubulin and Bax confirmed that all samples contained intact proteins that appeared to be present in roughly equivalent amounts, with the exception of testis which was underloaded in this particular blot (not shown). In *B*, immunoblot results for a few representative mouse tissues (*left panel*) and mouse tumor cell lines (*right panel*) are presented. All samples were normalized for total protein content (50 μg/lane).

[5] Unpublished observations.

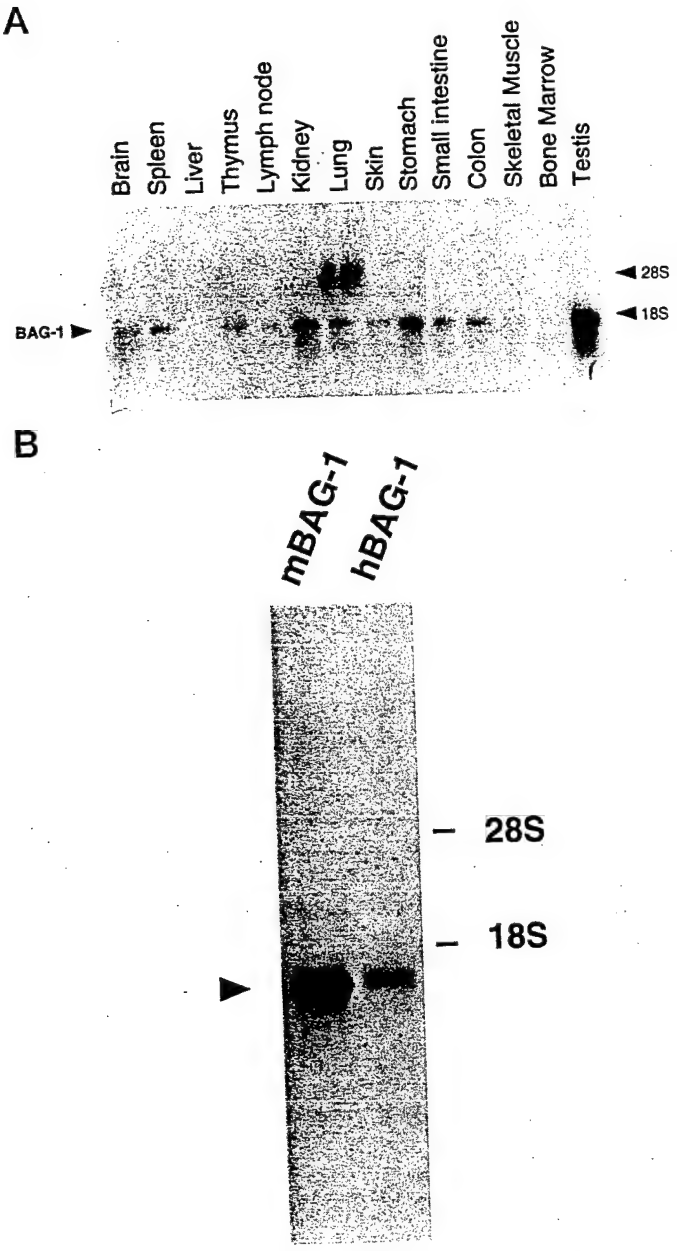

Fig. 2. RNA blot analysis of BAG-1 mRNA in tissues. Total cellular RNA was isolated from various mouse tissues (*A*) or from mouse S49.1 and human Jurkat T-cell leukemia cell lines (*B*) and analyzed by RNA blotting (20 μg/lane) using a ^{32}P-labeled muBAG-1 cDNA probe. Loading of approximately equivalent amounts of intact RNA was confirmed by visualization of the 28S and 18S rRNA bands in ethidium-stained gels (not shown). *Arrowheads*, positions of the ~1.8-kbp mouse and ~1.9-kbp human BAG-1 mRNAs.

region. The resulting *in vitro* translation products were then analyzed by SDS-PAGE/autoradiography (Fig. 4*A*) or by immunoblotting using a BAG-1 specific anti-peptide antiserum (not shown). As shown in Fig. 4*A*, *in vitro* translation of the mouse BAG-1 cDNA that lacked the upstream CTG containing region generated the expected ~29–30 kDa BAG-1 protein. In contrast, *in vitro* translation of the mouse BAG-1 cDNA that contained the 5′ upstream region resulted in the production of two BAG-1 immunoreactive proteins of 50 kDa and 29–30 kDa. No similar ^{35}S-labeled proteins or BAG-1 immunoreactive bands were observed when reticulocyte lysates were primed with pSK-II or pcDNA3 plasmids lacking BAG-1 cDNA inserts (not shown).

A similar result was obtained when human BAG-1 cDNAs were *in vitro* translated, except that the additional in-frame ATG codon generated another isoform of BAG-1, consistent with a recent report (14). For example, when a human BAG-1 cDNA, which contains both the originally described ORF plus the upstream in-frame ATG, was *in vitro* translated and the products were analyzed by either SDS-PAGE/autoradiography (Fig. 4*A*) or immunoblotting using an anti-BAG-1 monoclonal antibody (not shown), the anticipated ~36 kDa BAG-1 protein was observed as well as a longer ~52 kDa BAG-1 immunoreactive protein. Moreover, when a longer human BAG-1 cDNA was used that contains the 5′ in-frame CTG codons mentioned above, the predominant protein produced was a ~56–57 kDa BAG-1 immunoreactive band, with only very small amounts of translation initiation from the usual downstream ATG which generates the ~36 kDa BAG-1 protein and essentially none of the ~52 kDa protein predicted to arise from the 5′ in-frame ATG codon (Fig. 4*A*). Finally, comparisons were made with a human BAG-1 cDNA in which the first of the candidate noncanonical CTG start codons was mutated to ATG, thus forcing translation from this upstream site. As shown in Fig. 4*A*, *in vitro* translation of the human BAG-1 CTG→ATG mutant generated predominantly a ~56–57 kDa band, suggesting that the first CTG is the most likely site of translation initiation for generation of the ~56–57 kDa isoform of BAG-1. This ~56–57 kDa protein comigrated precisely in gels with the endogenous BAG-1 proteins seen in human tumor cell lines (see below). In contrast, the *in vitro* translation product derived from a BAG-1 cDNA in which the next CTG downstream was mutated to ATG resulted in a protein that migrated slightly faster in SDS-PAGE compared with the endogenous 56–57 kDa BAG-1 protein (not shown). None of the various ^{35}S-labeled proteins shown in Fig. 4 were observed when reticulocyte lysates were primed with control pSKII plasmid DNA, confirming the specificity of these results. We have designated the longer isoforms of human (~56–57 kDa) and mouse (~50 kDa) BAG-1 proteins that appear to arise from translation at noncanonical CTG codons as "BAG-1-long" (BAG-1L), and the intermediate length human BAG-1 protein which presumably arises from the in-frame upstream ATG codon as "BAG-1 medium" (BAG-1M).

To further verify that these proteins observed in the *in vitro* translation experiments corresponded to the BAG-1 immunoreactive species identified by immunoblot analysis of tissues, *in vitro* translated proteins were compared side-by-side in gels with the cell-derived BAG-1 proteins that either arise naturally in some cell lines or that were produced by gene transfection. For these experiments, a human BAG-1 cDNA that includes the 5′ upstream region where the CTG codons reside and the ORFs for BAG-1 and BAG-1M was *in vitro* translated, giving rise to a prominent ~56–57 kDa BAG-1L product and less abundant amounts of ~52 kDa BAG-1M and ~36 kDa BAG-1. These bands comigrated in SDS-PAGE with BAG-1 immunoreactive bands seen in some tumor cell lines such as Jurkat T-cell leukemia, which produces all three isoforms of BAG-1 (Fig. 4*B*). These same bands corresponding to BAG-1, BAG-1M, and BAG-1L were detected using all three of our anti-BAG-1 monoclonal antibodies raised against the ~36 kDa BAG-1 protein (data not shown).

The ability of a single BAG-1 cDNA to encode both the originally identified ~36 kDa BAG-1 protein and longer ~56–57 kDa BAG-1L isoform was confirmed by expressing in mammalian cells the same human BAG-1 cDNA that had been used for the *in vitro* transcription/translation experiments. For this purpose, the BAG-1 cDNA was subcloned downstream of the cytomegalovirus immediate early-region promoter in pcDNA-3, and this plasmid or the control pcDNA-3 plasmid was stably transfected into Rat-1 fibroblasts. Immunoblot analysis of lysates derived from these cells revealed the presence of two isoforms of BAG-1 having apparent molecular masses of ~36 kDa and ~56–57 kDa in the BAG-1-transfected Rat-1 cells but not in

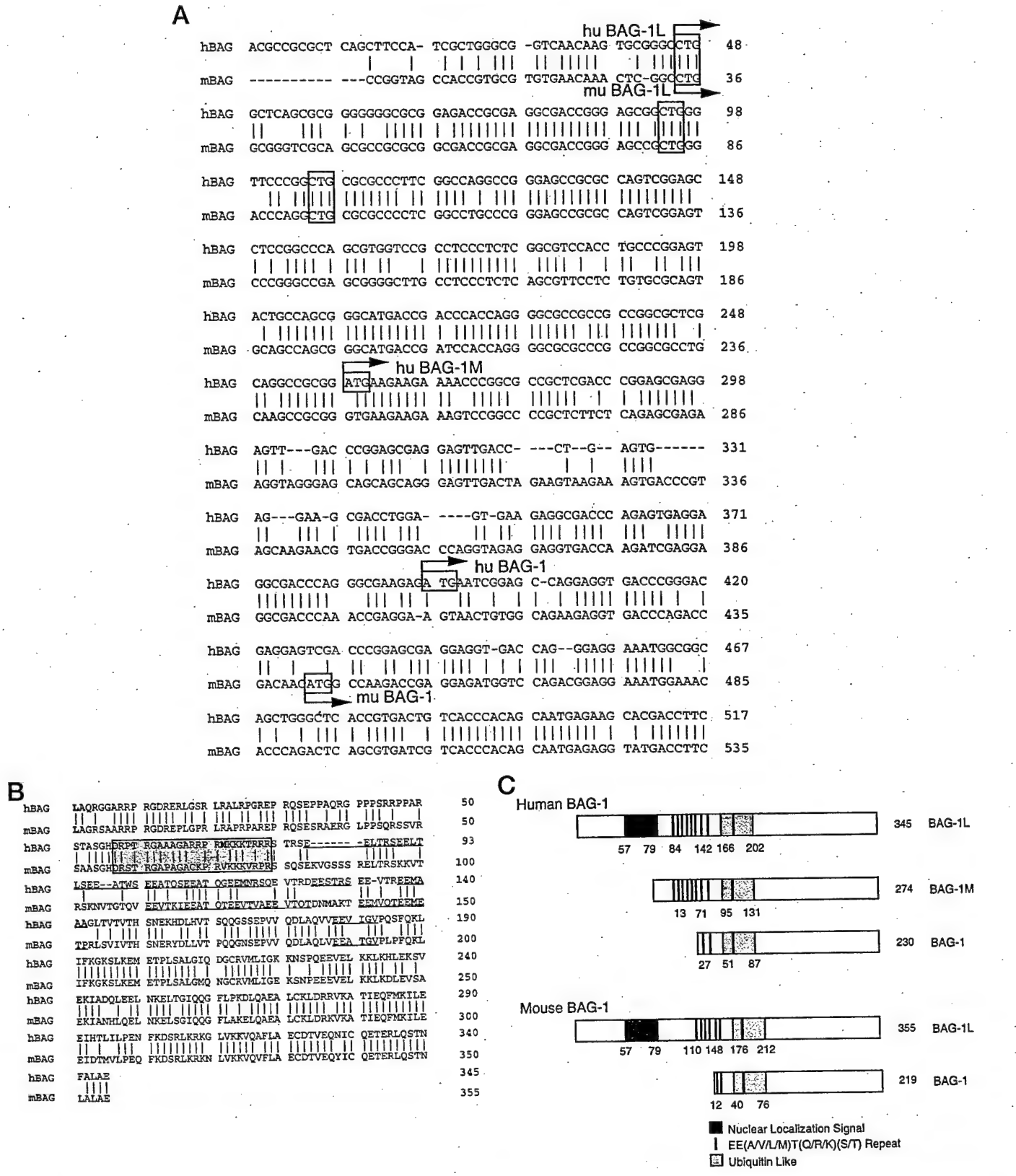

Fig. 3. Nucleotide and predicted amino acid sequences of human and mouse BAG-1 mRNAs and proteins. In *A*, a portion of the nucleotide sequences of human and mouse BAG-1 cDNAs are presented (submitted to GenBank). The locations of the predicted ATG start codons and the alternative upstream CUG codons are indicated in *boxes*. The CUG codon with the most favored context for translation initiation is indicated by an *arrow*. The two downstream CUGs have pyrimidines rather than the favored purines at positions −3 and/or +4 relative to the CUG (where C is +1). *B*, the predicted amino acid sequences of the human and mouse BAG-1L proteins are presented in single-letter code, assuming translation initiation from the most 5′ CUG codon. The methoniones corresponding to the AUG codon initiation sites are in *bold*. A basic region with similarity to NLS motifs is shaded. The six amino-acid EE motifs [most common sequence is E-E-(A/V/L/M)-T-(Q/R/K)-(S/T)] are *underlined*. In *C*, a schematic of the human and mouse BAG-1 isoforms is presented, illustrating the ubiquitin-like domain NLS and hexameric repeats (see "Discussion").

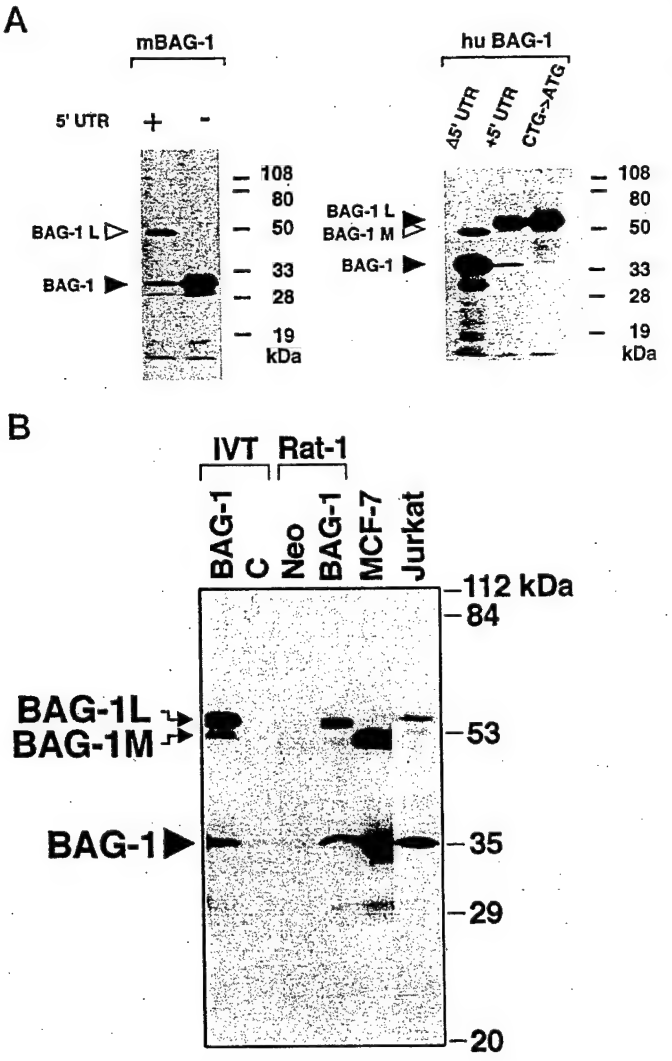

Fig. 4. The BAG-1L protein derives from use of noncanonical CTG codons for translation initiation. In *A*, *in vitro* translations were performed in the presence of [^{35}S]L-methionine using murine (*left panel*) and human (*right panel*) BAG-1 cDNAs that either contain or lack the 5′-untranslated region (*UTR*) where the CUG codons reside. The human BAG-1 cDNA encompasses position −345 bp to 690 bp relative to the ATG (A is +1) that initates the ORF encoding the shortest BAG-1 protein, whereas the murine BAG-1 cDNA encompasses positions −408 bp to 657 bp. The same human BAG-1 cDNA, but in which the 5′ most CUG codon was mutated to ATG, was also *in vitro* translated. Proteins were analyzed by SDS-PAGE/autoradiography. The BAG-1, BAG-1L, and BAG-1M proteins are indicated by *arrowheads*. In *B*, immunoblot analysis was performed using either *in vitro* translated proteins or lysates (50 μg/lane) derived from cells. *Lanes 1* and *2* represent reticulocyte lysates (3 μl) used for *in vitro* transcription/translation of either control pcDNA3 plasmid (*c*) without an insert or a huBAG-1 cDNA (pKK240) encoding nucleotides −390 to 880 bp relative to the AUG codon (A is 1+). *Lanes 3* and *4* are Rat-1 cells that had been stably transfected with either a control plasmid pcDNA-3 or pcDNA-3 containing the pKK241-1 huBAG-1 cDNA (−390 to 880 bp). Lysates were also included from MCF7 breast cancer cells stably transfected with a BAG-1 expression plasmid that produces both BAG-1M and BAG-1 but which lacks the upstream CTG required for BAG-1L (*Lane 5*) and from untransfected Jurkat T-cell leukemia cells which intrinsically express all three isoforms of BAG-1 (*Lane 6*). The blot was incubated with anti-huBAG-1 monoclonal antibody KS-6C8, followed by ECL-based detection. The positions of the BAG-1, BAG-1L, and BAG-1M proteins are indicated.

the control (Neo)-transfected cells. These two forms of BAG-1 detected in transfected Rat-1 cells comigrated in gels with the anti-BAG-1 immunoreactive bands seen in Jurkat and some other human cell lines (Fig. 4*B* and data not shown). The intermediate BAG-1M protein was not produced in these transfected Rat-1 cells. To demonstrate production of the BAG-1M protein in cells, MCF7 breast cancer cells were transfected with a BAG-1 cDNA containing the ORFs for BAG-1 and BAG-1M but lacking the 5′ region where the CTG codons reside. Deletion of the 5′ upstream region was empirically determined to allow for more efficient translation initiation from the downstream ATG codons. In these transfected MCF7 cells, abundant amounts of the ~52 kDa BAG-1M and ~36 kDa BAG-1 proteins were observed but not the longer BAG-1L protein (Fig. 4*B*).

Taken together, these data corroborate and extend recent observations (14) demonstrating that the human BAG-1 mRNA can potentially encode three isoforms having lengths of 345 (BAG-1L), 274 (BAG-1M), and 230 (BAG-1) amino acids, with BAG-1L arising from a noncanonical CUG and the BAG-1M and BAG-1 proteins arising from typical AUG codons. The cDNA cloning results presented here also provide evidence that the mouse BAG-1 mRNA can similarly encode two isoforms of 355 (BAG-1L) and 219 (BAG-1) amino acids in length (Fig. 3), with the longer of these arising from a noncanonical CUG codon.

BAG-1L and BAG-1M Proteins Retain Hsc70 Binding Activity. Recently, we reported that the shorter BAG-1 protein can bind to Hsp/Hsc70 family proteins and modulate their activities (5). We therefore explored whether the BAG-1L and BAG-1M variants of BAG-1 can also bind to molecular chaperones. For these experiments, a GST-fusion protein containing the ATP-binding domain of Hsc70 was tested for interactions *in vitro* with the BAG-1, BAG-1L, and BAG-1M proteins, which were produced by *in vitro* translation of BAG-1 cDNAs that either contained or lacked the region where the noncanonical CTG start codons reside. The COOH-terminal peptide-binding domain of Hsc70 was not included in the GST-fusion protein to avoid nonspecific association and because our previous experiments showed that BAG-1 binds directly to the ATP-binding domain

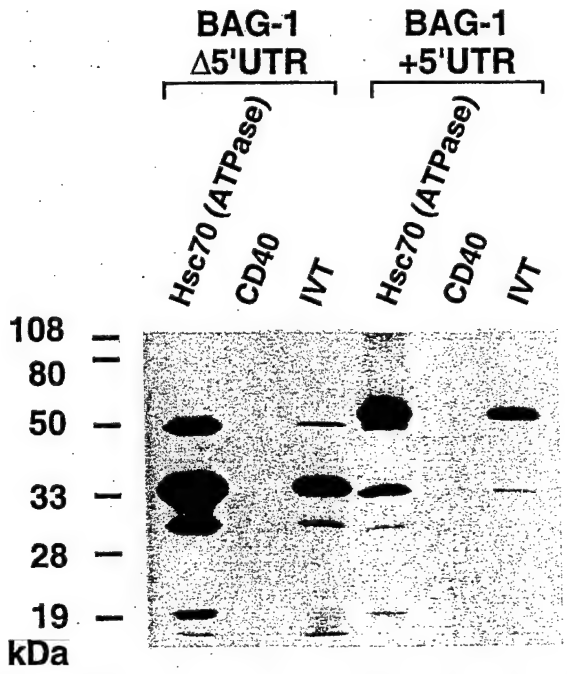

Fig. 5. Hsc70 binds to BAG-1, BAG-1L, and BAG-1M. Human BAG-1 cDNAs containing or lacking the region upstream of the originally identified ORF were *in vitro* translated (*IVT*) in the presence of [^{35}S]L-methionine, thus producing the BAG-1, BAG-1M, and BAG-1L proteins. The BAG-1 (*+5′UTR*) cDNA produces primarily BAG-1L, whereas the BAG-1 (*Δ5′UTR*) cDNA produces mostly BAG-1 along with some BAG-1M protein. IVT BAG-1 proteins were incubated with GST-Hsc70 (ATP-binding domain) or (as a negative control) GST-CD40 cytosolic domain immobilized on glutathione-Sepharose. After washing, proteins bound to beads were analyzed by SDS-PAGE/autoradiography. As a control, one-tenth the input volume of the IVT proteins was run directly in gels. Note that BAG-1, BAG-1M, and BAG-1L bind to GST-Hsc70 but not to GST-CD40. The small molecular weight proteins presumably represent partial degradation products of BAG-1 or translation initiation from internal AUG codons. These small proteins have not been detected *in vivo*, arising only in IVT experiments.

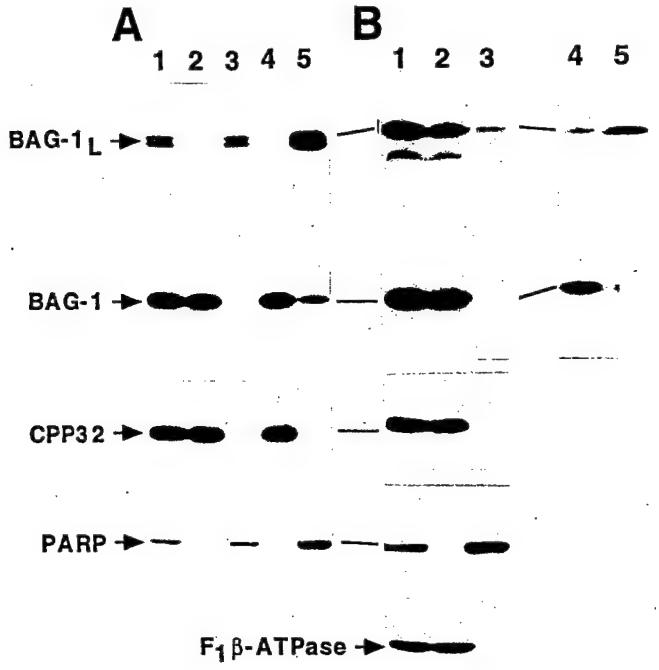

Fig. 6. Subcellular fractionation analysis of BAG-1 proteins. Nuclear and nonnuclear fractions were prepared from 267 prostate cancer (*A*) and Jurkat T-cell leukemia (*B*) cell lines. Lysates were normalized either for cell equivalents (4-10^5, *A*; 10^6, *B*) (*Lanes 1–3*) or for total protein content (50 μg/lane; *Lanes 4* and *5*). Whole-cell lysates were included for comparison (*Lane 1*). With cytosolic (*Lanes 2, 4*) and nuclear (*Lanes 3, 5*) extracts. After SDS-PAGE and transfer to nitrocellulose, blots were sequentially probed with antibodies specific for BAG-1, the cytosolic protein CPP32 (caspase-3), the nuclear protein poly(ADP-ribose) polymerase (*PARP*), or the mitochondrial protein $F_1$1-β-ATPase using a multiple antigen detection method (17). The positions of the BAG-1 and BAG-1L proteins are indicated. Jurkat T-cells (*B*) also contain some BAG-1M.

of Hsp70 and Hsc70 (5). As shown in Fig. 5, the BAG-1L, BAG-1M, and BAG-1 proteins all bound to GST-Hsc70(ATP domain) but not to a control GST fusion containing the cytosolic domain of CD40. Similar results were obtained in coimmunoprecepitation assays using lysates from cells that endogenously contain BAG-1, BAG-1M, and BAG-1L (not shown). Thus, BAG-1 and its variants BAG-1L and BAG-1M can all interact with Hsc70.

BAG-1 Proteins Can Reside in the Nucleus. The additional NH_2-terminal region found in both the human and mouse BAG-1 proteins is predicted to contain a basic stretch of amino acids resembling NLSs such as that found in nucleoplasmin (Fig. 3*B*; Refs. 27 and 28). We therefore explored the subcellular locations of these proteins by preparing nuclear and nonnuclear fractions from a human leukemia line, Jurkat, and a prostate cancer line 267 that contain relatively high endogenous levels of the BAG-1 and BAG-1L proteins. Jurkat T-cells also contain lower but detectable levels of BAG-1M.

In 267 prostate cancer cells, the shorter ~36 kDa BAG-1 protein was located predominantly in the nonnuclear fraction with only a small proportion of this observed in the nucleus (Fig. 6*A*). In contrast, the BAG-1L protein was found predominantly in the nuclear fraction, regardless of whether samples were normalized for cell equivalents or total protein content (Fig. 6*A*). In contrast, in Jurkat T-cells, most of the BAG-1, BAG-1L, and BAG-1M proteins resided in the nonnuclear fraction in Jurkat T-cells, as determined by immunoblot analysis where cell equivalents were used for sample normalization (Fig. 6*B*, *Lanes 1–3*). However, some of the BAG-1L protein was also detected in the nuclear fraction by immunoblot analysis. Reprobing the same blot with antibodies specific for a cytosolic protein (CPP32), a nuclear protein (PARP), and a mitochondrial protein (F1-β-ATPase) confirmed the purity of these subcellular fractions (Fig. 6). When the Jurkat nuclear and nonnuclear fractions were normalized for total protein content (Fig. 6*B*, *Lanes 4* and *5*), a reciprocal relation was observed between the relative amounts of BAG-1 and BAG-1L in these subcellular fractions, with higher levels of BAG-1 in the nonnuclear compared with the nuclear compartment and conversely higher levels of BAG-1L in the nuclear than the nonnuclear fractions. These findings therefore suggest that the BAG-1L protein is commonly located in the nucleus, whereas the shorter BAG-1 protein tends to be nonnuclear. Note however that some of the shorter ~36 kDa BAG-1 protein was also present in the nuclear fraction. Consequently, these data argue that BAG-1 and BAG-1L can reside in either the cytosol or the nucleus, although they may have preferences for one location or the other.

To further evaluate the intracellular locations of the BAG-1 and BAG-1L proteins, we used confocal immunofluorescence microscopy methods. In Rat-1a cells that had been transfected with a human BAG-1 cDNA and that expressed roughly equivalent amounts of the 56–57 kDa BAG-1L and 36 kDa BAG-1 proteins (see Fig. 4*B*), immunofluorescence-based detection of the human BAG-1 protein revealed localization predominantly in the nucleus (Fig. 7). In contrast, expression of human or murine BAG-1 plasmids capable of producing only the shorter BAG-1 protein in several types of cells generally resulted in a predominantly cytosolic distribution (not shown). Taken together, these observations derived from subcellular fractionation and immunofluorescence confocal microscopy confirm that BAG-1 proteins can reside in either the nucleus or the cytosol, with the BAG-1L protein apparently having a preference for the nucleus. However, the cellular background in which BAG-1 is expressed can influence whether it resides primarily in the cytosol or is also found in the nucleus.

Immunolocalization of BAG-1 Proteins in Human and Mouse Tissues by Immunohistochemistry. Using the anti-BAG-1 monoclonal antibody KS-6C8, an immunohistochemical analysis of BAG-1 expression in essentially all normal adult human tissues was performed. Although only the data for the KS-6C8 anti-human BAG-1 monoclonal, major portions of the immunostaining results were confirmed by use of the KS-10B6 and KS-5A6 anti-human BAG-1 monoclonals. All of these monoclonal antibodies react with the

Fig. 7. Confocal immunofluorescence analysis of intracellular distribution of BAG-1 proteins demonstrates nuclear location. Rat-1a cells, which had been stably tranfected with a huBAG-1 cDNA (encompassing nucleotides −390 to 880 bp relative to the AUG), were analyzed for huBAG-1 protein expression by immunofluorescence assay. After fixation, cells were incubated with either a mIgG1 control (*left*) or the anti-huBAG-1 monoclonal antibody KS-6C8, followed by a FITC-confugated secondary antibody.

Table 1 *Summary of immunohistochemical analysis of in vivo BAG-1 expression in normal tissues*

Organ/Tissue	Structure/Cell type	Intensity[a]
Skin		
Epidermis	Keratinocytes	
Stratum basale	Basal cell layer	1–3+c
Stratum spinosum	Spinous layer	2+d
Stratum granulosum	Granular layer	1–2+b
Stratum corneum	Cornified layer	0
Dermis		
Connective stroma	Fibroblasts	0–2+b
Sweat gland	Epithelium	2–3+b
Sabaceous gland	Epithelium	1–2+b
Musculoskeletal system		
Skeleton		
Cartilage	Chondrocytes	1–3+d
	Fibroblasts	0–1+b
Bone	Osteocytes	1–3+b
	Osteoclasts	1+b
Striated muscles	Muscle fibers	1–2+a,c
Cardiovascular system		
Heart		
Myocardium	Myocytes	1–2+d
	Fibroblasts	0–1+b
	Capillary endothelium	0
Arteries	Endothelial cells	0
	Smooth muscle cells	0–2+b
	Fibroblasts	0–1+b
Respiratory system		
Trachea		
Epithelium (pseudostratified columnar)	Basal cell layer	0–1+b
	Luminal cell layer	2–3+a
Submucosa	Fibroblasts	0–1+b
	Smooth muscle cells	0–1+b
	Sero-mucous glands	0
Cartilage	Chondrocytes	0–2+d
Lung		
Bronchi	Pseudostratified or simple columnar epithelium	2–3+a
Alveoli	Type I pneumocytes	0
	Type II pneumocytes	0
	Alveolar macrophages	2–3+a
Alimentary tract		
Salivary gland (submandibular gland)		
Secretory gland acini	Serous cells	0
	Mucous cells	0
	Salivary duct epithelium	1–3+a
Tongue/Esophagus		
Stratified squamous epithelium	Basal cell layer	0–1+c
	Spinous layer	1–2+d
	Granular layer	0–1+b
Muscularis externa	Smooth muscle cells	0–1+b
Stomach		
Cardiac region	Gastric pits/foveolar cells	2–3+d
	Cardiac glands/mucoid cells	0–3+a,c
Submucosal plexus (Meissner's plexus)	Ganglion cells	1+d
	Smooth muscle cells	0–1+b
Small intestine	Absorptive epithelium	1+d
	Paneth cells	0–1+b
Colon	Absorptive cells	1–2+b
	Goblet/mucous cells	0
Myenteric plexus (Auerbach's plexus)	Ganglion cells	0–1+d
Liver	Hepatocytes	1–3+a
	Sinusoidal endothelium	0–1+b
	Bile duct epithelium	2–3+a
Pancreas		
Exocrine	Acinar cells	2–3+a
	Ductal epithelium	1–2+b
Endocrine: Islets of Langerhans	A cells	2–3+a
	B cells	0–1+a
Urinary system		
Kidney		
Glomeruli	Mesangial cells	0
Bowman's capsule	Parietal layer/podocytes	0
	Visceral layer/squamous epithelium	0
Collecting tubules	Proximal convoluted tubules	0–1+d
	Loop of Henle, thin limb	1–2+a,d
	Distal convoluted tubules	2–3+a
Collecting ducts	Epithelial cells	1–3+a
Urinary bladder	Transitional epithelium	0–2+a
	Smooth muscle cells	0–1+b
Reproductive systems		
Male		
Testis	Leydig cells	0
Seminiferous tubules	Sertoli cells	0–3+b
	Spermatogonia	0–1+b
	Spermatocytes	0
	Spermatids	0
	Spermatozoa	0–3+d
Vas deferens	Pseudostratified columnar epithelium	0–1+b
Prostate		
Tubuloalveolar glands	Basal cells	1–3+d
	Luminal secretory cells	0–3+a
Fibromuscular stroma	Smooth muscle cells	0–1+b
	Fibroblasts	0–1+b
Female		
Uterus		
Endometrium	Columnar epithelium	0–3+a,c
	Stromal cells	0–1+b
Myometrium	Smooth muscle cells	0–1+b
Ovary		
Primordial/primary follicle	Oocytes	nf
	Follicular cells	0
Secondary follicle	Granulosa cells	0
	Theca internal cells	1+b
	Theca external cells	1+b
Corpus luteum	Granulosa lutein cells	0–1+b
	Theca lutein cells	0–2+d
Oviduct (Fallopian tube)		
Tunica mucosa	Ciliated columnar epithelium	2–3+a
	Secretory cells	0
Tunica muscularis	Smooth muscle cells	0–1+b
Mammary gland		
Tubuloalveolar glands	Cuboidal/columnar epithelium	1–3+d
Lactiferous ducts	Columnar epithelium	1–3+d
	Myoepithelial cells	0
Stroma	Fibroblasts	0–1+b
Hematolymphoid system		
Peripheral blood	Granulocytes	0–3+d
	Monocytes	0–2+b
	Lymphocytes	0
	Erythrocytes	0
Bone marrow	Erythroid precursors	0–1+b
	Myeloid precursors	0–1+b
	Megakaryocytes	2–3+c
	Mature neutrophils	1–3+d
	Plasma cells	0–1+d
	Monocytes	0–2+b
Thymus		
Cortex	Cortical thymocytes	0–1+b
	Macrophages (dendritic interdigitating cells)	0
Medulla	Epithelioreticular cells	1–3+b
	Hassall's corpuscles	0–2+b
	Medullary thymocytes	0–1+b
Tonsil/Lymph nodes		
Germinal center	Large noncleaved cells	0
	Small noncleaved cells	0
	Small cleaved cells	0
	Follicular dendritic cells	0
	Macrophages	1–3+a
Mantle zone	Lymphocytes	0
Interfollicular region	Small T-cells	0
	Large transformed cells	0
	Sinus histiocytes	0–1b
	Plasma cells/reactive	1–2+d
Spleen		
Periarteriolar sheets	B-lymphocytes	0
Marginal zone	T-lymphocytes	0
Interfollicular cells	Granulocytes	1–3+d
	Erythrocytes	0
Venous sinsues	Endothelium	1–3+a
Central nervous system		
Cortex and basal ganglia		
Gray matter	Normal neurons	0–3+d
	Axons	1–2+b
	Neuropil	0–1+b
White matter	Myelin sheath	0
Neuroglia	Astrocytes	0–3+a
	Oligodendroglia	0
Microglia	Resting cells	0
	Activated cells	0

Table 1 *Continued*

Organ/Tissue	Structure/Cell type	Intensity[a]
Ependyma	Ependymal cells	1–2+b
Leptomeninges	Arachnoid epithelium	0
Choroid plexus	Epithelium	0
Cerebellum		
Cortex	Purkinje cells	1–2+d
	Granular cells	0
	Golgi cells	0
Molecular layer	Stellate and basket cells	0
	Purkinje cell dendrites	0–1+b
	Astrocytes (Bergman glia)	2–3+a
Medulla	Dentate nucleus	0–1+d
	Myelin fibers	0
Spinal cord		
White matter	Axons	0–1+b
	Myelin sheath	0
Gray matter	Ventral horn motoneurons	1–3+d
	Dorsal horn sensory neurons	0–1+b
	Neuro-pil	0–1+b
Central channel	Epen-pil	1+b
Peripheral nervous system		
Dorsal root and cranial nerve ganglia	Ganglion cells	0–3+d
	Satellite cells	0
	Schwann cells	0
	Fibroblasts	0
Autonomic ganglia	Ganglion cells	0–3+d
	Satellite cells	0
	Schwann cells	0
	Fibroblasts	0
Peripheral nerve	Axons	1–2+b
	Myelin sheath	0
Endocrine system		
Thyroid	Follicle cells	0–1+b
Adrenal		
Cortex	Zona glomerulosa	0–1+b
	Zona fasciculata	0–2+b
	Zona reticularis	0–2+b
Medulla	Chromaffin cells	2–3+c

[a] Immunohistochemical analysis of *in vivo* patterns of BAG-1 expression was performed for both human and mouse tissues. Results were scored according to intensity of immunostaining as: 0, negative; 1, weakly positive; 2, moderate; and 3, strong. The intracellular locations of BAG-1 immunostaining varied as indicated: a, organellar/mitochondrial pattern of expression; b, cytosolic; c, nuclear; and d, both nuclear and organellar/cytosolic pattern of expression. nf, not found.

BAG-1, BAG-1L, and BAG-1M proteins.[5] Moreover, immunohistochemical analysis was also performed for murine tissues using an anti-peptide polyclonal antiserum that is specific for residues 26–45 of the mouse BAG-1 protein (1), yielding similar results.

Table 1 summarizes the results, and Fig. 8 provides some of the more salient examples of BAG-1 immunoreactivity in normal tissues. A few of these results are commented upon here. Three subcellular patterns of BAG-1 immunostaining were identified, existing either individually or in combinations depending on the particular type of cell. These consisted of: (*a*) nuclear; (*b*) diffuse cytosolic; and (*c*) punctate cytosolic staining typical of association with organelles.

In the epidermis, cytosolic BAG-1 immunostaining was present throughout all the sublayers of keratinocytes (Fig. 8.1). The basal cell layer of cells, however, also contained nuclear BAG-1 immunostaining. Thus, the subcellular distribution of BAG-1 appears to change during differentiation of these epithelial cells, with loss of BAG-1 from the nuclei occurring as the cells differentiate and migrate toward the body surface. Combinations of diffuse cytosolic and nuclear BAG-1 immunostaining were also seen in chondrocytes (Fig. 8.3), cardiac myocytes (Fig. 8.4), colonic enterocytes (Fig. 8.10), bladder urothelium (Fig. 8.17), spermatogonia of the testis (Fig. 8.21), and mammary epithelial cells (Fig. 8.22). In some other types of cells, however, predominantly nuclear BAG-1 immunostaining with relatively little or no cytosolic staining was observed in the cells of the gastric glands (Fig. 8.7 and 8.8), intestinal epithelium (Fig. 8.9), corpus luteum of the ovary (Fig. 8.23), megakaryocytes in the bone marrow (Fig. 8.26), cortical and spinal cord neurons (Fig. 8.28 and 8.29), and adrenal chromaffin cells (Fig. 8.30 and 8.31).

Coarse, cytosolic granules of BAG-1 immunostaining were evident in several types of cells, sometimes with a perinuclear distribution, either alone or in combination with nuclear immunostaining, diffuse cytosolic staining, or both. Among the cells with organellar-like staining were cardiac myocytes (Fig. 8.4), bronchial epithelial cells (Fig. 8.5), alveolar macrophages (Fig. 8.6), exocrine pancreas (Fig. 8.11), renal collecting duct epithelium (Fig. 8.14), bladder epithelial cells (Fig. 8.18), and thymic epithelial cells (Fig. 8.24).

Analysis of this organellar immunostaining pattern at higher magnification revealed association of BAG-1 with what may be mitochondria (Fig. 9). In many cases, cross-sections through these organelles were obtained, demonstrating BAG-1 immunostaining around the circumference, thus producing a donut-like appearance. Similar observations were made by laser scanning microscopic analysis of these BAG-1-immunostained tissue sections (Fig. 9*F*). These results are highly reminescent of previous studies of Bcl-2 subcellular distribution using the same methods (21).

A few observations concerning the levels and locations of BAG-1 protein deserve comment: (*a*) the location of BAG-1 in some types of cells may be under dynamic regulation. Evidence for this comes, for example, from comparisons of BAG-1 immunostaining in prostates derived from several individuals, where either the mitochondrial or nuclear patterns prevailed depending on the specimen (not shown) and from the epidermis where BAG-1 appeared to move from a nuclear to a cytosolic location during differentiation of keratinocytes (Fig. 8.1); and (*b*) the intensity of BAG-1 immunostaining varied within some types of cells during their differentiation. For instance, BAG-1 immunostaining increased in intensity along the crypt-villus axis in the colon and small intestine, implying that BAG-1 protein levels become elevated as these cells differentiate and migrate toward the lumen of the bowel (Fig. 8.10). BAG-1 immunostaining was also strikingly up-regulated during differentiation of bladder epithelial cells and down-regulated during differentiation of prostate epithelium.

Bcl-2 Targets BAG-1 to Intracellular Membranes and Organelles. The immunohistochemical analysis of BAG-1 protein in tissues suggested that this protein can be associated with intracellular organelles, possibly mitochondria, in some types of cells. To explore whether expression of the integral membrane protein Bcl-2 can cause a relocation of BAG-1 to the intracellular membranes where it resides, a GFP-BAG-1 fusion protein was expressed in HeLa cells by transient transfection, with or without Bcl-2. As shown in Fig. 10 (left panels), when expressed by itself, the GFP-BAG-1 protein was diffusely distributed through the cytosol of HeLa cells. In contrast, coexpression of GFP-BAG-1 with Bcl-2 caused a portion of the GFP-BAG-1 to associate with what appeared to be the nuclear envelope and perinuclear membranes as well as punctate cytosolic structures suggestive of mitochondria. Because the Bcl-2 protein exhibits a similar distribution in cells (21), we conclude that the intracellular location of the BAG-1 protein can be modulated by Bcl-2.

Analysis of BAG-1 Expression in Human Tumor Cell Lines. To preliminarily explore the expression of BAG-1 in cancers, an immunoblot analysis was performed using the National Cancer Institute screening panel of 60 human tumor cell lines. Because prostate cancers are underrepresented in this screening panel, the analysis was supplemented with an additional five human prostate cancer cell lines. An additional B-cell lymphoma line (RS11846) and a T-cell leukemia Jurkat were also included. For these experiments, whole-cell lysates were prepared from tumor lines and normalized for total protein content before SDS-PAGE/immunoblot assay. Results were scored for each of the three forms of BAG-1 (BAG-1, BAG-1L, and BAG-

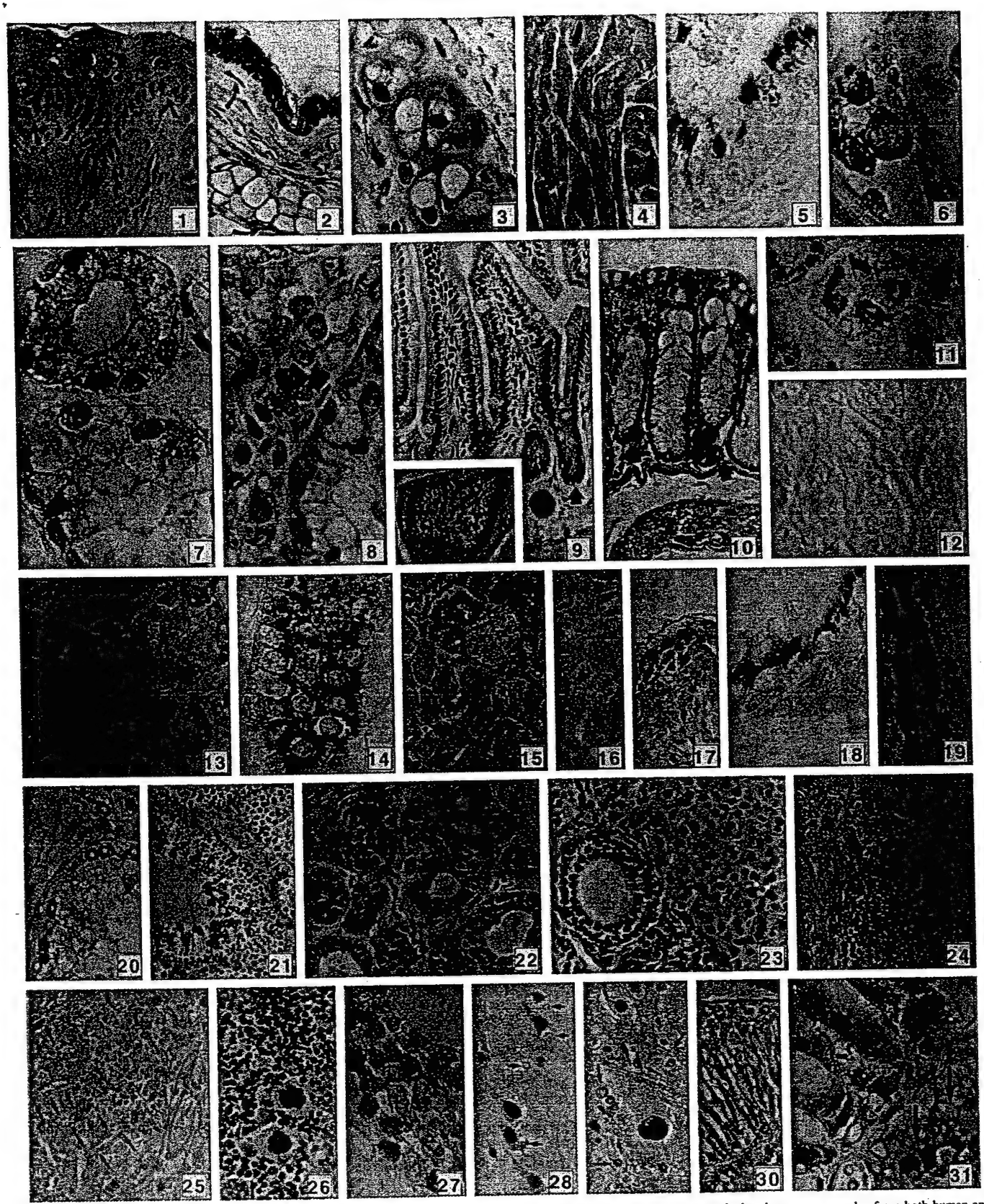

Fig. 8. Immunohistochemical analysis of BAG-1 expression *in vivo*. Representative BAG-1 immunostaining results are presented, showing some examples from both human and mouse tissues and representing 31 color photomicrographs taken with a 35-mm camera. Counterstaining of nuclei was performed with hexatoxylin, unless otherwise noted. *1*, human epidermis stained with KS6C8 demonstrating predominantly cytoplasmic immunoreactivity in all layers but nuclear BAG-1 in the basal cells lining the basement membranes (*arrows*); ×400. *2*, mouse epidermis from skin overlying the tail immunostained with anti-BAG-1 polyclonal antiserum, showing strong cytoplasmic and moderate nuclear BAG-1 immunoreactivity in keratinocytes in all layers of the epithelium. In the dermis below, faint cytoplasmic staining in fibroblasts and nuclear staining in perichondrial cells is present (*arrows*); ×200. *3*, cartilage from mouse, demonstrating strong nuclear and cytoplasmic BAG-1 immunostaining in chondrocytes. *Arrows*, immunopositive nuclei of cells in perichondrium; ×1000. *4*, mouse myocardium, showing cytosolic BAG-1 immunoreactivity, associated apparently with organelles, and nuclear BAG-1 expression; ×400. *5*, human bronchial epithelium, demonstrating intense BAG-1 immunostaining in a peri- or supranuclear distribution and having a clear granular pattern indicative of organella association (methylgreen counterstain). Faint diffuse cytoplasmic BAG-1 immunostaining is also present; ×1000. *6*, human alveolar macrophages exhibiting intense organellar-like BAG-1

1M), using a semiquantitative method that involved use of an internal control cell line to standardize results. As summarized in Table 2, the ~36 kDa BAG-1 protein was consistently the most abundant form of BAG-1 expressed in tumors. Among the tumor types with consistently higher relative levels of 36-kDa BAG-1 protein were breast, colon, and leukemia cell lines, although a variety of other types of tumor lines also expressed high levels of BAG-1 on a more variable basis. In contrast, the presence of the BAG-1L and BAG-1M proteins was highly variable. Prostate cancer, breast cancer, and leukemia cell lines were the most consistent expressors of BAG-1L, with seven of seven prostate, seven of eight breast, and four of five leukemia cell lines containing immunodetectable levels of this protein.

DISCUSSION

In this report, we explored the patterns of expression and intracellular distributions of the BAG-1 protein *in vivo* and in cultured cell lines. These data provide evidence that BAG-1 mRNAs and proteins are widely expressed *in vivo*, with the major form of BAG-1 protein representing the originally reported ~30 kDa mouse BAG-1 protein and a ~36 kDa human BAG-1 protein. The human and mouse BAG-1 proteins are predicted to be 230 and 219 amino acids in length, as deduced from cDNA cloning (1, 13), which coincides with proteins of ~26 kDa and ~25 kDa. Characterization of the BAG-1 protein by ultracentrifugation equilibrium sedimentation confirms this molecular mass.[5] However, like GrpE (29), molecular modeling and gel-sieve chromatography analysis suggest that BAG-1 is an elongated, rod-like molecule,[6] thus potentially accounting for its anomalous migration in SDS-PAGE. Moreover, both the human and mouse BAG-1 proteins are acidic (calculated pI of ~5.0 for human and ~4.8 for mouse) and thus may bind less SDS per unit mass, causing them to migrate slower in SDS-polyacrylamide gels than expected.

In addition to the originally described BAG-1 protein, we present evidence here that an additional generally less abundant form of BAG-1 can arise, most likely as a result of use of noncanonical CTG codons within BAG-1 mRNAs. Recent studies of human BAG-1 cDNAs by Packham *et al.* (14) also support this idea but lacked definitive evidence for an analogous configuration for murine BAG-1 cDNAs. Numerous studies have documented the ability of CUG codons to serve as alternatives to AUG for translation initiation, provided they are found within the proper sequence context (see for example Refs. 22 and 23). Based on predictions from cDNA cloning, the human and mouse BAG-1L proteins are expected to be 345 and 355 amino acids in length, respectively, assuming that the first of the available in-frame CTGs are used for translation initiation. Unlike the human BAG-1 cDNA, sequencing of murine BAG-1 cDNAs failed to reveal an in-frame upstream AUG codon that would give rise to a protein analogous to BAG-1M. Consistent with these DNA sequencing data, *in vitro* translation experiments resulted in the production of three isoforms of BAG-1 when the human cDNA was used compared with only two with the murine BAG-1 cDNA. It remains to be determined whether this species-specific difference is of functional importance, but immunoblot analysis of human tissues and multiple tumor cell lines indicated that BAG-1M (also known as RAP46) is by far the least abundant of the BAG-1 isoforms.

The originally described human and mouse BAG-1 proteins contain three copies of a 6-amino acid motif containing glutamic acid diamino acid (Glu-Glu) resides within their NH_2-terminal regions. The NH_2-terminal extensions present within the BAG-1L proteins of humans and mice add another six copies of this hexameric motif, for a total of nine copies. Although the function of this 6-amino acid motif is presently unknown, the preferred sequence is E-E-(A/V/L/M)-T-(Q/R/K)-(S/T). When this 6-amino acid motif is present in tandem copies, as is often the case in both huBAG-1 and muBAG-1, a consensus site for phosphorylation by creatine kinase-2 (T-R/Q-S-E) is generated. The first ~50 amino acids of the human and mouse BAG-1L proteins are also predicted to be proline rich. Moreover, in both the human and mouse BAG-1L proteins, this proline-rich region is followed by a stretch of basic residues resembling but not sharing perfect homology with NLSs (27, 28). Consistent with this idea, subcellular fractionation experiments and immunofluorescence confocal microscopy demonstrated the presence of BAG-1L within the nuclear compartment of at least some types of cells. The strong amino acid sequence homology shared by the human and mouse BAG-1 proteins within the NH_2-terminal domain created by translation from CUG codons implies an evolutionarily conserved purpose for this domain.

Comparison of the organization of mRNAs encoding bFGF reveals

[6] J. Stuart, D. Myszki, L. Joss, R. Mitchell, S. MacDonald, S. Takayama, Z. Xien, J. C. Reed, and K. Ely. Characterization of BAG-1 interactions with HSC70 molecular chaperones, submitted for publication.

immunostaining in their cytoplasm (methyl green counterstain); ×1000. *7* and *8*, human and mouse stomach, respectively, showing scattered cells within the gastric glands that contain strong nuclear BAG-1 immunostaining; ×1000. Human stomach was counterstained with methyl green (*panel 7*) to better demonstrate nuclear immunopositivity. *9*, murine small intestine demonstrating strong nuclear BAG-1 immunostaining in many of the enterocytes lining the surface of the villi. Note that the proportion of cells with nuclear immunopositivity increases toward the tip of villi (*arrow* points to base of villi where the BAG-1 immunopositive cells are more scarce; ×200. *Inset*, cross-section through a villus at higher magnification; ×400. *10*, colon from mouse, showing BAG-1 immunostaining associated with both nuclei and cytosol. The intensity of BAG-1 immunostaining appears to be greater within the epithelial cells at the apex of the crypts at the luminal surface and lower in the cells located in the bases of the crypts (*arrow*); ×200. *11*, human exocrine pancreas, demonstrating cells with perinuclear organellar-like BAG-1 immunostaining pattern that were counterstained with methyl green; ×1000. *12*, as a control, an adjacent section from the same pancreas was subjected to the immunostaining procedure using anti-BAG-1 monoclonal that had been preabsorbed with GST-BAG-1 fusion protein; ×1000. *13* and *14*, human kidney demonstrating immunonegative glomerulus but strong nuclear immunopositivity in the epithelial cells of proximal and distal convoluted tubules, with only faint cytoplasmic staining (*panel 13*; ×200); and strong cytosolic organellar-like BAG-1 immunostaining in collecting duct epithelium counterstained with methyl green (*panel 14*; ×1000), respectively. *15* and *16*, murine kidney showing same patterns of cell type specificity and intracellular location of BAG-1 immunostaining as observed in humans (*panel 15*; ×150) and demonstrating specificity by preadsorption of anti-muBAG-1 polyclonal antiserum (1735) with muBAG-1 26–45 peptide (*panel 16*; ×100). *17*, bladder urothelium of mouse with BAG-1 immunopositive cells in the subluminal layer with strong perinuclear immunostaining along with weaker diffuse nuclear and cytoplasmic immunoreactivity; ×200. *18*, human bladder transitional epithelium lining the human prostatic sinus with coarse granular cytoplasmic BAG-1 immunostaining of organelles and methylgreen counterstaining of nuclei. Note only faint BAG-1 positivity in the deeper, basal cell layer of the epithelium; ×1000. *19*, human prostate, showing strong cytoplasmic BAG-1 immunostaining in basal cells along the basement membrane but little or no staining of the overlying differentiated secretory cells facing the lumen of the gland; ×400. *20* and *21*, testes from human and mouse, respectively, showing examples of strong perinuclear and cytosolic BAG-1 immunostaining of spermatogonia (methylgreen counterstain; ×400) and BAG-1 immunopositivity of spermatozoa (×200), respectively. Note that the testes from aged human is atrophic compared with young mouse. *22*, proliferative human mammary gland alveoli with BAG-1 immunostaining within both cytoplasm and nuclei of mammary epithelial cells; ×400. *23*, murine ovary with BAG-1 immunopositive nuclei in luteal cells but not in the granulosa cells of a secondary follicle; ×400. *24*, human thymus, demonstrating strong BAG-1 immunopositivity in reticuloepithelial cells but no apparent immunostaining of thymocytes; ×200. *25*, human splenic white pulp demonstrating only weak BAG-1 immunopositivity of neutrophils and endothelium of splenic venous sinusoids (*arrows*) but absence of BAG-1 in lymphoid cells (methyl green counterstain); ×400. *26* and *27*, bone marrow from mouse and human, respectively, demonstrating strong BAG-1 immunostaining of megakaryocyte nuclei (×400) and moderate intensity immunostaining of mature monocytes (*arrow*) and granulocytes, with relatively less BAG-1 immunoreactivity in more immature hemopoeitic cells (×1000), respectively. *28* and *29*, human brain (frontal cortex) and mouse spinal cord, presenting examples of strong nuclear BAG-1 immunostaining in neurons. Note that surrounding macroglia (*arrows*) are immunonegative (methyl green counterstain; ×400). *30* and *31*, adrenal gland from mouse at low (×80) and high (×1000) magnification, illustrating predominantly cytosolic BAG-1 immunostaining of cortical cells and mostly nuclear immunostaining of medullary cells.

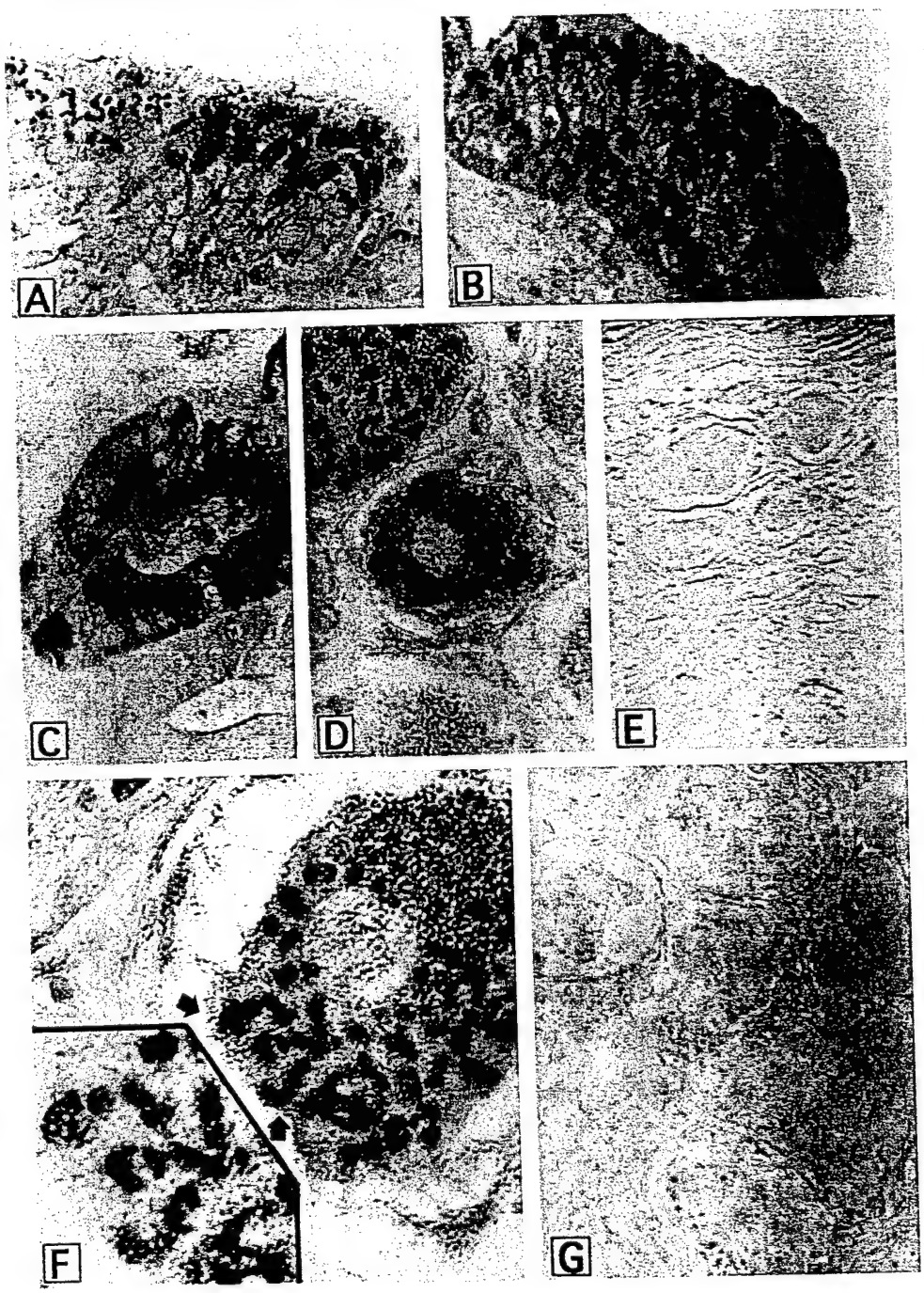

Fig. 9. Light- and laser-scanning microscopic analysis of BAG-1 protein demonstrates association with mitochondria. BAG-1 immunostained paraffin-embedded tissue sections (3 μm) were examined by light (*A–E*) or laser-scanning (*F* and *G*) microscopy. Typical examples of organellar immunostaining are presented from human pattern pseudocolumnar bronchial epithelium (*A*); transitional epithelium (*B*); gastric gland (*C*); and neurons of a dorsal root ganglion (*C*), as shown for sensory ganglia neurons on *D* (×1000). Laser scanning analysis of dorsal root ganglion neurons is presented in *F* (×3000). The *inset* shows a higher magnification view of immunostained mitochondria derived from the region indicated by the *arrows* (×5000). In *E* (×4000) and *G* (×3000), the anti-BAG-1 monoclonal antibody was preadsorbed with GST-BAG-1 fusion protein as a control for immunospecificity.

some striking similarities with BAG-1. Similar to BAG-1, the bFGF mRNA encodes a shorter ~18 kDa form of bFGF, which is predominantly found in the cytosol and which arises from a traditional AUG codon, as well as longer ~22–24-kDa bFGF isoforms that reside in the nucleus and arise from upstream, in-frame, noncanonical CUG codons (30). It may also be relevant that the nuclear targeting NH_2-terminal sequences of these longer isoforms of bFGF constitute a proline-rich domain similar to the predicted the NH_2-termini of the human and mouse BAG-1L proteins (31).

Despite the presence of a potential NLS and some similarity to the nuclear targeting NH_2-terminus of high molecular weight bFGF, the BAG-1L protein was also found to some extent in the nonnuclear fraction by subcellular fractionation, suggesting that its import into the nucleus is regulated rather than constitutive. In this regard, the immunohistochemical analysis of normal tissues implied dynamic regulation of BAG-1 entry into or exit from the nucleus in some types of cells. For example, whereas the basal cell layer of keratinocytes contained both nuclear and cytosolic BAG-1 immunostaining, the more differentiated cells in the upper layers of the epidermis generally contained only cytosolic BAG-1. In addition, specimen to specimen variation in the location of BAG-1 in the prostate gland also implied regulation of nuclear import or export. We have also observed variations among breast cancer specimens with regard to whether they contain BAG-1 in both cytosol and nucleus *versus* in the cytosol only.[7] Although the shorter mouse originally described human and mouse BAG-1 proteins lack regions with clear similarity to NLS

[7] M. Krajewska, C. Reynolds, S. Krajewski, S. Takayama, C. V. Clevenger, and J. C. Reed. Loss of nuclear BAG-1 immunostaining associated with reduced estrogen and progesterone receptor expression in breast cancer, submitted for publication.

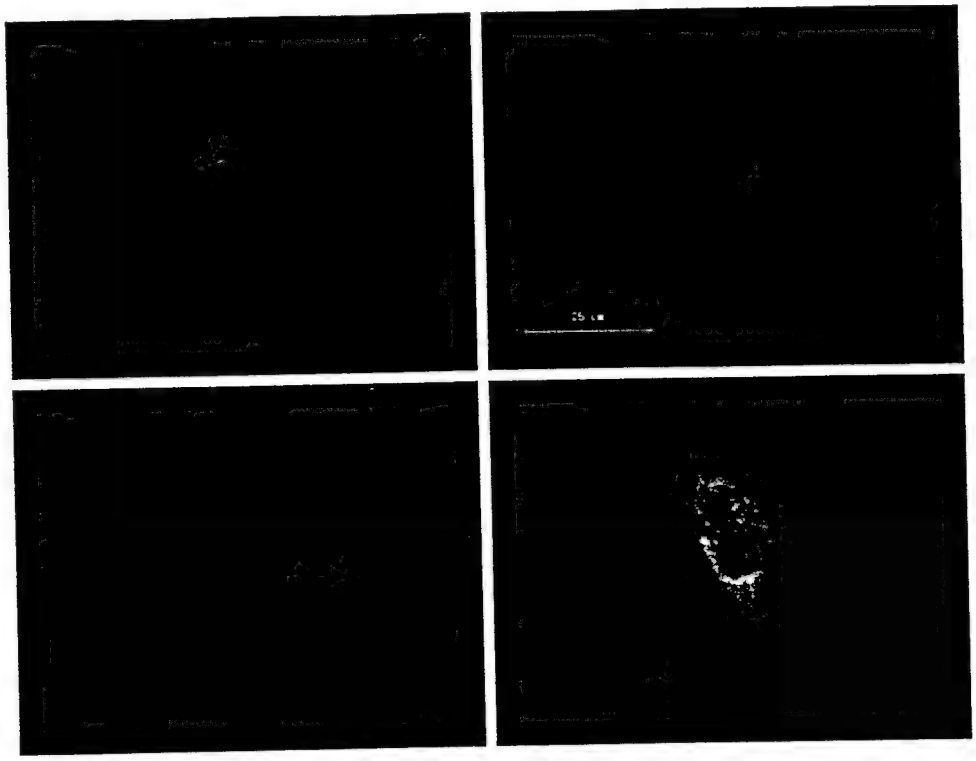

Fig. 10. Bcl-2 alters intracellular distribution of GFP-BAG-1. HeLa cells were transiently transfected with a plasmid encoding GFP-BAG together with equal amounts of either pRc/CMV control (*upper left panel*) or pRc/CMV-Bcl-2 (*other panels*) plasmids. Two days later, images were taken of representative cells using a confocal microscope.

motifs, the mouse BAG-1 protein has been shown to interact with retinoic acid receptors.[8] Thus, it is possible that the shorter BAG-1 protein could also gain entry into the nucleus through its interactions with other proteins. Moreover, because the BAG-1M protein (also known as RAP46) has been reported to interact with other steroid hormone receptors, including as ER, glucocorticoid receptor, progesterone receptor, and androgen receptor, its location theoretically could be controlled in part by associations with these receptors as they traffic between cytosol and nucleus in response to steroid hormones.

In many types of cells, BAG-1 immunostaining was present in the cytosol or in association with cytosolic organelles that morphologically resembled mitochondria, rather than in the nucleus. Association of BAG-1 with mitochondria is consistent with the reported interaction of this protein with Bcl-2 (1). The Bcl-2 protein resides in the outer mitochondrial membrane, oriented toward the cytosol. The immunostaining of BAG-1 seen around the circumference of mitochondria at high magnification by light and laser scanning microscopy supports the idea of BAG-1 association with the outer membrane of mitochondria and is highly reminiscent of previous results obtained for Bcl-2 by the same methods (21). Further studies including immuno-electron microscopy, however, are required for definitive confirmation of BAG-1 association with the outer membrane. BAG-1 immunostaining also occurred in a perinuclear distribution in some types of cells, not unlike Bcl-2 and some of its homologues that have been shown to reside in the nuclear envelope and parts of the endoplasmic reticulum (ER), as well as outer mitochondrial membranes (21, 32). Moreover, when coexpressed in cells, Bcl-2 resulted in targeting of a GFP-BAG-1 fusion protein to perinuclear membranes and cytosolic structures that probably represent mitochondria, providing direct evidence that Bcl-2 can alter the intracellular distribution of the BAG-1 protein. It should be noted, however, that an organellar or perinuclear pattern of BAG-1 immunostaining was not seen in all cell-types that are known to express Bcl-2 *in vivo*. Thus, unidentified events presumably determine whether BAG-1 is recruited to the organellar or nuclear membranes where Bcl-2 resides. Although many possibilities exist, one such event could be dimerization of Bcl-2 with antagonists such as Bax or BAD, which conceivably might prevent Bcl-2 from binding to BAG-1.

It remains to be determined whether the BAG-1L and BAG-1M proteins can interact with the same proteins reported for BAG-1. Previous studies have shown that the NH_2-terminal first 89 amino acids of the mouse BAG-1 protein are expendable for binding to Hsc70, Hsp70, Bcl-2, Raf-1, HGF-R, and PDGF-R (1, 5, 7, 11).[5] Thus, the NH_2-terminal Glu-Glu repeat domain and ubiquitin-like domains of BAG-1 are not required for those protein interactions. In contrast, the COOH-terminal 47 amino acids of mouse BAG-1 are critical for binding to Hsc70, Hsp70, and Raf-1, and the last 84 amino acids of BAG-1 are sufficient for binding to HGF-R and PDGF-R. Because BAG-1L differs from BAG-1 at the NH_2 rather than COOH terminus, it seems likely that it should also bind to these same proteins. Moreover, as shown here, BAG-1, BAG-1M, and BAG-1L all retain the ability to interact with Hsc70. Thus, BAG-1 and its variants BAG-1L and BAG-1M may have the potential to target Hsp70/Hsc70 family proteins to different compartments within cells, presumably facilitating the interactions of Hsp70/Hsc70 family proteins with other proteins in the cytosol, at the mitochondrial surface, or in the nucleus.

The survey of 67 human tumor lines performed here indicates that BAG-1 protein levels can vary widely among malignant cells. However, compared with other tumor lines, BAG-1 protein levels were consistently at high levels in leukemia and lymphoma cell lines, which contained high levels of BAG-1 protein in seven of seven cases. We cannot determine whether the relatively high levels of BAG-1 seen in leukemias and lymphomas as well as many types of solid tumor cell lines represent a pathological increase in the expression of this anti-apoptotic protein in the absence of direct comparisons with purified populations of the appropriate normal cell counterparts. However,

[8] R. Liu, S. Takayama, Y. Zheng, B. Froesch, G-Q. C., X. Zhang, J. C. Reed, and X-K. Zhang. Interaction of BAG-1 with retinoic acid receptor and its inhibition of retinoic acid-induced apoptosis in cancer cells, J. Biol. Chem., in press.

Table 2 *Summary of BAG-1 immunoblot data for human tumor cell lines*

Data represent estimated BAG-1 protein levels (ng per 50 μg of total protein) based on quantification of immunoblot data by densitometric scanning and extrapolation from a GST-BAG-1 standard curve. Data were scored as: 0, undetectable; +/−, 1 to ≤5 ng/50 μg; +, 5 to ≤10 ng/50 μg; ++, 10 to ≤15/50 μg; +++, 15 to ≤20/50 μg; and ++++, >20 ng/50 μg). Tumor lines are grouped by categories.

	BAG-1	BAG-1_M	BAG-1_L
Breast			
BT-549	+++	0	+
HS578T	+	0	0
MCF-7	++++	+/−	+/−
MCF7ADR/RES	+	+/−	+/−
MDA-MB-231	++++	+/−	+
MDA-MB-435	+++	+/−	+
MDA-N	+++	+/−	+/−
T47D	+	0	0
Colon			
COLO205	+	0	0
HCT-15	+++	+/−	+/−
HCT-116	+++	0	0
HCC-2998	+++	0	0
HT29	+/−	0	0
KM-12	++++	+/−	+/−
SW-620	++++	+/−	+/−
CNS			
SF-268	+++	+/−	+/−
SF-295	+++	0	0
SF-539	0	0	0
SNB-19	0	0	0
SNB-75	++	0	+/−
U251	+++	+/−	+/−
Leukemia/Lymphoma			
CCRF-CEM	+	−	+/−
HL-60	+++	+/−	0
K562	++++	+/−	+/−
MOLT-4	+++	+/−	+/−
RPMI-8226	+++	+/−	0
RS11846	++++	+	+
Jurkat	+++	+/−	++
SR	+++	0	0
Lung			
A549	++	0	+
EKVX	++++	+	++
HOP-62	+++	0	0
HOP-92	+/−	+/−	0
NCI-H322M	0	0	0
NCI-H226	+/−	+/−	+/−
NCI-H23	+/−	+/−	+/−
NCI-H522	+/−	0	0
NCI-H460	0	0	0
Melanoma			
LOX-IMVI	+/−	0	0
MALME-3M	++++	+/−	+/−
M14	++	0	0
SK-MEL-2	0	0	+/−
SK-MEL-5	++	+/−	+/−
SK-MEL-28	+	0	0
UACC-62	+	0	+/−
UACC-257	+	0	0
Ovarian			
IGROV1	++	0	+
OVCAR-3	++++	+/−	+
OVCAR-4	+/−	0	+/−
OVCAR-5	+/−	0	0
OVCAR-8	+/−	+/−	+/−
SK-OV-3	+	−	++
Prostate			
LNCap	++	+/−	++
DU-145	+++	+	++
PC-3	++	+/−	+/−
PPC-1	+++	+/−	+
ALVA-31	++	+/−	+/−
Tsu-PRL	+	0	+/−
JCA-1	+/−	0	+/−
Renal			
786-0	+++	+/−	+/−
A498	+	0	0
ACHN	+++	0	0
CAKI-1	0	0	0
RXF-393	+/−	0	0
SN12C	+++	+/−	+
TK-10	+++	0	0
UO-31	+	0	0

immunohistochemical analyses of some of the corresponding normal tissues, such as hemopoietic and lymphoid organs, suggest this might be the case.

With few exceptions, the ~36-kDa BAG-1 protein was clearly the most abundant form of BAG-1 found in tumor lines. The BAG-1M (RAP46) protein reproducibly constituted <10% of the total BAG-1 in these malignant cell lines and was the least abundant isoform of BAG-1. In contrast, the BAG-1L protein was more variable in its expression, and in a few instances BAG-1L levels approached or were equivalent to the levels of ~36-kDa BAG-1 in tumor lines such as the breast cancer BT-549, the prostate cancer lines DU-145 and LN-CaP, and the leukemia line Jurkat. Indeed, breast cancer, prostate cancer, and leukemia cell lines were the most consistent expressors of the BAG-1L protein, with seven of seven prostate, seven of eight breast, and four of five leukemia cell lines containing immunodetectable levels of this protein. An intriguing possibility is that BAG-1L, with its proclivity for nuclear targeting, may contribute to the regulation of nuclear hormone receptor function in these types of tumors, given the prominent role played by androgen receptor, ER, and glucocorticoid receptor in cancers of the prostate, breast, and lymphoid organs, respectively. Also of potential relevance to the issue of BAG-1 and steroid hormone receptors was the finding that ovary and testis contained the highest relative amounts of BAG-1L protein among normal tissues, given that these tissues represent the principal sources of estrogen and androgen production. Thus, unidentified tissue-specific factors presumably influence the extent to which translation initiation can occur at the upstream noncanonical CTG codons relative to the usual ATG codon start-site within BAG-1 mRNAs. It remains to be determined whether dynamic fluctuations in the relative ratios of BAG-1 and BAG-1L play a role in the apparent variations in the intracellular location of BAG-1 immunostaining in steroid hormone-dependent tissues such as the prostate gland.

In summary, the findings presented here demonstrate the existence of additional forms of the BAG-1 protein in both humans and mice, including one that appears to arise through translation initiation from an upstream CTG within BAG-1 transcripts. The expression of BAG-1 is highly tissue specific and can vary in some instances with differentiation in particular cell lineages. The intracellular locations of BAG-1 proteins also differ among cell types, suggesting that interactions with other proteins modulate the locations of BAG-1 within cells. Delineating the mechanisms that control the translation initiation decision that gives rise to BAG-1L, BAG-1M, or BAG-1; contrasting the functions and intracellular locations of the BAG-1, BAG-1M, and BAG-1L proteins; and understanding how BAG-1 expression and function may become altered in cancer represent goals for the future.

ACKNOWLEDGMENTS

We thank T. Brown for manuscript preparation and Xiaokun Xiao for technical assistance.

REFERENCES

1. Takayama, S., Sato, T., Krajewski, S., Kochel, K., Irie, S., Millan, J. A., and Reed, J. C. Cloning and functional analysis of BAG-1: a novel Bcl-2 binding protein with anti-cell death activity. Cell, *80:* 279–284, 1995.
2. Clevenger, C. V., Thickman, K., Ngo, W., Chang, W-P., Takayama, S., and Reed, J. C. Role of Bag-1 in the survival and proliferation of the cytokine-dependent lymphocyte lines, Ba/F3 and Nb2. Mol. Endocrinol., *11:* 608–618, 1997.
3. Schulz, J. B., Bremen, D., Reed, J. C., Lommatzsch, J., Takayama, S., Wullner, U., Loschmann, P-A., Klockgether, T., and Weller, M. Cooperative interception of neuronal apoptosis by BCL-2 and BAG-1 expression: prevention of caspase activation and reduced production of reactive oxygen species. J. Neurochem., *69:* 2075–2086, 1997.
4. Terada, S., Fukuoka, K., Fujita, T., Komatsu, T., Takayama, S., Reed, J. C., and Suzuki, E. Anti-apoptotic proteins, bag-1 and bcl-2, improve survival and antibody

production by hybridoma cells under conditions of thymidine excess and serum deprivation. Cytotechnology, *25:* 17–23, 1997.
5. Takayama, S., Bimston, D. N., Matsuzawa, S., Freeman, B. C., Aime-Sempe, C., Xie, Z., Morimoto, R. J., and Reed, J. C. BAG-1 modulates the chaperone activity of Hsp70/Hsc70. EMBO J., *16:* 4887–4896, 1997.
6. Danen-van Oorschot, A. A. A. M., den Hollander, A., Takayama, S., Reed, J. C., van der Eb, A. J., and Noteborn, M. H. M. BAG-1 inhibits p53-induced but not apoptin-induced apoptosis. Apoptosis, *2:* 395–402, 1997.
7. Bardelli, A., Longati, P., Albero, D., Goruppi, S., Schneider, C., Ponzetto, C., and Comoglio, P. M. HGF receptor associates with the anti-apoptotic protein BAG-1 and prevents cell death. EMBO J., *15:* 6205–6212, 1996.
8. Jeffers, M., Rong, S., and Woude, G. F. Hepatocyte growth factor/scatter factor-Met signaling in tumorigenicity and invasion/metastasis. J. Mol. Med., *74:* 505–513, 1996.
9. Frisch, S. M., and Francis, H. Disruption of epithelial cell-matrix interactions induces apoptosis. J. Cell Biol., *124:* 619–626, 1994.
10. Adachi, M., Sekiya, M., Torigoe, T., Takayama, S., Reed, J. C., Miyazaki, T., Minami, Y., Taniguchi, T., and Imai, K. Interleukin-2 (IL-2) upregulates *BAG-1* gene expression through serine-rich region within IL-2 receptor beta c chain. Blood, *88:* 4118–4123, 1996.
11. Wang, H-G., Takayama, S., Rapp, U. R., and Reed, J. C. Bcl-2 interacting protein, BAG-1, binds to and activates the kinase Raf-1. Proc. Natl. Acad. Sci. USA, *93:* 7063–7068, 1996.
12. Hohfeld, J., and Jentsch, S. GrpE-like regulation of the hsc70 chaperone by the anti-apoptotic protein bag-1. EMBO J., *16:* 6209–6216, 1997.
13. Takayama, S., Kochel, K., Irie, S., Inazawa, J., Abe, T., Sato, T., Druck, T., Huebner, K., and Reed, J. C. Cloning of cDNAs encoding the human BAG1 protein and localization of the human *BAG1* gene to chromosome 9p12. Genomics, *35:* 494–498, 1996.
14. Packham, G., Brimmell, M., and Cleveland, J. L. Mammalian cells express two differently localized Bag-1 isoforms generated by alternative translation initiation. Biochem. J., *328:* 807–813, 1997.
15. Zeiner, M., and Gehring, U. A protein that interacts with members of the nuclear hormone receptor family: identification and cDNA cloning. Proc. Natl. Acad. Sci. USA, *92:* 11465–11469, 1995.
16. Reed, J., Meister, L., Cuddy, M., Geyer, C., and Pleasure, D. Differential expression of the *bcl-2* proto-oncogene in neuroblastomas and other human neural tumors. Cancer Res., *51:* 6529–6538, 1991.
17. Krajewski, S., Zapata, J. M., and Reed, J. C. Detection of multiple antigens on Western blots. Anal. Biochem., *236:* 221–228, 1996.
18. Krajewski, S., Krajewska, M., Shabaik, A., Miyashita, T., Wang, H-G., and Reed, J. C. Immunohistochemical determination of *in vivo* distribution of bax, a dominant inhibitor of bcl-2. Am. J. Pathol., *145:* 1323–1333, 1994.
19. Krajewski, S., Krajewska, M., Shabaik, A., Wang, H-G., Irie, S., Fong, L., and Reed, J. C. Immunohistochemical analysis of *in vivo* patterns of Bcl-X expression. Cancer Res., *54:* 5501–5507, 1994.
20. Krajewski, S., Bodrug, S., Krajewska, M., Shabaik, A., Gascoyne, R., Berean, K., and Reed, J. C. Immunohistochemical analysis of Mcl-1 protein in human tissues: differential regulation of Mcl-1 and Bcl-2 protein production suggests a unique role for Mcl-1 in control of programmed cell death *in vivo*. Am. J. Pathol., *146:* 1309–1319, 1995.
21. Krajewski, S., Tanaka, S., Takayama, S., Schibler, M. J., Fenton, W., and Reed, J. C. Investigation of the subcellular distribution of the bcl-2 oncoprotein: residence in the nuclear envelope, endoplasmic reticulum, and outer mitochondrial membranes. Cancer Res., *53:* 4701–4714, 1993.
22. Chomczynski, P. One-hour downward alkaline capillary transfer for blotting of DNA and RNA. Anal. Biochem., *201:* 134–139, 1992.
23. Sambrook, J., Fritsch, E. F., and Maniatis, T. Molecular Cloning: A Laboratory Manual, Ed. 2. Cold Spring Harbor, NY: Cold Spring Harbor Laboratory, 1989.
24. Hennighausen, L., and Lubon, H. Interaction of protein with DNA *in vitro*. Methods Enzymol., *152:* 721–735, 1987.
25. Kozak, M. Recognition of AUG and alternative initiator codons is augmented by G in position +4 but is not generally affected by the nucleotides in positions +5 and +6. EMBO J., *16:* 2482–2492, 1997.
26. Grunert, S., and Jackson, R. J. The immediate downstream codon strongly influences the efficiency of utilization of eukaryotic translation initiation codons. EMBO J., *13:* 3618–3630, 1994.
27. Robbins, J., Dilworth, S. M., Laskey, R. A., and Dingwall, C. Two interdependent basic domains in nucleoplasmin nuclear targeting sequence: identification of a class of bipartite nuclear targeting sequence. Cell, *64:* 615–623, 1991.
28. Dingwall, C., and Laskey, R. A. Nuclear targeting sequences—a consensus? Trends Biochem. Sci., *16:* 478–481, 1991.
29. Harrison, C. J., Hayer-Hartl, M., Di Liberto, M., Hartl, F-U., and Kuriyan, J. Crystal structure of the nucleotide exchange factor grpE bound to the ATPase domain of the molecular chaperone DnaK. Science (Washington DC), *276:* 431–435, 1997.
30. Florkiewicz, R. Z., Baird, A., and Gonzalez, A. M. Multiple forms of bFGF: differential nuclear and cell surface localization. Growth Factors, *4:* 265–275, 1991.
31. Quarto, N., Finger, F. P., and Rifkin, D. B. The NH2-terminal extension of high molecular weight bFGF is a nuclear targeting signal. J. Cell. Physiol., *147:* 311–318, 1991.
32. Monaghan, P., Robertson, D., Andrew, T., Amos, S., Dyer, M. J. S., Mason, D. Y., and Greaves, M. F. Ultrastructural localization of bcl-2 protein. J. Histochem. Cytochem., *40:* 1819–1825, 1992.

THE JOURNAL OF BIOLOGICAL CHEMISTRY
Vol. 276, No. 16, Issue of April 20, pp. 12718–12724, 2001
Printed in U.S.A.

Structure-Function Analysis of Bag1 Proteins

EFFECTS ON ANDROGEN RECEPTOR TRANSCRIPTIONAL ACTIVITY*

Received for publication, November 30, 2000, and in revised form, January 19, 2001
Published, JBC Papers in Press, January 19, 2001, DOI 10.1074/jbc.M010841200

Deborah A. Knee‡, Barbara A. Froesch‡§, Ulrike Nuber, Shinichi Takayama, and John C. Reed¶

From The Burnham Institute, La Jolla, California 92037

Bag1 is a regulator of heat shock protein 70 kDa (Hsp70/Hsc70) family proteins that interacts with steroid hormone receptors. Four isoforms of Bag1 have been recognized: Bag1, Bag1S, Bag1M (RAP46/HAP46), and Bag1L. Although Bag1L, Bag1M, and Bag1 can bind the androgen receptor (AR) *in vitro*, only Bag1L enhanced AR transcriptional activity. Bag1L was determined to be a nuclear protein by immunofluorescence microscopy, whereas Bag1, Bag1S, and Bag1M were predominantly cytoplasmic. Forced nuclear targeting of Bag1M, but not Bag1 or Bag1S, resulted in potent AR coactivation, indicating that Bag1M possesses the necessary structural features provided it is expressed within the nucleus. The ability of Bag1L to enhance AR activity was reduced with the removal of an NH_2-terminal domain of Bag1L, which was found to be required for efficient nuclear localization and/or retention. In contrast, deletion of a conserved ubiquitin-like domain from Bag1L did not interfere with its nuclear targeting or AR regulatory activity. Thus, both the unique NH_2-terminal domain and the COOH-terminal Hsc70-binding domain of Bag1L are simultaneously required for its function as an AR regulator, whereas the conserved ubiquitin-like domain is expendable.

Steroid receptors play a crucial role in the development and maintenance of many organs. The androgen receptor (AR)[1] is a ligand-activated transcription factor that is a member of the nuclear receptor superfamily (1). One tissue that exhibits profound dependence on the ligand for this nuclear hormone receptor is the prostate gland. In normal prostate, androgens induce production of growth factors in the stromal cells that cause growth of the luminal secretory epithelial cells (reviewed in Ref. 2). The AR controls gene expression programs in these epithelial cells, resulting in the expression of various proteins characteristic of the differentiated state including prostate-specific antigen (3). Tumors develop from the prostatic epithelial cells and ultimately become independent of the androgenic hormones. Endocrine therapy, either by reducing the levels of androgen or by blockading androgens at the level of the AR, usually results in a favorable clinical response and a dramatic regression of prostate cancer due to apoptotic cell death (4). However, after an initial response to androgen ablation, the prostate cancers eventually become unresponsive if endocrine therapy is continued long term (5).

It remains an open question whether the AR continues to play a role in hormone-independent prostate cancers. Many hormone-insensitive tumors have been found to retain a wild-type AR gene. Moreover, the AR gene is sometimes amplified, or its transcriptional activity may be increased in advanced prostate cancer (6). Therefore, a need exists to understand more about the factors that control the functions of the AR so that the mechanisms responsible for resistance to endocrine therapy can be revealed and eventually alleviated.

In the absence of the ligand, AR and most steroid hormone receptors are maintained in an inactive state complexed with heat shock proteins. Upon binding of the cognate ligand, the receptor dissociates from the inactive complex and translocates to the nucleus in which it binds specific response elements in the promoter and/or enhancer regions of responsive genes (reviewed in Ref. 7). Once bound to the nuclear response element, the nuclear receptor up-regulates or down-regulates transcription by transmitting signals directly to the transcriptional machinery via direct protein-protein interactions. In addition, another class of proteins called coactivators is recruited and serves as bridging molecules between the transcription initiation complex and the nuclear receptor (reviewed in Ref. 8).

Recently, an isoform of the human Bag1 protein (known as Bag1L) has been reported to bind the AR and enhance transcriptional activity in the presence of the ligand (9). Bag1 contains a COOH-terminal "BAG" domain that binds the ATPase domain of heat shock protein 70 kDa (Hsp70/Hsc70) family proteins (10–14) and modulates the activity of Hsc70/Hsp70 family chaperones *in vitro* and *in vivo*. Through this interaction with Hsc70, Bag1 is able to interact with a variety of intracellular proteins and regulate diverse cellular processes relevant to cancer including cell division, cell survival, and cell migration (15–20). However, it is also possible that other non-Hsc70-binding domains in the NH_2-terminal portion of Bag1 mediate interactions with target proteins, thus providing a mechanism for directing Hsc70 family chaperones to specific proteins in the cells. For example, Bag1 contains a ubiquitin-like (UBL) domain, which has been proposed to permit its direct binding to the 26 S proteosome (21). However, the significance of this and other NH_2-terminal regions in Bag1 for

* This work was supported in part by the United States Army Department of Defense Prostate Cancer Research Program Grant DAMD17-98-1-8584, the National Institutes of Health/National Cancer Institute Grant CA-67329, the Susan G. Komen Breast Cancer Foundation (to D. A. K.), The Schweizerische Stiftung fuer medizinisch-biologische Stipendien (to B. A. F.), and the State of California Cancer Research Program Grant CCRP99-00567V-10110). The costs of publication of this article were defrayed in part by the payment of page charges. This article must therefore be hereby marked "*advertisement*" in accordance with 18 U.S.C. Section 1734 solely to indicate this fact.

‡ Both authors contributed equally to the work.

§ Current address: Dept. of Molecular Biology, University of Zurich, Winterthurerstrasse 190, 857 Zurich, Switzerland.

¶ To whom correspondence should be addressed: The Burnham Inst., 10901 N. Torrey Pines Rd., La Jolla, CA 92037. Tel.: 858-646-3140; Fax: 858-646-3194; E-mail: jreed@burnham-inst.org.

[1] The abbreviations used are: AR, androgen receptor; Hsp, heat shock protein; UBL, ubiquitin-like; NLS, nuclear localization sequences; CAT, chloramphenicol acetyltransferase; CT-FBS, charcoal-treated fetal bovine serum; GST, glutathione *S*-transferase; PAGE, polyacrylamide gel electrophoresis; ARE, androgen response element.

transactivation of AR or other steroid hormone receptors is unknown.

It has been shown that at least four isoforms of Bag1 protein can arise from alternative initiation of translation within a common mRNA: Bag1S, Bag1, Bag1M (RAP46/HAP46), and Bag1L (22, 23). These isoforms all contain the Hsc70-binding BAG domain near the COOH terminus as well as the upstream UBL domain, but they differ in the lengths of their amino-terminal regions. Additional motifs have been recognized within the NH_2-terminal segment of the Bag1 proteins including candidate nuclear localization sequences (NLS) and variable numbers of TXSEEX repeat sequences (23, 24). Bag1L, the longest isoform, contains both an SV40-LargeT-like and nucleoplasmin-like candidate NLS preceded by a unique ~50 amino acid-domain. This Bag1 isoform is predominantly nuclear (23). Bag1M (RAP46/HAP46) contains only a portion of the candidate NLS and has been shown to reside in the cytosol unless stimulated to traffic into the nucleus by associating with other proteins, such as the glucocorticoid receptor (24). Bag1 and the shorter and rarer isoform of Bag1S are predominantly found in the cytosol (23).

Bag1 proteins have been reported to interact with and regulate the activity of several members of the nuclear receptor superfamily. For example, Bag1M and Bag1L have been found to repress the activity of the glucocorticoid receptor (24, 25), and Bag1 represses the transcriptional activity of retinoic acid receptors (27). Conversely, Bag1L but not Bag1M or Bag1 can potentiate the transcriptional activity of the AR (9). In this report, we have extended structure-function analysis of Bag1 protein with respect to their regulation of the AR.

MATERIALS AND METHODS

Plasmids—The plasmids pcDNA3-Bag1L, pcDNA3-Bag1L_C, and pcDNA3-Bag1 have been described previously (9). pcDNA3-Bag1M was generated from pcDNA3-Bag1/Bag1M (9) by mutating the initiation codon that gave rise to Bag1 from an ATG to an ATC so that this construct now can give rise only to Bag1M.

The cDNAs encoding various fragments of Bag1 were generated by polymerase chain reaction from the plasmid pcDNA3-Bag1L (9) using the following forward (F) and reverse (R) primers containing *Eco*RI and *Xho*I sites: Bag1S, 5′-GGGAATTCGCCACCATGGCGGCA-3′ (F1) and 5′-CCCTCGAGTCACTCGGCCAGGGCAAAG-3′ (R1); Bag1LΔ1–50, primer 5′-GCGGAATTCGCCACCATGACTGCCAGC-3′ (F2) and R1; Bag1LΔ1–16, 5′-GGGAATTCGAGCGGATGGGTTCCCG-3′ (F3) and R1; Bag1MΔC83, 5′-GGGAATTCATGAAGAAGAAAACCCGGCGCC-3′ (F4) and 5′-CCCCTCGAGTCAAAAACCCTGCTGGATTCCAG-3′ (R2); and Bag1C83 5′-GGGAATTCCTGCCCAAGGATTTGCAAGCTG-3′ and R1.

The polymerase chain reaction products were digested with *Eco*RI and *Xho*I and then directly cloned into the *Eco*RI and *Xho*I sites of the mammalian expression vector pcDNA3 (Bag1S and Bag1LΔ1–50) or pcDNA3-Myc (Bag1LΔ1–16, Bag1MΔC83, and Bag1C83).

The GST-Bag1 fusion proteins were generated from pGEX-4T-Bag1L, pGEX-4T-Bag1LΔC, pGEX-4T-Bag1, pGEX-4T-Bag1ΔC, pGEX-4T-Bag1M, pGEX-4T-Bag1MΔC83, and pGEX-4T-1-Bag1C83. These plasmids were all generated by subcloning the appropriate cDNAs from pcDNA3 clone into the *Eco*RI and *Xho*I sites of pGEX-4T-1 (Amersham Pharmacia Biotech). To generate the nuclear-targeted Bag1 proteins, the appropriate cDNA was subcloned from pcDNA3 clone into the *Eco*RI and *Xho*I sites of pcDNA3-NLS (generated by the insertion of an oligonucleotide containing the SV40-LargeT-like NLS into the *Hin*dIII-*Eco*RI sites of pcDNA3.1).

The reporter pLCI plasmid contains the full-length mouse mammary tumor virus long terminal repeat sequence linked with the chloramphenicol acetyltransferase (CAT) gene (28, 29). The pSG5-AR plasmid contains the cDNA for the wild-type AR (28).

Cell Culture—The monkey kidney COS-7 cell line was obtained from the American Type Culture Collection (Manassas, VA). Cells were maintained in a humidified atmosphere with 5% CO_2 in Dulbecco's modified Eagle's medium supplemented with 10% fetal calf serum, 3 mM glutamine, 100 units/ml penicillin, and 100 μg/ml streptomycin (Life Technologies, Inc.). One day prior to experiments, cells were transferred into charcoal-treated fetal bovine serum (CT-FBS) and Dulbecco's modified Eagle's medium minus Phenol Red to reduce background levels of steroids. R1881 (PerkinElmer Life Sciences) was dissolved in ethanol and added to the cultures at a minimum dilution of 0.0001% (v/v). Control cells received an equivalent amount of solvent only.

Transfections and Enzyme Assays—COS-7 cells at 60% confluency in 12-well plates (Nunc) were transfected by a lipofection method. 1.1 μg of DNA was diluted into 176.5 μl of Opti-MEM (Life Technologies, Inc.) and combined with 3 μl of LipofectAMINE (Life Technologies, Inc.) in 185.5 μl of Opti-MEM. After incubation for 20 min, 0.375 ml of Opti-MEM was added, and the mixtures were overlaid onto monolayers of cells. After culturing with 5% CO_2 for 5 h at 37 °C, 0.75 ml of Opti-MEM containing 20% CT-FBS was added to the cultures. At 32–36 h after transfection, cells were stimulated with 0.1 nM R1881. Cell extracts were prepared 48 h after transfection. For reporter gene assays, cell lysates were made as described previously (30), and assays for β-galactosidase and CAT activity were performed. All transfection experiments were carried out in duplicate, repeated at least three times, and normalized for β-galactosidase activity.

In Vitro Binding Assays—The AR was *in vitro* translated in reticulocyte lysates (TNT lysates, Promega) containing [^{35}S]methionine and then preincubated with 10 nM R1881 for 30 min. Glutathione *S*-transferase (GST) fusion proteins were immobilized on glutathione-Sepharose and blocked in NET-N buffer (20 mM Tris, pH 8.0, 20 mM NaCl, 1 mM EDTA) containing 0.1% Nonidet P-40 and 15% milk for 30 min. The immobilized GST proteins (10 μg) were incubated for 2 h with 10 μl of R1881 treated *in vitro* translated AR in NET-N buffer containing 0.1% Nonidet P-40, proteinase inhibitors, and 10 nM R1881. The beads were washed three times in NET-N buffer containing 0.5% Nonidet P-40 and then boiled in Laemmli SDS sample buffer. The use of equivalent amounts of intact GST fusion proteins and successful *in vitro* translated of the AR was confirmed by SDS-PAGE analysis using Coomassie Blue staining or autoradiography, respectively.

Immunofluorescence—Transfected COS-7 cells were fixed with a −20 °C chilled mix of methanol and acetone (1:1) for 2 min at 20 °C. After fixation the cells were blocked with phosphate-buffered saline containing 3% bovine serum albumin, 2% FBS, and 0.1% goat serum and then incubated for 4 h at 20 °C with anti-Bag1 antibody (Dako Corp., Carpinteria, CA) diluted 1:50 in blocking solution (31). After this incubation, cells were rinsed three times for 10 min with phosphate-buffered saline at 20 °C and then incubated with fluorescein isothiocyanate-conjugated anti-mouse IgG (Dako Corp.), diluted 1:50 in blocking solution for 2 h at 37 °C. Excess secondary antibody was thoroughly washed off with phosphate-buffered saline. The slides were then treated with Mowiol containing 1,4-diazabicylo[2.2.2]octane, and glass coverslips were applied. The stained slides were observed using a laser-scanning confocal microscope (Bio-Rad 1024MP).

Hormone Binding Assay—COS-7 cells at 60% confluency in 10-cm^2 plates were transiently transfected either with empty vectors or a combination of expression vectors encoding for AR, Bag1L, or Bag1 by a lipofection procedure. 10 μg of DNA was incubated with 26 μl of LipofectAMINE (Life Technologies, Inc.) for 20 min, and the mixtures were overlaid onto monolayers of cells. After culturing with 5% CO_2 at 37 °C for 5 h, 1 volume of Opti-MEM containing 20% charcoal-stripped fetal bovine serum (CT-FBS) was added to the cultures. Cells were transferred into 24-well plates 1 day later and grown in CT-FBS medium for an additional 24 h. To determine the hormone binding affinities of the transfected AR, cells were incubated for 2 h with increasing concentrations (0.1–10 nM) of [^{3}H]R1881 (86 ΔCi/nmol, PerkinElmer Life Sciences) in the presence or absence of a 100-fold molar excess of cold R1881. Cells were then washed three times with ice cold phosphate-buffered saline, and radioactivity was determined by scintillation counting. Specific binding was calculated by subtracting the counts/min of cells transfected with a control plasmid from the counts/min of samples transfected with the AR expression plasmid that was treated with the same concentration of the hormone. The results represent the means of three independent experiments.

RESULTS

BAG Domain of Bag1 Is Sufficient to Bind AR in Vitro—The human Bag1 protein exists as four isoforms (Fig. 1A), which all contain the same COOH-terminal Hsc70-binding domain and an upstream ubiquitin-like domain but differ in the lengths of their NH_2-terminal regions (23). The Bag1L and Bag1M (RAP46) isoforms of the human Bag1 protein have been previously shown to bind the AR *in vitro* (9, 25). To determine

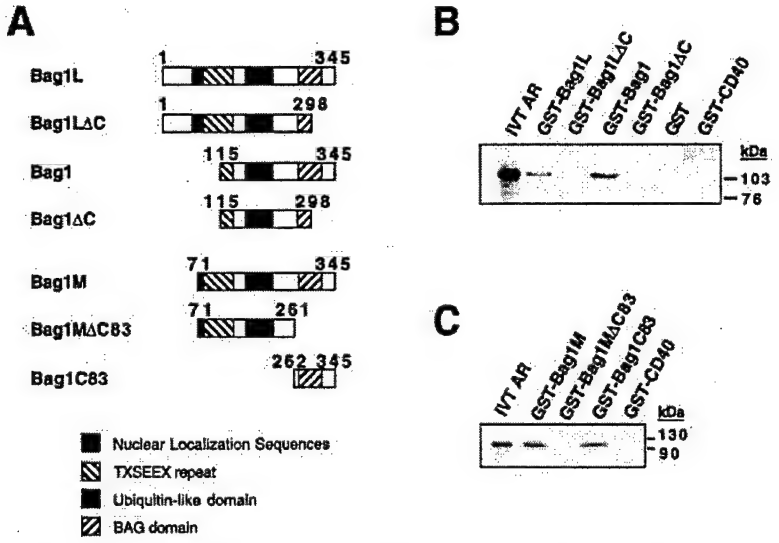

FIG. 1. **The BAG domain is necessary and sufficient for interacting with the AR *in vitro*.** *A*, a *schematic* shows the isoforms of the Bag1 protein, Bag1L, Bag1, Bag1M, and the following deletion mutants: Bag1ΔC and Bag1LΔC, which lack the COOH-terminal last 47 amino acids; Bag1M ΔC83, which lacks the COOH-terminal last 83 amino acids; and Bag1C83, which contains only the last 83 amino acids. The regions encoding the candidate nuclear localization sequences (*black box*), TXSEEX repeat (*downward diagonal striped box*), ubiquitin-like domain (*gray box*), and BAG domain (*upward diagonal striped box*) have been indicated. The *sequence numbers* all refer to the nucleotide numbers of Bag1L and indicate the start codon position for each isoform of Bag1 with respect to Bag1L. *B*, the interaction of the AR with various isoforms of Bag1 or COOH-terminal deletion mutants of these Bag1 proteins was tested by *in vitro* binding assays. The Bag1 isoforms and COOH-terminal mutants were expressed as GST fusion proteins and incubated with AR *in vitro* translated in the presence of [^{35}S]methionine. GST and GST fused to the cytoplasmic domain of CD40 were included as negative controls. GST-Bag1S failed to fold properly and could not be tested. *C*, the interaction of the AR with deletion mutants of Bag1 was tested by *in vitro* binding assays. The Bag1MΔC83 and Bag1C83 were expressed as GST fusion proteins and incubated with AR that was prepared by *in vitro* translation in the presence of [^{35}S]methionine.

whether other isoforms of the human Bag1 protein could interact with the AR, we performed *in vitro* protein interaction assays. The Bag1 isoforms were fused to GST and incubated with *in vitro* translated radiolabeled AR. As shown in Fig. 1*B*, the AR specifically interacted with Bag1L and Bag1 but not with the control proteins GST and GST-CD40. Mutants of Bag1L and Bag1, which lack the COOH-terminal Hsc70-binding domain (ΔC), were unable to interact with the AR in these assays, indicating that the BAG domain is required for interactions with the AR. Moreover, a GST-fusion protein containing only the last COOH-terminal 83 amino acids, GST-Bag1C83, was sufficient for binding to AR under these conditions (Fig. 1*C*). Therefore, we conclude that the BAG domain of Bag1 protein is necessary and sufficient for associating with the AR.

Nuclear Targeting of the Cytoplasmic Bag1 Is Insufficient for Potentiating AR Activity—Although all isoforms of Bag1 interact with the AR *in vitro*, only the Bag1L protein significantly enhances the transcriptional activity of the AR *in vivo* (9). Because the ligand-bound AR is localized to the nucleus (7), only isoforms of the Bag1 protein that are nuclear would be expected to enhance the transcriptional activity of the AR. Therefore, we checked the compartmentalization of the Bag1 proteins by immunofluorescence. COS-7 cells were transfected with plasmids encoding the various Bag1 isoforms followed by immunostaining with an anti-Bag1 monoclonal antibody and analysis by confocal laser-scanning microscopy. Bag1L is exclusively a nuclear protein, whereas all other Bag1 isoforms are predominantly cytosolic (Fig. 2, *left panels*). These findings are consistent with the presence of both nucleoplasmin-like and SV40-LargeT-like nuclear-targeting sequence in the Bag1L protein (22, 23) but not Bag1M, Bag1, or Bag1S. Although the Bag1M (RAP46/HAP46) isoform contains a region of basic residues suggestive of a nuclear targeting sequence (25), it is evidently transported inefficiently into the nucleus. Interestingly, the Bag1L protein may be associated with nuclear substructures given the speckled pattern of the immunofluorescence observed (Fig. 2).

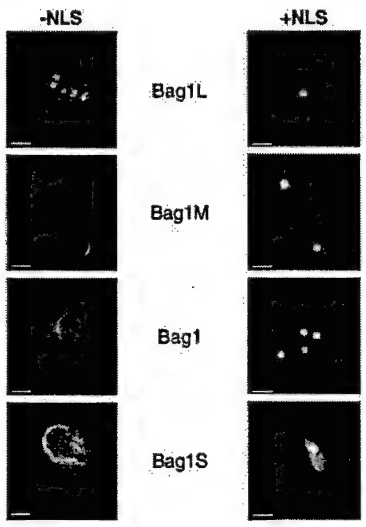

FIG. 2. **Bag1L is the only isoform of Bag1 that is nuclear.** COS-7 cells were transfected with 0.5 μg of pcDNA3-Bag1L, pcDNA3-Bag1M, pcDNA3-Bag1, pcDNA3-Bag1S, pcDNA3-NLS-Bag1L, pcDNA3-NLS-Bag1M, pcDNA3-NLS-Bag1, or pcDNA3-NLS-Bag1S. At 30 h post-transfection, cells were fixed, stained with a monoclonal antibody recognizing Bag1, and visualized using a laser confocal microscope. The nucleus and nucleoli are immunopositive in all transfectants involving NLS-targeted proteins (*right column*).

The difference in cellular distribution of the Bag1 proteins represents a possible explanation for the inability of the cytosolic Bag1 isoforms to enhance the transcriptional activity of the AR. To address this issue, we constructed plasmids that express Bag1L, Bag1M, Bag1, or Bag1S fused to SV40-LargeT-like nuclear-targeting sequences. Nuclear localization of these

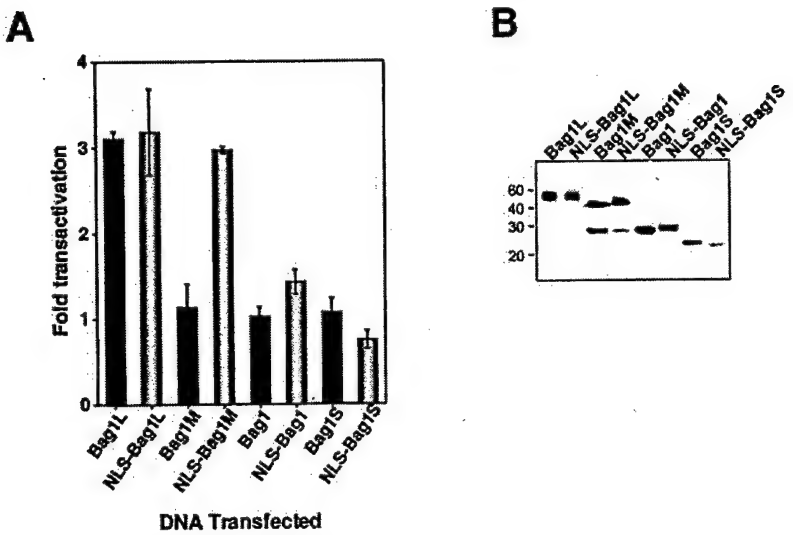

FIG. 3. **Targeting of Bag1M but not the shorter Bag1 isoforms to the nucleus confers the ability to enhance AR-mediated transactivation.** *A*, COS-7 cells were transfected with 0.06 μg of pSG5-AR, 0.5 μg of pLCI, 0.04 μg of pCMV-β-galactosidase, and various amounts of one of the following Bag1 expression plasmids: pcDNA3-Bag1L, pcDNA3-Bag1M, pcDNA3-Bag1, pcDNA3-Bag1S, pcDNA3-NLS-Bag1L, pcDNA3-NLS-Bag1M, pcDNA3-NLS-Bag1, or pcDNA3-NLS-Bag1S. Total DNA was maintained at 1.1 μg by the addition of pcDNA3 control plasmid. At 30 h after transfections, cells were stimulated with 1 nM R1881. Cell extracts were prepared and assayed for CAT and β-galactosidase activity at 40 h after transfection (mean ± S.E., $n = 2$). *B*, COS-7 cells were transfected with one of the following Bag1 expression plasmids: pcDNA3-Bag1L, pcDNA3-Bag1M, pcDNA3-Bag1, pcDNA3-Bag1S, pcDNA3-NLS-Bag1L, pcDNA3-NLS-Bag1M, pcDNA3-NLS-Bag1, or pcDNA3-NLS-Bag1S. At 30 h after transfection, cells were lysed in radioimmune precipitation buffer. Cell extracts (25 μg of total protein) were subjected to SDS-PAGE/immunoblot assay and probed with an antibody to Bag1. The Bag1 expression plasmid pcDNA3-Bag1M produces both the Bag1M and Bag1 proteins due to translational initiation from an internal AUG in Bag1M.

NLS-Bag1 proteins was verified by transfecting COS-7 cells with plasmids expressing the nuclear-targeting Bag1 isoforms and then immunostaining with an antibody that recognizes Bag1 (Fig. 2, *right panels*). Confocal laser-scanning microscopy analysis revealed that all the Bag1 isoforms are located exclusively in the nucleus of transfected cells.

The effects of these nuclear-targeted Bag1 isoforms on AR transcriptional activity were then tested by transfection into COS-7 cells together with an AR-expressing plasmid and an ARE-containing reporter gene. The cells were stimulated with R1881 to activate AR. As shown in Fig. 3*A*, the fusion of heterologous nuclear-targeting sequences to the 5′ end of Bag1L did not alter its ability to enhance the transcriptional activity of the AR. Targeting of Bag1M to the nucleus but not Bag1 or Bag1S was sufficient to enhance the transcriptional activity of the AR. Taken together, these results suggest that the first 70 amino acids of Bag1L are expendable for AR coactivation, whereas the NH_2-terminal region of Bag1M corresponding to amino acids 71–115 of Bag1L is required in conjunction with nuclear localization for enhancing AR function.

Immunoblot analysis showed that the levels of all Bag1 isoforms produced in cells (except Bag1S) were comparable to the nuclear-targeted isoforms, excluding quantitative differences in the levels of these proteins as a trivial explanation for the results (Fig. 3*B*). The difference in the level of expression of Bag1S and NLS-Bag1S makes it difficult to conclude that NLS-Bag1S is without effect on AR-mediated transactivation. The absence of Bag1S from the nucleus would argue against its role in transactivation.

The NH_2-terminal Region of Bag1L Is Required for Efficient Nuclear Localization—The observation that Bag1L is the only isoform that is nuclear suggests that the unique NH_2-terminal domain of Bag1L might perform a role in nuclear targeting or retention. We therefore generated two NH_2-terminal truncation mutants of Bag1L lacking either the first 16 amino acids of Bag1L (Bag1LΔ1–16) or retaining the nuclear-targeting sequences of Bag1L but lacking the NH_2-terminal 50 amino acids that differentiate it from the Bag1M protein (Bag1LΔ1–50).

Both the Bag1LΔ1–16 and Bag1LΔ1–50 proteins retain the candidate nuclear-targeting sequences of Bag1L and therefore should target to nuclei similar to Bag1L. To explore this option, COS-7 cells were transfected with plasmids encoding Bag1LΔ1–16, Bag1LΔ1–50, or Bag1L, and the localization of the resulting proteins was determined by immunofluorescence confocal microscopy. Bag1L and Bag1LΔ1–16 exhibited essentially the same compartmentalization pattern within the cell (Fig. 4*B*, *upper panels*), demonstrating a nuclear speckled pattern of immunostaining. In contrast, the Bag1LΔ1–50 protein was more promiscuous in its subcellular localization. Whereas Bag1LΔ1–50 was found in the same nuclear substructures as Bag1L, the protein was also found in a diffuse cytosolic staining pattern in transfected cells. This finding suggests that amino acids 17–50 of Bag1L may contain sequences necessary for optimal retention of Bag1L in the nucleus.

To contrast these subcellular localization results with coactivation function, COS-7 cells were cotransfected with the AR, an ARE-containing reporter gene, and plasmids encoding Bag1L, Bag1LΔ1–16, or Bag1LΔ1–50. The transfected cells were then stimulated with the synthetic androgen R1881. Bag1LΔ1–50 but not Bag1LΔ1–16 exhibited a decreased ability to enhance the transcriptional activity of the AR (Fig. 4*D*). Taken together, these observations suggest that the correct nuclear targeting/retention of Bag1L is required for optimal functional interactions of Bag1L and the AR.

To confirm this finding, we fused a nuclear-targeting sequence to Bag1L, Bag1LΔ1–16, and Bag1LΔ1–50 and transiently transfected the NLS-fusion constructs into COS-7 cells. Confocal immunofluorescence analysis revealed that NLS-Bag1L, NLS-Bag1LΔ1–16, and NLS-Bag1LΔ1–50 exhibit essentially the same nuclear pattern within the cell (Fig. 4*B*, *lower panels*). Targeting of Bag1L and Bag1LΔ1–16 to the nucleus did not significantly alter their effect on the AR, however, nuclear-targeting of Bag1LΔ1–50 markedly improved its ability to enhance AR transcriptional activity (Fig. 4*D*). Immu-

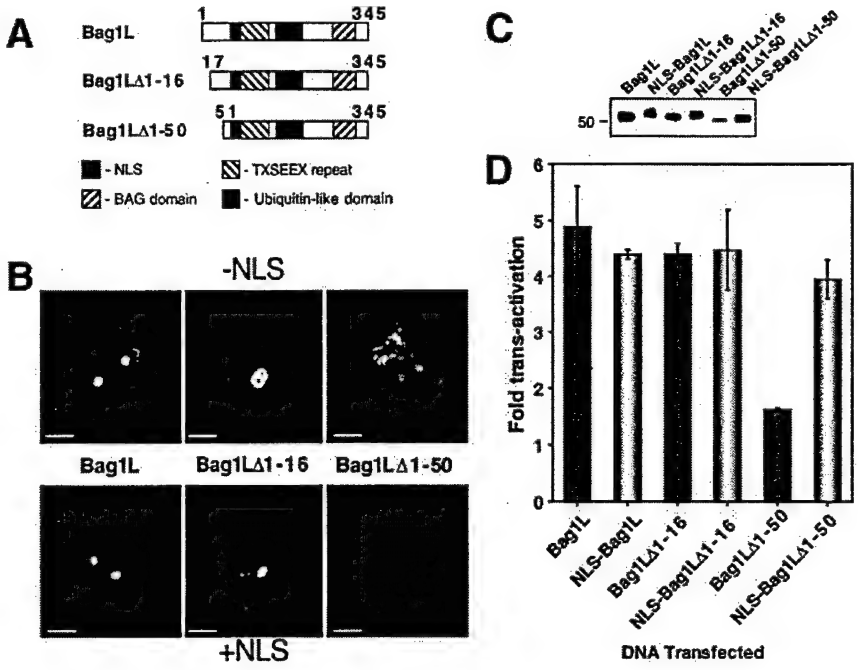

FIG. 4. **The NH_2 terminus of Bag1L is required for its targeting/retention in the nucleus.** *A*, a *schematic* is presented showing deletion mutants of Bag1L, which are lacking the NH_2-terminal 16 (*Bag1LΔ1–16*) or 50 amino acids (*Bag1LΔ1–50*). *B*, COS-7 cells were translated with the following Bag1 expression plasmids: pcDNA3-Bag1L, pcDNA3-Bag1LΔ1–16, pcDNA3-Bag1LΔ1–50, pcDNA3-NLS-Bag1L, pcDNA3-NLS-Bag1LΔ1–16, or pcDNA3-NLS-Bag1LΔ1–50. At 30 h post-transfection, cells were fixed, stained, and examined by laser confocal microscopy. *C*, COS-7 cells were transfected as in *A*, and after 30 h the cells were lysed in radioimmune precipitation buffer. Cell extracts (25 μg of total protein) were subjected to SDS-PAGE/immunoblot assay and probed with an antibody to Bag1. *D*, COS-7 cells were transfected with 0.06 μg of pSG5-AR, 0.5 μg of pLCI, 0.04 μg of pCMV-β-galactosidase, and various amounts of the Bag1 expression plasmids used in *B*. Total DNA was maintained at 1.1 μg by the addition of pcDNA3 control plasmid. At 30 h after transfection, cells were stimulated with 1 nM R1881. Cell extracts were prepared and assayed for CAT and β-galactosidase activity at 40 h after transfection (mean ± S.E., $n = 2$).

noblot analysis revealed that all Bag1 isoforms were expressed at similar levels (Fig. 4*C*).

The Ubiquitin-like Domain of Bag1L Is Not Required for Enhancing Transcriptional Activity of AR—The Bag1 protein contains a UBL domain that is conserved within the Bag1 homologues of *Caenorhabditis elegans* and *Schizosaccharomyces pombe* (32). To explore whether this region has functional significance in the enhancement of AR-mediated transcription, we constructed a deletion mutant of Bag1L lacking this region (Bag1LΔUBL) (Fig. 5*A*). COS-7 cells were cotransfected with plasmids expressing Bag1LΔUBL, AR, and an ARE-containing reporter gene plasmid and then stimulated with R1881. As illustrated in Fig. 5*B*, deletion of the UBL domain from Bag1L did not alter its ability to enhance AR-mediated transcription in reporter gene assays, suggesting that this region of Bag1L is not required for functional interactions of Bag1L and the AR. Immunoblot analysis showed that the levels of Bag1LΔUBL produced in cells was comparable to Bag1L (Fig. 5*C*). COS-7 cells were transfected with plasmids encoding Bag1LΔUBL or Bag1L, and the localization of the resulting proteins was determined by immunofluorescence confocal microscopy. Bag1L and Bag1LΔUBL exhibited essentially the same compartmentalization pattern within the cell (Fig. 5*D*), demonstrating a nuclear speckled pattern of immunostaining.

Bag1 Proteins Do Not Alter the Affinity of the AR for Its Ligand—Heat shock proteins and other molecular chaperones are required for placing steroid hormone receptors into a state that is competent to bind steroid ligands (33, 34). The ability of Bag1 proteins to bind and modulate the function of Hsp70/Hsc70 family molecular chaperones (10), therefore, could conceivably alter the ability of AR to bind androgenic hormones. Therefore, we determined the hormone binding affinity of the AR in whole cells in the absence or presence of overexpressed Bag1 or Bag1L. As depicted in Fig. 6*A*, the presence of elevated levels of either Bag1 or Bag1L did not significantly influence the amount of hormone bound to the receptors at any of the hormone concentrations tested. In addition, as revealed by Scatchard analysis (Fig. 6, *B–D*), neither Bag1 nor Bag1L significantly altered the apparent equilibrium binding constant (K_d) for R1881. Therefore, Bag1L exerts its influence on AR-mediated transcription at a stage other than ligand binding.

DISCUSSION

The data presented here confirm that Bag1L is the only isoform of Bag1 capable of enhancing the transcriptional activity of the AR (9). Thus, despite evidence that Bag1M and Bag1 can interact with the AR *in vitro*, only Bag1L interacts with AR in cells (9) and alters its transactivation function. Because Bag1L is the only isoform that is constitutively present in the nucleus, one possible explanation is that the higher nuclear levels of Bag1L may be responsible for its physical and functional interactions with AR complexes. Previous studies have shown that Bag1L does not alter the ligand-dependent nuclear translocation of the AR (9).

The appendage of an exogenous nuclear-targeting sequence to Bag1M, Bag1, and Bag1S is sufficient to force these proteins into the nucleus. This forced nuclear targeting bestowed upon Bag1M but not Bag1 or Bag1S the ability to coactivate the AR. Therefore, it appears that additional structural differences in Bag1L and Bag1M compared with Bag1 and Bag1S play an important role in the differential effects of these proteins on the AR. Recent papers have suggested that the TXSEEX repeat found in 8, 8, and 2 copies, respectively, in Bag1L, Bag1M, and Bag1 is required for repression of the transcriptional activity of the glucocorticoid receptor (24). Thus, these TXSEEX motifs may be important for functional collaboration of Bag1 with AR as both Bag1L and Bag1M are effective at potentiating AR function when expressed within the nucleus, whereas Bag1 is not.

By deleting the NH_2-terminal region of Bag1L, we demonstrated a function for this unique proline-rich domain for the first time. Subcellular localization experiments indicated that although Bag1L and Bag1LΔ1–16 were localized to nuclear substructures, Bag1LΔ1–50 protein was present diffusely throughout the cells. Therefore, the region between amino acids 17 and 50 of Bag1L was found to be required for its efficient import into nuclei or retention within the nucleus. We speculate that this NH_2-terminal region of Bag1L participates

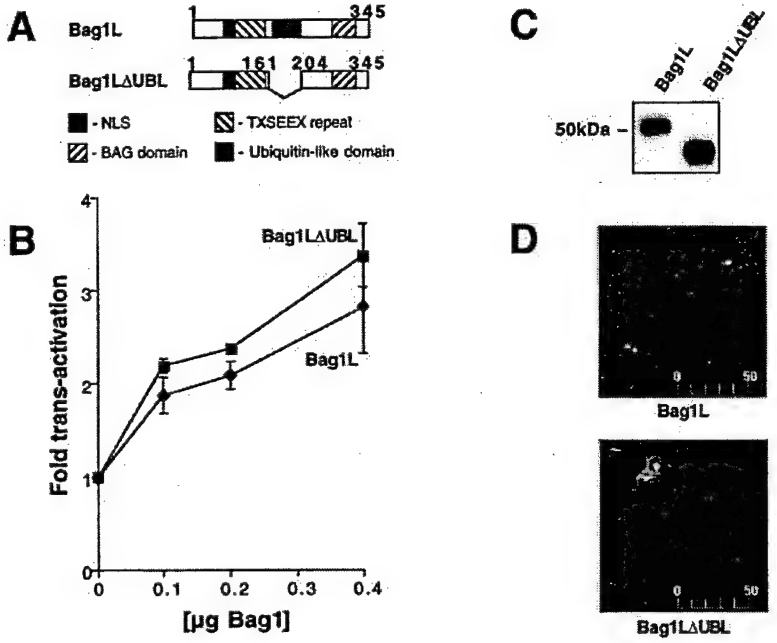

FIG. 5. **Deletion of the ubiquitin-like domain of Bag1L does not alter its ability to enhance AR-mediated transactivation of an ARE-containing reporter.** *A,* a *schematic* is presented showing a deletion mutants of Bag1L that lacks the ubiquitin-like domain. *B,* COS-7 cells were transfected with 0.06 μg of pSG5-AR, 0.5 μg of pLCI, 0.04 μg of pCMV-β-galactosidase, and various amounts of pcDNA3-Bag1L or pcDNA3-Bag1LΔUb. Total DNA was maintained at 1.1 μg by the addition of pcDNA3 control plasmid. At 30 h after transfection, cells were stimulated with 1 nM R1881. Cell extracts were prepared and assayed for CAT and β-galactosidase activity at 40 h after transfection (mean ± S.E., $n = 2$). *C,* COS-7 cells were transfected as in *B*, and after 30 h the cells were lysed in radioimmune precipitation buffer. Cell extracts (25 μg of total protein) were subjected to SDS-PAGE/immunoblot assay and probed with an antibody to Bag1. *D,* COS-7 cells were transfected as in *B*, and at 30 h post-transfection, cells were fixed, stained with a monoclonal antibody recognizing Bag1, and visualized under a laser confocal microscope.

in interactions with the nuclear proteins that serve to anchor Bag1L firmly in the nucleus.

In contrast, deletion of the UBL domain from Bag1L did not impair subcellular targeting or functional collaboration with the AR. A wide variety of proteins have been shown to contain UBLs (reviewed in Ref. 35). These domains can mediate direct interactions with subunits of the proteosome that recognize polyubiquitin chains on proteins that have been targeted for destruction. Recently, Bag1 was reported to bind the 26 S proteosome *in vitro*. The UBL domain is found within all four Bag1 isoforms and is conserved in the Bag1 homologues of other species including the yeast *S. pombe* and the nematode *C. elegans* (32), implying an evolutionarily conserved role for this domain in some aspect of Bag1 function. However, deletion of the UBL domain did not abrogate the stimulatory effect of Bag1L on AR function. Thus, whatever the function of the conserved UBL domain of Bag1 may be, it is expendable for coactivation of steroid hormone receptors.

Similar to the NH_2-terminal unique domain, the COOH-terminal region of Bag1 that is required for Hsc70 binding was found to be essential for potentiation of AR activity. The data reported here and elsewhere indicate that the COOH-terminal Hsc70-binding domain of Bag1 and Bag1L is required for interactions with AR *in vitro* and for coimmunoprecipitation of Bag1L with AR from cell lysates (9). Moreover, we presented novel evidence here that the BAG domain of Bag1 is sufficient for association with the AR *in vitro*. It has therefore been postulated that the interaction of Bag1L with the AR may involve Hsp70. Hsp70/Hsc70 along with Hsp90 and Hsp56 are involved in maintaining nuclear receptors in an inactive conformation in the cytoplasm. Thus, it is possible that Hsc70/Hsp70 family molecular chaperones provide a bridge between the AR and Bag1L. Alternatively, Hsp70 and AR may compete for binding to the BAG domain as has been determined recently for Hsp70 and Raf-1 (36).

Molecular chaperones perform several important functions in the regulation of steroid hormone receptors. For example, a variety of chaperones including Hsc70/Hsp70 is required to achieve receptor conformations that are competent to bind steroid ligands. Thus, enhanced ligand binding represents one possible explanation for the mechanism by which Bag1L poten-

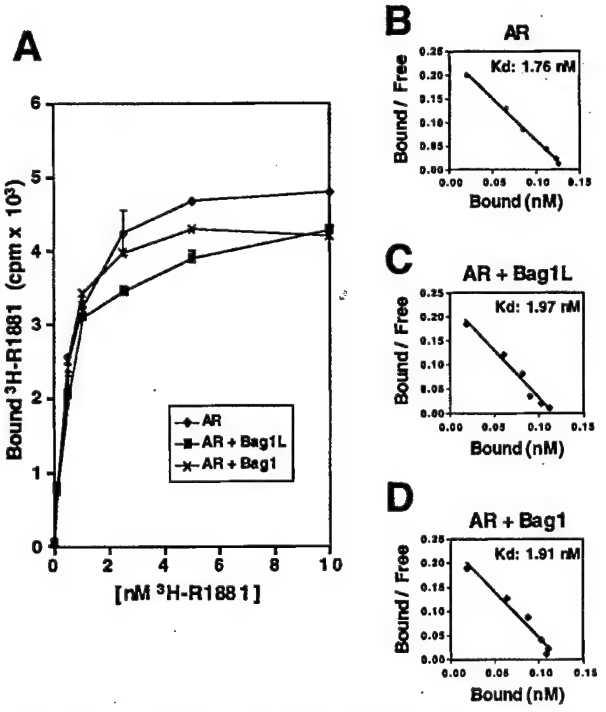

FIG. 6. **Effect of Bag1 and Bag1L on R1881 binding affinity of the AR.** COS-7 cells were transfected with either an empty vector or with expression vectors encoding AR and Bag1 or Bag1L. At 2 days after transfection, cells were incubated in the indicated concentration of [^{3}H]R1881 in the presence or absence of a 100-fold molar excess of cold R1881. The bound radioactivity was calculated by subtracting the amount of radioactivity incorporated in the presence of competitor from the amount incorporated in the absence of competitor. *A,* bound [^{3}H]R1881 as a function of hormone concentration in cells transfected with AR alone (*diamonds*) or in combination with either Bag1 (*crosses*) or Bag1L (*squares*). *B–D,* Scatchard analyses of the data represented in *A*, indicating the calculated K_d for R1881 of AR in the presence or absence of Bag1 and Bag1L. Data represent the mean ± S.E. of three independent experiments.

tiates AR function. If true, however, we would have expected the other isoforms of Bag1 also to potentiate AR activity, given that translation and folding of the AR occurs in the cytosol where the unliganded AR resides in a complex with Hsp90 and other chaperones. Thus, the data reported here demonstrating a lack of effect of Bag1 on the ligand binding affinity of the AR are consistent with the observed differences in the ability of nuclear and cytosolic isoforms of Bag1 to enhance AR activity. In addition, because heat shock proteins sequester AR in the cytosol in an inactive state until bound by specific steroid ligands, it was also possible that Bag1 proteins might regulate cytosol to nuclear translocation of AR, however, we previously demonstrated that this is not the case (9).

Given that Bag1L does not alter the affinity of AR for steroid ligands and does not modulate nuclear translocation of AR, we speculate that it potentiates AR function either by affecting coactivator binding to AR or by altering AR affinity for DNA-binding sites. Interestingly, it has been reported that Bag1M is able to bind to DNA and stimulate basal transcription machinery directly *in vitro* (25). Thus, Bag1L interactions with AR could conceivably increase the affinity of AR-containing transcription complexes for DNA, thereby enhancing transcriptional output of AR-responsive genes. However, given that we failed to see any affect of Bag1L on the binding of the AR to an ARE in gel retardation assays (data not shown), this observation alone cannot account for the unique effects of Bag1L on AR.

Taken together, the data reported here imply that at least two domains within Bag1L are important for its functional collaboration with the AR, namely the TXSEEX repeats and the COOH-terminal BAG domain, which binds Hsp70/Hsc70 family molecular chaperones. Multiple explanations can be envisioned for how these two domains might participate in the regulation of AR. For example, both of these domains might directly or indirectly bind AR. In this regard, it may be relevant that several coactivators of nuclear receptors, such as GRIP-1 and SRC-1, make multiple interactions with nuclear receptors through different domains (26, 37). However, it is equally probable that the BAG domain alone mediates interactions of Bag1L with AR, whereas the TXSEEX repeats associate with other proteins such as coactivators. Difficulties in producing soluble stable TXSEEX repeats alone have precluded us from distinguishing these two mechanisms to date. Another aspect of Bag1L effects on AR is that they may be indirect, involving Bag1L/Hsc70-induced conformational changes in AR that enhance its interactions with coactivators or reduce interactions with corepressors.

Given that only the Bag1L isoform of Bag1 collaborates functionally with the AR, one mechanism by which tissues could alter their responsiveness to androgens is by adjusting the levels of the Bag1L protein produced. The human *bag1* mRNA can generate up to four protein products through alternative mRNA translation from various canonical AUG or non-canonical CUG codons (22, 23). The mouse *bag1* mRNA similarly can produce up to three protein products but lack the AUG that is responsible for generating Bag1M (RAP46) (23). In human tissues and tumor cell lines, it has also been shown that Bag1 and Bag1L are by far the most abundant isoforms of Bag1 produced with little or no Bag1M or Bag1S present (23). Interestingly, whereas Bag1 is ubiquitously expressed throughout the organs of mice and humans, Bag1L production is tissue-specific and found predominantly in hormone-sensitive tissues, such as the testis, ovary, breast, and prostate. Also, in human tumor cell lines, levels of Bag1L tend to be highest in hormone-dependent cancers, such as prostate (AR), breast (estrogen receptor (ER), progesterone receptor (PR), and lymphoid (glucocorticoid receptor) malignancies in which steroid hormones are known to play major roles in the regulation of cell growth, differentiation, and death. Given that Bag1L enhances the transactivation function of AR and that it has been shown to render AR less inhibitable by anti-androgenic drugs (9), it will be interesting to determine whether the levels of Bag1L change during the progression of prostate cancers as they undergo conversion from hormone-responsive to hormone-refractory disease.

Acknowledgments—We thank Dr. Chawnshang Chang for AR and ARE-CAT plasmids and Rachel Cornell for manuscript preparation.

REFERENCES

1. Evans, R. M. (1988) *Science* **240,** 889–895
2. Thompson, T. C. (1990) *Cancer Cells* **2,** 345–354
3. Wolf, D. A., Schulz, P., and Fittler, F. (1992) *Mol. Endocrinol.* **6,** 753–762
4. Westin, P., Stattin, P., Damber, J. E., and Bergh, A. (1995) *Am. J. Pathol.* **146,** 1368–1375
5. Lepor, H., Ross, A., and Walsh, P. C. (1982) *J. Urol.* **128,** 335–340
6. de Vere, W. R., White, R., Meyers, F., Chi, S. G., Chamberlain, S., Siders, D., Lee, F., Stewart, S., and Gumerlock, P. H. (1997) *Cancer Res.* **57,** 314–319
7. Tsai, M. J., and O'Malley, B. W. (1994) *Annu. Rev. Biochem.* **63,** 451–486
8. Freedman, L. P. (1999) *Cell* **97,** 5–8
9. Froesch, B. A., Takayama, S., and Reed, J. C. (1998) *J. Biol. Chem.* **273,** 11660–11666
10. Takayama, S., Bimston, D. N., Matsuzawa, S., Freeman, B. C., Aime-Sempe, C., Xie, Z., Morimoto, R. J., and Reed, J. C. (1997) *EMBO J.* **16,** 4887–4896
11. Zeiner, M., Gebauer, M., and Gehring, U. (1997) *EMBO J.* **16,** 5483–5490
12. Höhfeld, J., and Jentsch, S. (1997) *EMBO J.* **16,** 6209–6216
13. Bimston, D., Song, J., Winchester, D., Takayama, S., Reed, J. C., and Morimoto, R. I. (1998) *EMBO J.* **17,** 6871–6878
14. Nollen, E. A., Brunsting, J. F., Song, J., Kampinga, H. H., and Morimoto, R. I. (2000) *Mol. Cell. Biol.* **20,** 1083–1088
15. Takayama, S., Sato, T., Krajewski, S., Kochel, K., Irie, S., Millan, J. A., and Reed, J. C. (1995) *Cell* **80,** 279–284
16. Wang, H.-G., Takayama, S., Rapp, U. R., and Reed, J. C. (1996) *Proc. Natl. Acad. Sci. U. S. A.* **93,** 7063–7068
17. Bardelli, A., Longati, P., Albero, D., Goruppi, S., Schneider, C., Ponzetto, C., and Comoglio, P. M. (1996) *EMBO J.* **15,** 6205–6212
18. Clevenger, C. V., Thickman, K., Ngo, W., Chang, W.-P., Takayama, S., and Reed, J. C. (1997) *Mol. Endocrinol.* **11,** 608–618
19. Matsuzawa, S., Takayama, S., Froesch, B. A., Zapata, J. M., and Reed, J. C. (1998) *EMBO J.* **17,** 2736–2747
20. Naishiro, Y., Adachi, M., Okuda, H., Yawata, A., Mitaka, T., Takayama, S., Reed, J., Hinoda, Y., and Imai, K. (1999) *Oncogene* **18,** 3244–3251
21. Luders, J., Demand, J., and Höhfeld, J. (2000) *J. Biol. Chem.* **275,** 4613–4617
22. Packham, G., Brimmell, M., and Cleveland, J. L. (1997) *Biochem. J.* **328,** 807–813
23. Takayama, S., Krajewski, S., Krajewska, M., Kitada, S., Zapata, J. M., Kochel, K., Knee, D., Scudiero, D., Tudor, G., Miller, G. J., Miyashita, T., Yamada, M., and Reed, J. C. (1998) *Cancer Res.* **58,** 3116–3131
24. Schneikert, J., Hübner, S., Martin, E., and Cato, A. C. B. (1999) *J. Cell Biol.* **146,** 929–940
25. Zeiner, M., and Gehring, U. (1995) *Proc. Natl. Acad. Sci. U. S. A.* **92,** 11465–11469
26. Ma, H., Hong, H., Huang, S. M., Irvine, R. A., Webb, P., Kushner, P. J., Coetzee, G. A., and Stallcup, M. R. (1999) *Mol. Cell. Biol.* **19,** 6164–6173
27. Liu, R., Takayama, S., Zheng, Y., Froesch, B., Chen, G.-Q., Zhang, X., Reed, J. C., and Zhang, X.-K. (1998) *J. Biol. Chem.* **273,** 16985–16992
28. Lee, H. J., Kokontis, J., Wang, K. C., and Chang, C. (1993) *Biochem. Biophys. Res. Commun.* **194,** 97–103
29. Mowszowicz, I., Lee, H. J., Chen, H. T., Mestayer, C., Portois, M. C., Cabrol, S., Mauvais-Jarvis, P., and Chang, C. (1993) *Mol. Endocrinol.* **7,** 861–869
30. Nielsen, D. A., Chang, T. C., and Shapiro, D. J. (1989) *Anal. Biochem.* **179,** 19–23
31. Takayama, S., Kochel, K., Irie, S., Inazawa, J., Abe, T., Sato, T., Druck, T., Huebner, K., and Reed, J. C. (1996) *Genomics* **35,** 494–498
32. Takayama, S., Xie, Z., and Reed, J. (1999) *J. Biol. Chem.* **274,** 781–786
33. Veldscholte, J., Berrevoets, C. A., Brinkmann, A. O., Grootegoed, J. A., and Mulder, E. (1992) *Biochemistry* **31,** 2393–2399
34. Fang, Y., Fliss, A. E., Robins, D. M., and Caplan, A. J. (1996) *J. Biol. Chem.* **271,** 28697–28702
35. Jentsch, S., and Pyrowolakis, G. (2000) *Trends Cell Biol.* **10,** 335–342
36. Beere, H. M., Wolf, B. B., Cain, K., Mosser, D. D., Mahboubi, A., Kuwana, T., Tailor, P., Morimoto, R. I., Cohen, G. M., and Green, D. R. (2000) *Nat. Cell Biol.* **2,** 469–475
37. Onate, S. A., Boonyaratanakornkit, V., Spencer, T. E., Tsai, S. Y., Tsai, M.-J., Edwards, D. P., and O'Malley, B. W. (1998) *J. Biol. Chem.* **273,** 12101–12108

THE JOURNAL OF BIOLOGICAL CHEMISTRY
Vol. 275, No. 52, Issue of December 29, pp. 40749–40756, 2000
Printed in U.S.A.

BAG1L Enhances Trans-activation Function of the Vitamin D Receptor*

Received for publication, June 8, 2000, and in revised form, August 30, 2000
Published, JBC Papers in Press, August 30, 2000, DOI 10.1074/jbc.M004977200

Meral Guzey‡§¶, Shinichi Takayama‡, and John C. Reed‡‖

From the ‡Burnham Institute, La Jolla, California 92037 and §RIGEB, MAM-TÜBITAK, P. K. 21 Gebze 41 470, Kocaeli, Turkey

The vitamin D receptor (VDR) is a member of the steroid/retinoid receptor superfamily of nuclear receptors that has potential tumor-suppressive functions. We show here that VDR interacts with and is regulated by BAG1L, a nuclear protein that binds heat shock 70-kDa (Hsp70) family molecular chaperones. Endogenous BAG1L can be co-immunoprecipitated with VDR from prostate cancer cells (ALVA31; LNCaP) in a ligand-dependent manner. BAG1L, but not shorter non-nuclear isoforms of this protein (BAG1; BAG1M/Rap46), markedly enhanced, in a ligand-dependent manner, the ability of VDR to trans-activate reporter gene plasmids containing a vitamin D response element in transient transfection assays. Mutant BAG1L lacking the C-terminal Hsc70-binding domain suppressed (in a concentration-dependent fashion) VDR-mediated trans-activation of vitamin D response element-containing reporter gene plasmids, without altering levels of VDR or endogenous BAG1L protein, suggesting that it operates as a trans-dominant inhibitor of BAG1L. Gene transfer-mediated elevations in BAG1L protein levels in a prostate cancer cell line (PC3), which is moderately responsive to VDR ligands, increased the ability of natural (1α,25(OH)$_2$ vitamin D$_3$) and synthetic (1α,25-dihydroxy-19-nor-22(*E*)-vitamin D$_3$) VDR ligands to induce expression of the VDR target gene, p21^{Waf1}, and suppress DNA synthesis. Thus, BAG1L is a direct regulator of VDR, which enhances its trans-activation function and improves tumor cell responses to growth-suppressive VDR ligands.

1α,25(OH)$_2$ vitamin-D$_3$ is a member of a steroid hormone family which controls calcium homeostasis, and bone formation (reviewed in Refs. 1 and 2). The effects of 1α,25(OH)$_2$ vitamin D$_3$ are largely mediated via interaction with a specific nuclear vitamin D$_3$ receptor (VDR).[1] The VDR is a ligand-dependent transcriptional regulator, belonging to the nuclear receptor (NR) superfamily (reviewed in Ref. 3). VDR primarily interacts with specific DNA sequences composed of a hexanucleotide of direct repeat, binding as either a homodimer or as heterodimer with retinoid X receptors (RXRs) (4).

Known target genes of VDR regulation include the cell cycle inhibitors p21^{Waf1} and p27^{Kip1} (5), perhaps accounting in part for the anti-proliferative effects of VDR ligands on some types of cells. Growth suppressive effects of VDR ligands on epithelial cancer cells *in vitro* have prompted interest in the possibility of applying natural or synthetic VDR ligands for the treatment of cancer (reviewed in Ref. 6). Prostate cancer is among the types of tumor cells with documented sensitivity to VDR ligands. 1α,25(OH)$_2$ vitamin D$_3$ and its less calcemic synthetic analogues have been shown to inhibit *in vitro* growth of established human prostate carcinoma cell lines and primary cultures of normal and prostate cancer cells (7, 8). Depending on the particular cell line tested, VDR ligands can induce cell cycle arrest, differentiation, apoptosis, or combinations of these events (9). Functional VDR is necessary for the growth-inhibitory effect of VDR. However, prostate cancer cell lines vary in their sensitivity to 1α,25(OH)$_2$ vitamin D$_3$ and its synthetic analogues in ways that cannot be explained by differences in VDR protein levels or rates of ligand metabolism, suggesting the existence of mechanisms for modulating VDR function at a post-ligand binding step. This variability in bioresponses to synthetic vitamin D$_3$ analogues has also been observed *in vivo* in clinical trials involving men with advanced prostate cancer (10).

The human *BAG1* gene encodes several proteins, including BAG1, BAG1M (Rap46), and BAG1L, which differ in the length of their N-terminal domains but which all share a conserved C-terminal domain that binds the ATPase domain of heat shock 70-kDa (Hsp70) family molecular chaperones (11). Some of the BAG1 protein isoforms have been shown to interact with and regulate the activity of certain members of the steroid hormone/retinoid superfamily of NRs (12–14). For example, BAG1 binds and suppresses retinoic acid receptors (RARs) (13), BAG1M (Rap46) interacts with and inhibits glucocorticoid receptors (15), and BAG1L associates with and enhances the trans-activation function of androgen receptors (AR) (14). In this report, we examined the relation of BAG1 proteins to VDR. Our findings indicate that the longest of the BAG1 protein isoforms, BAG1L, interacts with VDR in a ligand-inducible manner, enhancing VDR function and improving prostate cancer cellular responses to the growth suppressive effects of vitamin D$_3$ analogues. Thus, levels of BAG1L may be one of the determinants of vitamin D$_3$ responses in normal and malignant tissues.

MATERIALS AND METHODS

VDR Ligands—1α,25(OH)$_2$ vitamin D$_3$ and 1α,25-dihydroxy-19-nor-22(*E*)-vitamin D$_3$ were generously provided by Dr. H. F. DeLuca (Uni-

* This work was supported in part by Department of Defense Prostate Research Program Grant DAMD17-98-1-8584. The costs of publication of this article were defrayed in part by the payment of page charges. This article must therefore be hereby marked "*advertisement*" in accordance with 18 U.S.C. Section 1734 solely to indicate this fact.

¶ Recipient of International Union Against Cancer fellowships from Yamagiwa-Yoshida Memorial and the American Cancer Society Young Investigators.

‖ To whom correspondence should be addressed: Burnham Inst., 10901 N. Torrey Pines Rd., La Jolla, CA 92037. Tel.: 858-646-3140; Fax: 858-646-3194; E-mail: jreed@burnham-inst.org.

[1] The abbreviations used are: VDR, vitamin D receptor; VDRE, vitamin D response element; RXR, retinoid X receptor; RAR, retinoic acid receptor; BSA, bovine serum albumin; PBS, phosphate-buffered saline; CMV, cytomegalovirus; tk, thymidine kinase; CAT, chloramphenicol acetyltransferase; PAGE, polyacrylamide gel electrophoresis; BrdUrd, bromodeoxyuridine; NR, nuclear receptor; AR, androgen receptor.

versity of Wisconsin, Madison, WI) (16). These VDR ligands were prepared as 10^{-3} M stock solutions in ethanol and stored at −20 °C. Stock solution concentrations were confirmed by spectroscopy (Spectra Max 190, Molecular Devices), using an extinction coefficient at 220–290 nm of 18,300 for 1α,25(OH)$_2$ vitamin D$_3$. The spectroscopic confirmation for 1α,25-dihydroxy-19-nor-22(*E*)-vitamin D$_3$ was slightly modified as described previously (16).

Cell Culture—The human prostate cancer cell lines PC-3 and LNCaP, the transformed human embryonal kidney line 293, and monkey kidney COS-7 cell lines were obtained from the American Type Culture Collection (Rockville, MD). The ALVA 31 human prostate cancer cell line was generously provided by Dr. G. Miller (17). Cells were maintained in a humidified atmosphere with 5% CO_2 in RPMI 1640 (PC3, LNCaP, ALVA31) or Dulbecco's modified Eagle's medium (293 and COS-7) supplemented with 10% fetal calf serum, 1 mM glutamine, 100 units/ml penicillin, and 100 μg/ml streptomycin (Life Technologies, Inc.). For most experiments, cells were cultured in medium in which the serum had been preadsorbed with activated charcoal to deplete steroid hormones (14).

Transfections—COS-7 and 293T cells were transiently transfected by a LipofectAMINE method. Cells at ~50% confluence (~2 × 10^5 cells) were seeded per well in six-well (9.4 cm^2) plates (Corning, New York) in 2 ml/well of steroid-depleted medium. The next day, 2.2 μg of DNA was combined with 6 μl of LipofectAMINE in a total volume of 375 μl of Opti-MEM medium (Life Technologies, Inc.) and incubated for ~ 0.5 h. Adherent cells were washed twice with serum-free pre-warmed Opti-MEM, and then DNA/LipofectAMINE mixtures were applied in 750 μl of Opti-MEM. After culturing at 37 °C and 5% CO_2 for 3 h, 1.5 ml of 20% csFBS-containing medium was added per well. The following day, various concentrations of 1α,25(OH)$_2$ vitamin D$_3$ or 1α,25-dihydroxy-19-nor-22(*E*)-vitamin D$_3$ were added and cells were cultured for up to 3 days before preparing lysates for various assays.

For stable transfections, 2.2 μg of either supercoiled or *Sca*I-cleaved pRc/CMV-BAG1L plasmid DNA, encoding BAG1L protein (11) or pRc/CMV parental vector was transfected into PC-3 cells using the LipofectAMINE method, essentially as described above. After 2 days, cells were cultured in medium containing 0.6 mg/ml (active drug) G418 (Life Technologies, Inc.). Medium was replaced twice weekly, until colonies of stably transfected clones arose. Clones were individually recovered and expanded in culture.

Reporter Gene Assays—Transient transfection reporter gene assays were employed for monitoring VDR trans-activation function. Briefly, cells were transiently transfected as described above with various amounts (20, 50, 100, and 150 ng) of pcDNA3 plasmids encoding BAG1L, BAG1L(ΔC), BAG1M, BAG1, BAG1S, or BAG1 (20–800 ng) (11, 14) (see Fig. 1), together with 250 ng of a plasmid encoding one copy of a VDRE upstream of a thymidine kinase minimal promoter and chloramphenicol acetyltransferase (CAT) reporter gene (18, 19), and 400 ng of pCMV-βGal, encoding β-galactosidase under the control of a CMV immediate-early region promoter (14), with or without 100 ng of pcDNA3/VDR, a plasmid encoding the human VDR under the control of a CMV promoter (18). For some experiments, VDRE-tk-CAT was replaced with p21^{Waf1}-CAT, a plasmid containing 2.4 kilobase pairs of the human p21^{Waf1} promoter cloned upstream of a CAT gene (20). After 36–48 h, cell lysates were prepared using Promega reporter lysis buffer (Promega), normalized for total protein content, and relative levels of CAT and β-galactosidase activity were measured as described (14). CAT data were first normalized relative to β-galactosidase, then expressed as -fold activation relative to a defined control, usually cells cultured without VDR ligands or cells transfected without BAG1-encoding plasmids.

Cell Cycle Analysis—The percentage of cells undergoing DNA synthesis was measured by incorporation of bromodeoxyuridine (BrdUrd), essentially as described (21, 22). Stably transfected clones of PC-3 cells containing pRc-CMV control ("Neo") or pRc/CMV-BAG1L plasmids were seeded at 7.5 × 10^3 cells/six-well plate in 2 ml of normal medium for 24 h, then changed to medium in which the serum had been preadsorbed with activated charcoal to deplete steroid hormones. In some cases, VDR ligands were added, as indicated, and cultures were continued for up to 48 h. Cells were then cultured with 10 μM BrdUrd (Sigma) for 1 h, collected by trypsinization, and fixed in 70% ethanol (final concentration ~10^6 cells/100 μl). Fixed cells were then washed in phosphate-buffered saline (pH 7.4) containing 0.5% (w/v) bovine serum albumin (BSA), then exposed to 2 M HCl, 0.5% BSA at room temperature for 20 min before re-washing with PBS/BSA and re-suspending in 0.5 ml of 0.1 M sodium borate ($Na_2B_4O_7$) (pH 8.7) for 2 min at room temperature, and washing a final time with PBS/BSA. Cells were incubated in PBS/BSA with 20 μl/10^6 cells fluorescein isothiocyanate-conjugated anti-BrdUrd antibody (PharMingen) for 20 min in the dark. Finally, propidium iodide (50 μg/ml) was added, and the cells were analyzed using a fluorescence-activated cell sorter (Becton Dickinson FACStar-Plus) using the Cell Quest and Mod-Fit programs.

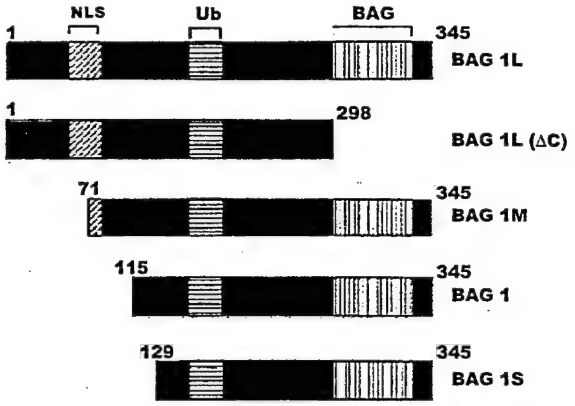

FIG. 1. **Structure of BAG1 protein isoforms.** The structures of the human BAG1 protein isoforms are depicted, showing the conserved BAG domain, as well as other domains found in selected members of the family such as ubiquitin-like domain (*Ub*), and nuclear targeting sequences (*NLS*). The longest of the BAG1L proteins is a predicted 345 amino acids in length. All others are presented relative to BAG1L. The BAG1L(ΔC) mutant is also depicted (14).

Antibodies and Immunoblotting—Cell lysates were prepared using radioimmunoprecipitation assay buffer (10 mM Tris (pH 7.4), 150 mM NaCl, 1% Triton X-100, 1% deoxycholate, 0.1% SDS, 5 mM EDTA), normalized for total protein content (25 μg of protein), and subjected to SDS-PAGE using 12% gels, followed by electrotransfer to 0.45-μm nitrocellulose transfer membranes (Bio-Rad). Blots were incubated as described (11, 14), with the following primary antibodies, including 1:1000 (v/v) of a mouse monoclonal specific for human VDR (IVG8C11) (gift of Dr. H. F. DeLuca) (23), 1:1000 (v/v) of a rabbit polyclonal anti-VDR IgG (Santa Cruz Biotechnology, Inc., Santa Barbara, CA), 1:1000 (v/v) control normal rabbit IgG (Santa Cruz Biotechnology, Inc.), 1:1000 (v/v) control mouse IgG$_1$ (Dako, Inc.), 1:1000 (v/v) of mouse monoclonal (IgG$_1$) specific for human BAG1 (KS6C8) (11, 24), and 1/250 (v/v) of mouse anti-human p21 monoclonal antibody (IgG$_1$) (PharMingen, San Diego, CA). Immunodetection was accomplished essentially as described (11, 14) using horseradish peroxidase-conjugated secondary antibody (Amersham Pharmacia Biotech) and an enhanced chemiluminescence detection method (ECL) (Amersham/Pharmacia Biotech.) with exposure to x-ray film (XAR, Eastman Kodak Co.).

Co-immunoprecipitations—Untransfected ALVA31 and LN-CaP cells or 293T cells transfected with plasmids encoding BAG1L or BAG1L(ΔC) were cultured with or without 5 × 10^{-8} M 1α,25(OH)$_2$ vitamin D$_3$, and collected at 70% confluence. Cells were lysed on ice in HKMEN (10 mM HEPES (pH 7.2), 142 mM KCl, 1 mM EGTA, 1 mM EDTA, 0.2% Nonidet P-40) containing protease inhibitors (Roche Molecular Biochemicals), then either passed several times through a ~21-gauge needle to disrupt nuclei or NE-PER nuclear extraction reagent (Pierce) was added according to the manufacturer's protocol. After centrifugation at 10,000 × *g* for 25 min, the resulting supernatants from equivalent numbers of cells were subjected to immunoprecipitations in HKMEN using the anti-BAG1 monoclonal KS6C8, anti-VDR monoclonal IVG8C11, or anti-VDR polyclonal antiserum, bound to protein G-agarose (Zymed Laboratories Inc., San Francisco, CA). Control immunoprecipitations were performed using mouse IgG$_1$ (Dako) or non-immune rabbit serum (Santa Cruz). Immune-complexes were washed three times with 1 ml of HKMEN and analyzed by SDS-PAGE/immunoblotting, as above.

RESULTS

BAG1L Enhances Trans-activation Function of VDR—We initially explored the effects of BAG1 proteins on the trans-activation function of the VDR using transient transfection reporter gene assays in HEK 293T and COS-7 cells. Several isoforms of the BAG1 protein were compared, as depicted in Fig. 1. These isoforms of BAG1 all contain a conserved C-terminal domain "BAG domain" responsible for high affinity interactions with Hsc70/Hsp70 molecular chaperones and they

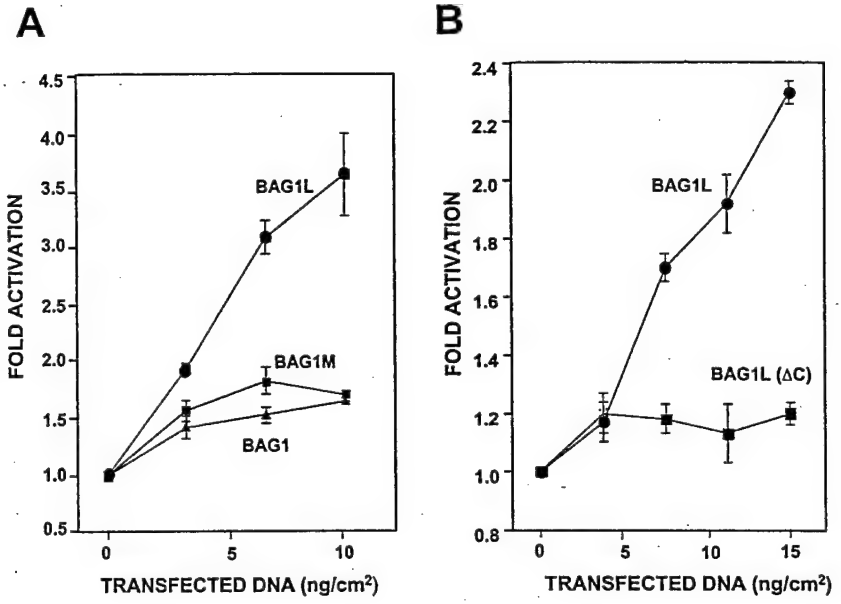

FIG. 2. **BAG1L enhances trans-activation function of VDR.** COS-7 cells at ~50% confluence in six-well plates (area 9.4 cm^2) in steroid-depleted medium were transfected by a LipofectAMINE method with VDR encoding plasmid (100 ng), VDRE-CAT reporter plasmid (250 ng), pCMV-βgal (400 ng), and various amounts of BAG1-encoding plasmids as indicated, normalizing total DNA to 2.2 μg/well. After 1 day, cells were stimulated with 5×10^{-9} M $1\alpha,25(OH)_2$ vitamin D_3. Cell extracts were prepared and assayed for CAT and β-galactosidase activity, expressing normalized data as a ratio relative to transfected cells which received pcDNA3 control DNA instead of a BAG1-expression plasmid (mean ± S.E.; $n = 3$). In *A*, plasmids encoding BAG1 (*triangles*), BAG1M (*squares*), or BAG1L (*circles*) were transfected in amounts of 20, 50, and 100 ng (reported as ng/cm^2). In *B*, plasmids encoding BAG1L (*circles*) or BAG1L(ΔC) mutant (*squares*) were transfected using 20, 50, 100, or 150 ng of these plasmid DNAs, as indicated.

possess an upstream ubiquitin-like domain, but they differ in the length of their N-terminal domains. The various isoforms of BAG1L arise by translation from alternative initiation codons within a common mRNA (11, 25). Among these proteins, only BAG1L contains both nucleoplasmin-like and SV40 large T-like candidate nuclear targeting sequences and is constitutively localized to nuclei (11, 25).

To enforce expression of selected isoforms of BAG1, a cDNA encoding the longest isoform, BAG1L, and various 5′-truncated versions of cDNAs encoding BAG1M, BAG1, and BAG1S were subcloned into an expression plasmid, with additional modifications as described previously (11, 14, 24). These plasmids were then co-transfected in various amounts with a fixed amount of plasmid encoding VDR and a VDRE-CAT reporter gene plasmid. Cells were supplied with physiologically relevant concentrations (5×10^{-9} M) of $1\alpha,25(OH)_2$ vitamin D_3. All data were normalized relative to cells stimulated with $1\alpha,25(OH)_2$ vitamin D_3 in the absence of BAG1 expression plasmids.

As shown in Fig. 2, the longest isoform, BAG1L, enhanced the trans-activation function of VDR in a concentration-dependent manner, resulting in a 2–4-fold increase in VDRE-tk-CAT reporter gene activation under these conditions. In contrast, BAG1M, BAG1, and BAG1S had little effect on VDR activity (Fig. 2 and data not shown). Moreover, although full-length BAG1L effectively enhanced VDR activity, a mutant of BAG1L lacking the C-terminal Hsc70/Hsp70-binding domain did not. This observation confirms the specificity of these finding obtained with full-length BAG1L and also suggests that the C-terminal BAG domain of BAG1L is required for potentiating VDR activity.

Immunoblot analysis was performed to verify production of the BAG1L, BAG1L(ΔC), BAG1M, BAG1, and BAG1S proteins in transfected cells. As shown in Fig. 3, BAG1L, BAG1L(ΔC), BAG1, and BAG1S were produced at comparable levels. The BAG1M protein was also produced, but due to internal translation initiation from the AUG, which normally gives rise to the shorter BAG1 protein, the steady-state levels of BAG1M achieved were only about half the other isoforms. Nevertheless, BAG1M protein was produced at levels far in excess of endogenous BAG1 and BAG1L, which migrate at ~35 and ~55 kDa and which can be seen as faint bands in the immunoblot analysis (Fig. 3). We conclude, therefore, that the selective enhancement of VDR activity seen with BAG1L but not with other BAG1 isoforms in transient transfection reporter gene assays

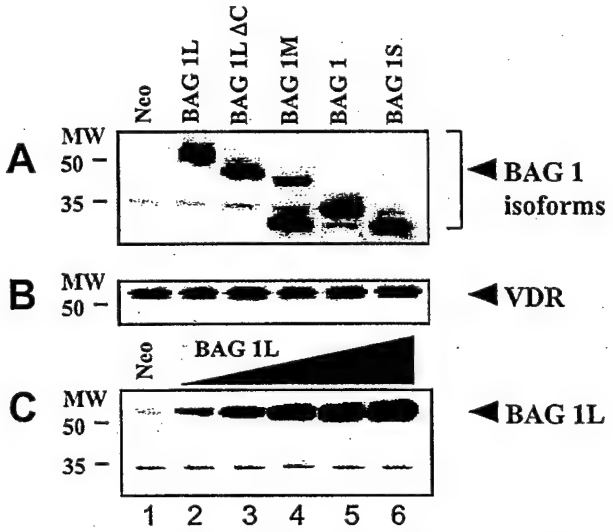

FIG. 3. **Immunoblot analysis of expression of BAG1 isoforms in transfected cells.** COS-7 cell plasmids in 60-mm dishes (growth area; 21 cm^2) were transiently transfected using a LipofectAMINE reagent with 220 ng of VDR and 330 ng of either pcDNA3 (neo) or pcDNA3-plasmids encoding BAG1L, BAG1M, BAG1L(ΔC), BAG1, or BAG1S. After 2 days, whole cell lysates were prepared, normalized for total protein content (25 μg/lane), and subjected to SDS-PAGE/immunoblot assay, using anti-BAG1 (*A*) or anti-VDR (*B*) antibodies in conjunction with an ECL-based detection method. In *C*, 293T cells were transfected with 220 ng of VDR and increasing amounts of pcDNA3-BAG1L DNA (*lanes 2–6*, 44, 110, 220, 330, and 440 ng, respectively) (reported as ng/cm^2 for area of 21 cm^2), normalizing total DNA content (~5 μg in 60-mm dishes) with pcDNA3 (Neo) vector. Lysates were prepared after 2 days and analyzed as above using anti-BAG1 antibody. Molecular size markers are indicated in kilodaltons.

is unlikely to be due to differences in the levels of production of these proteins. Importantly, expression of the various isoforms of BAG1 had no effect on levels of VDR, thus excluding alterations in the receptor for $1\alpha,25(OH)_2$ vitamin D_3 as a trivial explanation for the results obtained in reporter gene assays (Fig. 3*B*). Immunoblotting also confirmed the concentration dependence of BAG1L protein production in response to transfection of various amounts of expression plasmid DNA (Fig. 3*C*), further validating the results obtained by reporter gene assays.

$1\alpha,25(OH)_2$ Vitamin D_3 Induces Association of BAG1L with

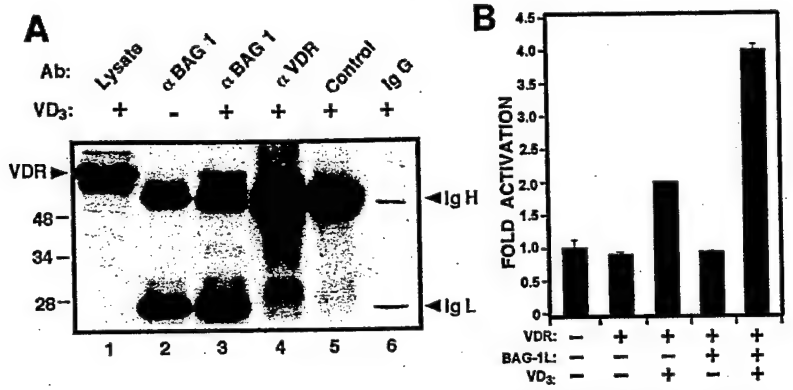

FIG. 4. **BAG1L associates with and modulates function of VDR in a ligand-dependent manner.** In *A*, lysates were prepared using HKMEN solution from ALVA31 prostate cells grown in the absence (−) or presence (+) of 5×10^{-8} M $1\alpha,25(OH)_2$ vitamin D_3. Immunoprecipitations were performed using anti-BAG1 monoclonal (IgG_1) KS6C8 (14) (*lanes 2* and *3*), rabbit polyclonal IgG VDR antibody (Santa Cruz) (*lane 4*), rabbit IgG_1 control (*lane 5*), or mouse IgG control (*lane 6*). Immune complexes were analyzed by SDS-PAGE/immunoblotting using a polyclonal rabbit anti-VDR with ECL-based detection. As a control, lysate (25 μg) from $1\alpha,25(OH)_2$ vitamin D_3-treated cells was also directly loaded in the gel (*lane 1*). The positions of the heavy (*IgH*) and light (*IgL*) chains of the primary antibodies are indicated (*right*), as well as the position of the VDR (*left*). In *B*, COS-7 cells in steroid-depleted medium were transfected as described in Fig. 2, using 100 ng of pcDNA3-BAG1L (+) or pcDNA3 control (−) plasmid DNA. After 1 day, either 5×10^{-9} M $1\alpha,25(OH)_2$ vitamin D_3 (+) or control diluent (−) was added to cultures. Lysates were prepared 48 h later, and relative CAT production from the VDR-CAT reporter gene plasmid was measured, normalizing for β-galactosidase and expressing the data as -fold activation relative to cells that received neither the VDR nor BAG1L plasmids and which were not stimulated with VDR ligand.

VDR—The functional collaboration of BAG1L with VDR prompted us to explore whether these proteins physically interact, particularly given evidence that BAG1L can associate with certain other members of the NR family (13–15). Co-immunoprecipitation assays were performed using lysates from untransfected ALVA-31 (Fig. 4) and LNCaP (data not shown) prostate cancer cells to explore whether the endogenous BAG1L and VDR proteins can form complexes. These lines were chosen because they contain relatively high intrinsic levels of both BAG1L and VDR, and because they are sensitive to $1\alpha,25(OH)_2$ vitamin D_3-induced growth suppression (10).[2] BAG1L was immunoprecipitated from lysates prepared from unstimulated and $1\alpha,25(OH)_2$ vitamin D_3-treated cells, and the resulting immune complexes were analyzed by SDS-PAGE/immunoblotting using an anti-VDR antibody.

Anti-BAG1 immunoprecipitates prepared from lysates of $1\alpha,25(OH)_2$ vitamin D_3 -treated cells contained associated VDR, whereas VDR was not found associated with BAG1L immune complexes derived from unstimulated ALVA31 (Fig. 4) or LNCaP (data not shown) cells. Control immunoprecipitates prepared using mouse IgG_1 instead of anti-BAG1 antibody confirmed the specificity of these results. Comparisons of the levels of VDR and BAG1L proteins in ALVA31 and LNCaP lysates before and after treatment with $1\alpha,25(OH)_2$ vitamin D_3 revealed no demonstrable difference, indicating that the association is not merely secondary to ligand-induced changes in the amounts of these proteins (data not shown). We conclude, therefore, that VDR associates with BAG1L in a ligand-dependent manner.

The ligand-dependent association of BAG1L with VDR predicts that BAG1L should enhance VDR trans-activation function only when appropriate steroid ligand is provided. Accordingly, we performed transient transfection reporter gene assays in which cells were cultured with or without $1\alpha,25(OH)_2$ vitamin D_3 in medium containing steroid-depleted serum. Co-expression of BAG1L with VDR in the absence of ligand did not increase VDR-mediated reporter gene trans-activation (Fig. 4*B*). However, when $1\alpha,25(OH)_2$ vitamin D_3 was provided, BAG1L more than doubled the levels of VDR-mediated induction of the VDRE-CAT reporter gene plasmid compared with COS-7 cells, which received VDR and $1\alpha,25(OH)_2$ vitamin D_3 in the absence of BAG1L. Taken together, these results demonstrate that BAG1L associates with and potentiates the function of VDR complexes in a ligand-dependent manner.

A BAG1L Mutant Lacking the Hsc70/Hsp70-binding Domain Inhibits VDR Activity—It has been shown that the last 47 amino acids of the BAG1 protein are required for binding to the ATPase domain of Hsc70 and Hsp70 chaperones (11, 26). To explore the functional consequences of removing the C-terminal domain from BAG1L on VDR, transient transfection reporter gene assays were performed, assaying VDR-mediated trans-activation of the VDRE-CAT reporter gene plasmid in the presence of increasing amounts of co-transfected pcDNA3-BAG1L (ΔC), which encodes a truncation mutant of BAG1L lacking the Hsp70/Hsc70-binding domain. As shown in Fig. 5*A*, co-transfection of the BAG1L(ΔC) expression plasmid failed to enhance VDR activity and instead inhibited VDR activity in a concentration-dependent manner, reducing trans-activation of the VRE-CAT reporter gene by approximately half. Immunoblot analysis demonstrated dose-dependent production of the BAG1L(ΔC) protein, which reached levels roughly equivalent to full-length BAG1L at the highest concentrations of plasmid DNA transfected (Fig. 5*B*). We conclude, therefore, that the Hsc70/Hsp70-binding domain of BAG1L is necessary for its stimulatory effects on VDR, and that deletion of this domain converts BAG1L from a stimulator to an inhibitor of VDR, presumably functioning as a trans-dominant competitor of the endogenous wild-type BAG1L protein.

To explore the mechanism of the BAG1L(ΔC) protein further, comparisons were made of the ability of BAG1L and BAG1L(ΔC) to associate with VDR, as determined by co-immunoprecipitation experiments (Fig. 5*C*). Although VDR could be readily co-immunoprecipitated with BAG1L from $1\alpha,25(OH)_2$ vitamin D_3-stimulated cells, VDR association with BAG1L(ΔC) was not detected. Immunoblot analysis of the cell lysates derived from transfected 293T cells used for these experiments confirmed production of both the full-length BAG1L and truncated BAG1L(ΔC) proteins (Fig. 5*C*). Thus, deletion of the C-terminal region of BAG1L abrogates its ability to associate with the VDR.

BAG1L Enhances VDR-mediated Trans-activation of the $p21^{Waf1}$ Promoter—The promoter of the gene encoding the cell cycle regulator, $p21^{Waf1}$, is known to contain a VDRE (27). To extend the analysis of BAG1L effects on VDR to a more natural

[2] M. Guzey, S. Takayama, and J. C. Reed, unpublished observations.

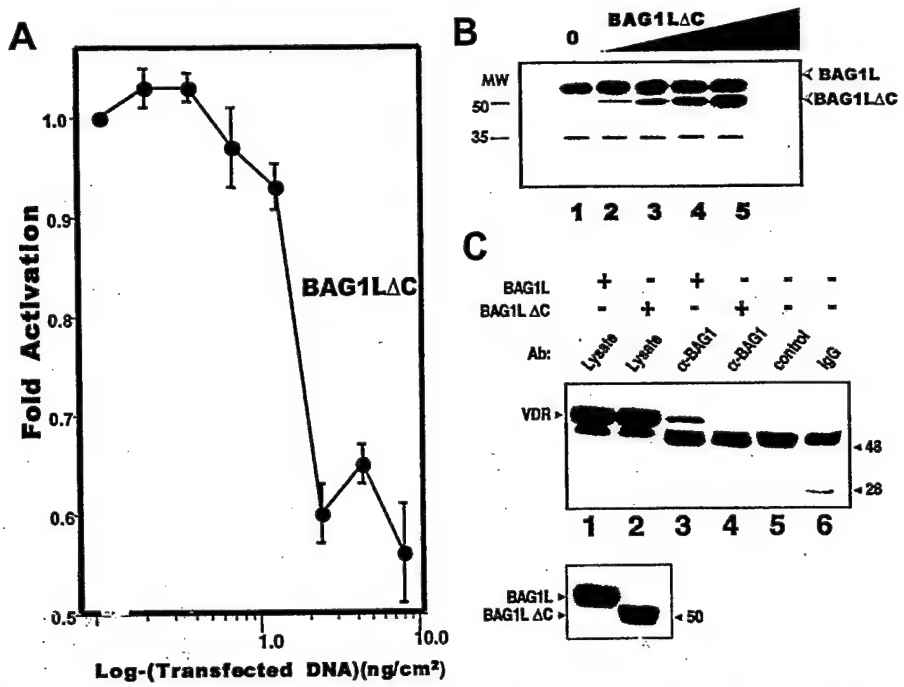

FIG. 5. **BAG1L(ΔC) mutant inhibits VDR function.** *A*, HEK 293T cells were transiently transfected with 200 ng of VDR, 250 ng of the VDRE-CAT, 400 ng of pCMV-βgal, 250 ng of pcDNA3-BAG1L, and various amounts of pcDNA3-BAG1L(ΔC) (20–800 ng, reported as ng/cm²) or an equal amount of pcDNA3 control plasmid, total DNA normalized to 2.2 μg/well (six-well plates, growth area 9.4 cm²) by addition of pcDNA3 control plasmid. After 1 day, cells were stimulated with 5×10^{-9} M 1α,25(OH)$_2$ vitamin D$_3$ and cell extracts were prepared 2 days later and assayed for CAT and β-galactosidase activity. Data were normalized using β-galactosidase, and results expressed as -fold activation relative to 1α,25(OH)$_2$ vitamin D$_3$ -stimulated cells, which received the VDR expression vector in combination with pcDNA3 control plasmid. *B*, COS-7 cells in 60-mm dishes (area 21 cm²) were transiently transfected with 330 ng of pcDNA3-BAG1L, 220 ng of VDR, and increasing amounts of pcDNA3-BAG1L(ΔC) (*lanes 2–5*, 44 , 110, 220, 330, and 440 ng, respectively) (reported as ng/cm²). After 2 days, whole cell lysates were prepared, normalized for total protein content (25 μg/lane), and subjected to SDS-PAGE/immunoblot assay using anti-BAG1 antibody. The positions of the BAG1L and BAG1L(ΔC) proteins are indicated (*arrowheads*). Molecular size markers are indicated in kilodaltons. *C*, 293T cells in 100-mm dishes were transiently transfected with equivalent amounts of plasmids (~1 μg each) encoding VDR, and either full-length BAG1L or BAG1L(ΔC). Cells were treated 1 day later with 5×10^{-8} M 1α25(OH)$_2$ vitamin D$_3$, then collected at 2 days after transfection, lysed on ice in HKMEN buffer, and immunoprecipitations were performed using either anti-BAG1 monoclonal KS6C8 or mouse IgG control antibody. Immune complexes were analyzed by SDS-PAGE immunoblotting, using a polyclonal rabbit anti-VDR antiserum with ECL-based detection. Lysates (25 μl) were also run directly in the gel for comparison with immunoprecipitates. The blot was reprobed with anti-BAG1 antibody (*lower panel*) to verify production of the BAG1L and BAG1L(ΔC) proteins (indicated by *arrowheads*).

promoter context, we asked whether BAG1L protein could enhance VDR-mediated trans-activation in a CAT reporter gene plasmid containing the p21^{Waf1} promoter. For these experiments, COS-7 or HEK 293T cells were transiently co-transfected with various amounts of plasmid DNA encoding BAG1L, together with fixed amounts of VDR and p21-CAT plasmids. Cells were cultured in the presence of either the natural VDR ligand, 1α,25(OH)$_2$ vitamin D$_3$ (5×10^{-9} M) (Fig. 6, *A* and *B*) or the synthetic vitamin D$_3$ analogue 1α,25-dihydroxy-19-nor-22(*E*)-vitamin D$_3$ (5×10^{-9} M) (Fig. 6, *C* and *D*).

BAG1L induced a dose-dependent increase in VDR-mediated trans-activation of the p21-promoter in these transient transfection reporter gene assays when VDR ligands were supplied (Fig. 6) but not in the absence of ligands (data not shown). The effect of BAG1L appeared to be more pronounced, in terms of -fold enhancement of reporter gene activation, when the vitamin D$_3$ analogue 1α,25-dihydroxy-19-nor-22(*E*)-vitamin D$_3$ was employed, compared with the natural VDR ligand, 1α,25(OH)$_2$ vitamin D$_3$. However, because maximal BAG1L plasmid DNA concentrations (plateau) were not reached in these experiments, quantitative comparisons should be interpreted cautiously.

BAG1L enhances VDR-mediated induction of the endogenous p21^{Waf1} gene. To extend the analysis of BAG1L to an endogenous target of VDR, we explored the effects of VDR ligands on induction of p21^{Waf1} protein production in PC3 cells. PC3 cells contain moderate levels of VDR (800 fmol/mg protein), but express BAG1L at low levels (10).[2] For these experiments, therefore, PC3 cells were stably transfected with either a control plasmid or BAG1L-encoding plasmid and several clones were characterized. Immunoblot analysis revealed several stably transfected clones with elevated levels of BAG1L protein compared with control-transfected or parental PC3 cells. These clones were then cultured with either natural VDR ligand, 1α,25(OH)$_2$ vitamin D$_3$ (5×10^{-8} M) or vitamin D$_3$ analogue 1α,25-dihydroxy-19-nor-22(*E*)-vitamin D$_3$ (5×10^{-8} M) for 1–3 days, and lysates were prepared for immunoblot analysis of p21^{Waf1} protein levels.

Both natural and synthetic VDR ligands induced greater increases in p21^{Waf1} protein levels in BAG1L-overexpressing PC3 cells compared with controls. Increases in p21 were also sometimes more rapid in BAG1L-overexpressing compared with control-transfected cells. Re-probing the blots with an antibody to β-actin verified loading of equivalent amounts of total protein. Although representative data are provided for two clones in Fig. 7, similar findings were obtained with others (data not shown).

BAG1L Sensitizes PC3 Cells to Growth Inhibition by VDR Ligands—The effects of VDR ligands on p21^{Waf1} expression in PC3 cells suggested that BAG1L-overexpressing cells might display greater sensitivity to the growth suppressive effects of vitamin D$_3$ analogues. Accordingly, clones of PC3 control (Neo)-transfected and BAG1L-transfected cells were cultured in steroid-depleted medium with or without 5×10^{-8} M 1α,25(OH)$_2$ vitamin D$_3$ for 2 days, and the percentage of replicating cells was then estimated by labeling with BrdUrd, which is incor-

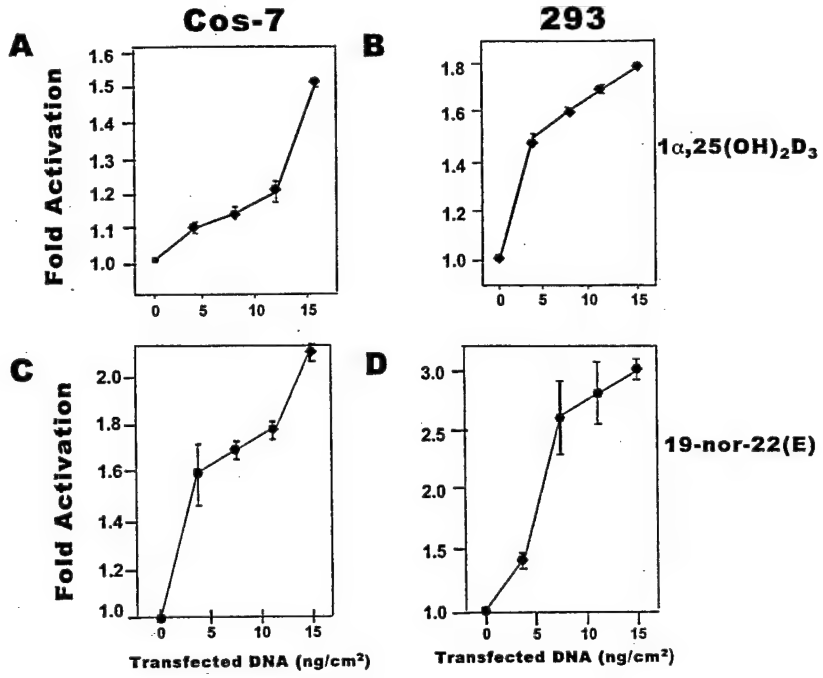

FIG. 6. **BAG1L enhances VDR-mediated trans-activation of $p21^{Waf1}$ promoter.** COS-7 monkey kidney cells (*A* and *C*) and HEK 293T human embryonic kidney cells (*B* and *D*) were transfected by a LipofectAMINE method in 9.4-cm^2 dishes with VDR-encoding plasmid (100 ng), 250 ng of p21-CAT reporter plasmid, 400 ng of pCMV-β-galactosidase, and increasing amounts of pcDNA3-BAG1L expression plasmid, as indicated. One day later, transfected cells were treated with 5×10^{-9} M either 1α,25$(OH)_2$ vitamin D_3 (*A* and *B*) or 1α,25-dihydroxy-19-nor-22(*E*)-vitamin D_3 (19-nor-22(*E*)) (*C* and *D*) and CAT activity was measured 2 days later, normalizing data relative to β-galactosidase and reporting results as -fold activation relative to cells transfected with pcDNA3 control plasmid instead of pcDNA3-BAG1L. BAG1L did not enhance VDR activity when VDR ligands were omitted from cultures (data not shown).

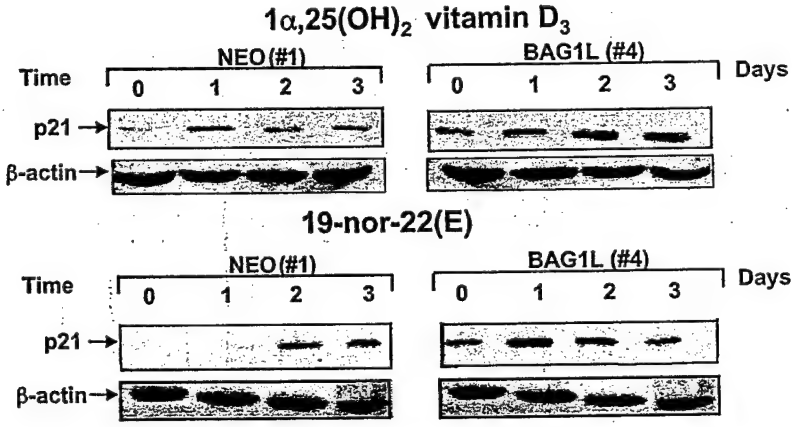

FIG. 7. **BAG1L increases induction of endogenous $p21^{Waf1}$ expression by VDR ligands.** PC-3 cells stably transfected with empty pcDNA3 vector (Neo) or pcDNA3-BAG1L were cultured with 5×10^{-8} M 1α,25$(OH)_2$ vitamin D_3 (*top*) or 19-nor-22(*E*) (*bottom*). Cell lysates were prepared after 0, 1, 2, or 3 days of culture, normalized for total protein content (25 μg/lane) and subjected to SDS-PAGE/immunoblot assay using anti-p21 and anti-β-actin antibodies in conjunction with an ECL-based detection method. Data obtained using representative clones (Neo clone 1; BAG1L clone 4) are presented.

porated into the DNA of cells in S-phase. Comparisons were made between two Neo control-transfected clones of PC3 and six BAG1L-transfected clones. The percentage inhibition of cell proliferation induced by VDR ligand was significantly greater for the BAG1L-transfected compared with the Neo-control transfected PC3 cell clones, as determined by contrasting BrdUrd incorporation in each clone when cultured without *versus* with 1α,25$(OH)_2$ vitamin D_3 ($p < 0.005$ by unpaired t test). Similar results were obtained using the synthetic VDR ligand, 1α,25-dihydroxy-19-nor-22(*E*)-vitamin-D_3, and when cell cycle analysis was performed by measuring DNA content of propidium iodide-stained cells instead of by BrdUrd labeling (data not shown). Analysis of cell viability indicated that VDR ligands induced growth arrest without causing a substantial increase in cell death during the time course of these experiments. Immunoblot analysis confirmed that the levels of BAG1L protein were elevated by ~3–10-fold in the BAG1L-transfected clones compared with Neo-control clones of PC3 cells (Fig. 8). In contrast, levels of VDR protein were not different among these clones. Taken together, these data suggest that BAG1L can influence the sensitivity of cells to VDR ligands, with overexpression of BAG1L increasing the sensitivity of prostate cancer cells to the growth-inhibitory effects of VDR ligands.

DISCUSSION

In this report, we provide the first evidence that BAG1L can interact with and regulate the activity of VDR. In contrast, shorter isoforms of BAG1, including BAG1M, BAG1, and BAG1S, lacked the ability to enhance the trans-activation function of VDR. In human cells, at least four BAG1 isoforms can arise from translation-initiation from alternative start codons within a common mRNA, resulting in proteins that all share a common C terminus but that can be distinguished by the length of their N termini: BAG1S, BAG1, BAG1M (previously also termed Rap 46/Hap 46), and BAG1L. Of these, BAG1 and BAG1L are the most abundant *in vivo*, with only scant amounts of BAG1M or BAG1S generally observed (11). Similarly, in mice, BAG1 and BAG1L are the most prevalent isoforms. Moreover, the *bag1* mRNA molecules of mice lack the ATG required for production of BAG1M (11, 25). BAG1 is predominantly, although not exclusively, a cytosolic protein, whereas BAG1L is located entirely in the nucleus of cells (11, 14, 25, 26).

The unique ability of BAG1L to enhance VDR function in cells may be related to the nuclear location of this protein. BAG1L contains candidate nuclear localization sequences, which are not found in other BAG1 isoforms, including nucleoplasmin-like and SV40 large-T antigen-like basic amino acid

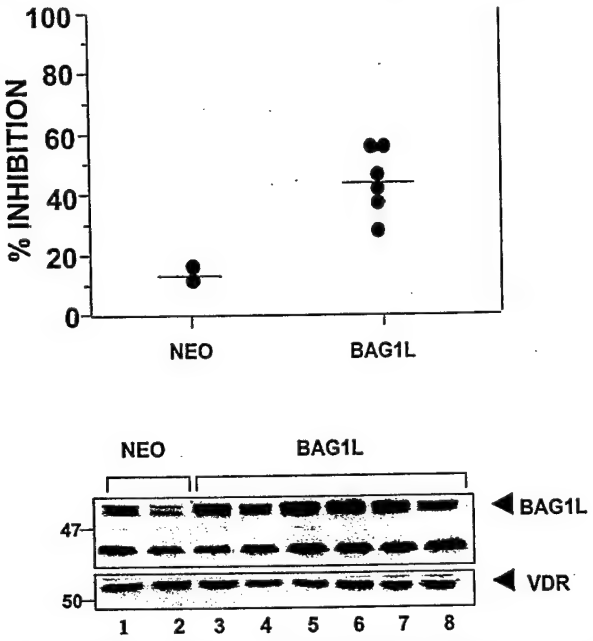

FIG. 8. **BAG1L overexpression increases sensitivity of PC3 cells to growth suppression by 1α,25(OH)$_2$ vitamin D$_3$.** *A*, various clones of control (Neo) or BAG1L-transfected PC3 cells were cultured with or without 5×10^{-8} M 1α,25(OH)$_2$ vitamin D$_3$. BrdUrd was then added to the cultures for 1 h, and cells were recovered, fixed, and stained with anti-BrdUrd antibody, determining the percentage of cells that incorporated BrdUrd into DNA by a flow cytometry method. Data are presented as percentage inhibition based on comparison of untreated and vitamin D$_3$-treated cells. Mean values are indicated by *bars*. *B*, immunoblot data are presented for each of the stably transfected PC3 clones, using lysates normalized for total protein content and probing blots with antibodies specific for BAG1 (*top*) or VDR (*bottom*). The position of BAG1L is indicated by an *arrowhead*. The endogenous BAG1 protein is also seen in the gel (not labeled). Molecular size markers are indicated in kilodaltons.

motifs commonly associated with nuclear import. In contrast, BAG1M contains only a portion of one of these candidate nuclear localization sequences and has been shown to reside in the cytosol unless stimulated to traffic into the nucleus by associating with other proteins, such as glucocorticoid receptors. However, the unique ~50-amino acid N-terminal domain of BAG1L also contains several additional copies of (EEX_4) repeat sequences, which conceivably may have relevance to the ability of this protein to associate with and enhance the function of VDR. In this regard, it has been suggested that these EEX_4 repeats in the BAG1M protein allow it to associate with DNA (28). Thus, the presence of additional copies of this repeating motif in the longer BAG1L protein conceivably could improve its ability targeting to DNA, indirectly enhancing its functional interactions with nuclear hormone receptors. However, other sequences found in the unique N-terminal region of BAG1L might account for its ability to collaborate with VDR, independently of possible DNA binding activity, such as through interactions with co-activator proteins.

The VDR binds its cognate response elements in target genes as either a homodimer (VDR/VDR) or heterodimer (VDR/RXR), leading to activation or repression of transcription via interaction with transcriptional co-factors and the basal transcriptional machinery. Moreover, VDR also can form heterodimers with RAR (29). Previously, we reported that the shorter BAG1 isoform can antagonize RAR activity through what appears to be a direct interaction with RAR, inhibiting binding of RAR/RXR heterodimers to retinoid response elements *in vitro* and suppressing RAR function in cells (13). In contrast, BAG1 does not interact with RXR and does not interfere with RXR signaling in cells. Since the shorter BAG1 protein had no detectable effect on VDR trans-activation function, we consider it unlikely that the observed effects of the longer BAG1L protein on VDR can be attributed to an indirect interaction with this steroid hormone receptor caused by its heterodimerization with RAR.

Association of BAG1L with VDR in co-immunoprecipitation assays was found to be ligand-dependent. Similarly, BAG1L-mediated enhancement of VDR transcriptional activity was also dependent on the presence of VDR ligands. Ligand-dependent effects of BAG1L have also been reported for the AR, where BAG1L likewise enhances trans-activation function of AR in a ligand-dependent manner (14). All members of the NR family of transcription factors contain a ligand-independent and ligand-dependent trans-activation domain: AF1 and AF2, respectively (reviewed in Refs. 29–31). We presume, therefore, that interaction of BAG1L with VDR depends upon the ligand-binding AF2 domain. However, it is unknown at present whether BAG1L binds directly to VDR *versus* associating indirectly through interactions with other VDR-binding proteins whose interactions with VDR are ligand-dependent.

One protein that conceivably could mediate BAG1L interactions with VDR is Hsp70 or Hsc70. All known isoforms of BAG1 contain a conserved C-terminal ~45 amino acid domain (the "BAG domain") that binds the ATPase domain of Hsp70/Hsc70 molecular chaperones with high affinity (11, 26). Thus, if ligand binding to steroid hormone receptors causes conformational changes that permit stable Hsp70/Hsc70 binding, then this could possibly provide a mechanism by which Hsp70/Hsc70 bridges BAG1L to VDR and other members of the NR family. Indeed, deletion of the C-terminal Hsp70/Hsc70-binding domain from BAG1L abrogated its ability to associate with VDR, as determined by co-immunoprecipitation experiments. In this regard, it has been reported that Hsp70 can be found complexed to ligand-activated steroid hormone receptors (*i.e.* estrogen receptor, glucocorticoid receptor, and prolactin receptor) bound to DNA (32–35), further supporting this idea. However, analysis of a mutant of BAG1L lacking the C-terminal Hsc70/Hsp70-binding domain revealed a trans-dominant inhibitory function for this protein, where it suppressed rather than enhanced VDR trans-activation function. A similar trans-dominant inhibitory effect of BAG1L(ΔC) has also been reported previously for AR (14). If the only mechanism for functional interaction of BAG1L with VDR were through association with VDR/Hsp70 complexes, then we would expect deletion of the Hsp70-binding domain to nullify BAG1L effects on VDR but not to interfere with VDR in a trans-dominant manner. Since physiochemical analysis of recombinant BAG1 protein has revealed it to be a monomer (36), it also seems unlikely that the BAG1L(ΔC) mutant interfered with endogenous BAG1L by forming heterodimers/hetero-oligomers with the wild-type BAG1L protein. Thus, we favor the interpretation that BAG1L requires both the Hsc70-binding domain and other upstream regions of this protein for regulating VDR. The purpose of the upstream regions of BAG1L in this context remains to be clarified, but could include interactions with DNA, chromatin, co-activator proteins, or other types of proteins that influence nuclear hormone receptor function.

The mechanism by which BAG1L enhances the trans-activation function of VDR is currently unknown. Given the ability of this protein to bind Hsp70/Hsc70 molecular chaperones, it seems reasonable to speculate that BAG1L may act in collaboration with Hsp70/Hsc70 to produce conformational changes in VDR or VDR-associated proteins such as co-activators that result in a net enhancement of ligand-dependent transcription. However, alternative models are possible. For example, all BAG1 isoforms contain a conserved ubiquitin-like domain,

which has been suggested based on circumstantial evidence to mediate interactions with the 26 S proteosome (37). Accordingly, BAG1L conceivably could facilitate the turnover of proteins within VDR transcription complexes. Although no effect of BAG1L on the steady-state levels of VDR was observed, we cannot exclude the possibility of effects on the turnover of VDR-associated proteins not examined here.

1α,25(OH)$_2$ vitamin D$_3$ and its synthetic analogues can have growth-suppressive effects on certain types of tumor cells, including adenocarcinomas of the prostate (10). However, responses to natural and synthetic VDR ligands vary widely among tumor lines, despite their expression of functional VDR, suggesting that a variety of factors may modulate sensitivity to VDR ligands. The evidence presented here suggests that BAG1L protein levels may represent one determinant of sensitivity to growth inhibition by VDR ligands. Using a prostate cancer cell line, which expresses moderate levels of VDR (800 fmol/mg) but which contains little BAG1L and which displays little responsiveness to VDR ligands, we found that gene transfer-mediated overexpression of BAG1L increased cell cycle arrest induced by VDR ligands. This enhanced sensitivity to growth arrest induced by VDR ligands was associated with increased expression of p21^{Waf1}, a known target gene of VDR (27). However, it remains to be determined whether VDR-mediated growth repression is directly attributable to p21^{Waf1} gene induction by this steroid hormone receptor, and it should be recognized that VDR is likely to affect expression of a wide variety of target genes in cells. Although it cannot be excluded that the down-regulation of p21^{Waf1} seen in PC3 cells treated with natural or synthetic VDR ligands is a consequence rather than a cause of the growth suppressive effects of these compounds, our studies of the p21^{Waf1} promoter in transient transfection reporter gene assays demonstrated that BAG1L is capable of augmenting VDR-mediated transcription of this promoter.

Prostate cancer is the most common lethal form of cancer currently diagnosed in American men, second only to lung cancer as the leading cause of malignancy-associated death among males (38). The primary therapy for men with metastatic disease entails use of anti-androgens and androgen ablation. Hormonal therapy, however, has a limited time of efficacy, and essentially all patients eventually relapse with hormone-refractory disease (10). Androgen ablation therapy also decreases the quality of life as it causes "hot flashes," muscle wasting, and impotence in many men, as well as increasing the risk of osteoporosis. As a result, many physicians prefer to observe rather than treat asymptomatic patients, particularly elderly patients whose PSA levels are rising slowly. An effective, relatively nontoxic agent such as 1α,25(OH)$_2$ vitamin D$_3$ thus could be an ideal type of therapy for use in palliative treatment of metastatic prostate cancer. However, variability in responses to 1α,25(OH)$_2$ vitamin D$_3$-based therapies limits opportunities for clinical applications. Improved understanding of the role of BAG1L and other factors in the regulation of VDR activity and tumor suppression by VDR ligands may contribute to more rational selection of patients for therapy with 1α,25(OH)$_2$ vitamin D$_3$ or its synthetic analogues.

Acknowledgments— We thank H. F. DeLuca for providing vitamin D$_3$ analogues and antibodies, S. Kitada for assistance with fluorescence-activated cell sorter assays, B. Froesch for plasmids, X. Zhang for helpful discussions and reagents, and R. Cornell for manuscript preparation.

REFERENCES

1. Feldman, D. (1997) *Vitamin D* (Feldman, D., Glorieux, F. H., and Pike, J. W., eds.) pp. 3–11, Academic Press, San Diego
2. DeLuca, H. F. (1988) *FASEB J* **2,** 224–236
3. Darwish, H. M., and DeLuca, H. F. (1996) *Prog. Nucleic Acid Res. Mol. Biol.* **53,** 321–344
4. Glass, C. K. (1994) *Endocrine Rev.* **15,** 391–407
5. Silberstein, G. B., and Daniel, C. W. (1987) *Science* **237,** 291–293
6. van Leeuwen, J. P. T. M., and Pols, H. A. P. P. (1997) in *Vitamin D* (Feldman, D., Glorieux, F. H., and Pike, J. W., eds) pp. 1089–1105, Academic Press, San Diego
7. Ly, L. H., Zhao, X.-Y., Holloway, L., and Feldman, D. (1999) *Endocrinology* **140,** 2071
8. Zhao, X. Y., Ly, L. H., Peehl, D. M., and Feldman, D. (1999) *Endocrinology* **140,** 1205–1212
9. Guzey, M., and DeLuca, H. (1997) *Res. Commun. Mol. Pathol. Pharmacol.* **98,** 3–18
10. Gross, C., Peehl, D. M., and Feldman, D. (1997) in *Vitamin D* (Feldman, D., Glorieux, F. H., and Pike, W. P., eds) pp. 1125–1200, Academic Press, San Diego
11. Takayama, S., Krajewski, S., Krajewska, M., Kitada, S., Zapata, J. M., Kochel, K., Knee, D., Scudiero, D., Tudor, G., Miller, G. J., Miyashita, T., Yamada, M., and Reed, J. C. (1998) *Cancer Res.* **58,** 3116–3131
12. Zeiner, M., Gebauer, M., and Gehring, U. (1997) *EMBO J.* **16,** 5483–5490
13. Liu, R., Takayama, S., Zheng, Y., Froesch, B., Chen, G.-q., Zhang, X., Reed, J. C., and Zhang, X.-K. (1998) *J. Biol. Chem.* **273,** 16985–16992
14. Froesch, B. A., Takayama, S., and Reed, J. C. (1998) *J. Biol. Chem.* **273,** 11660–11666
15. Kullmann, M., Schneikert, J., Moll, J., Heck, S., Zeiner, M., Gehring, U., and Cato, A. C. B. (1998) *J. Biol. Chem.* **273,** 14620–14625
16. Perlman, K. L., Sicinski, R. R., Schnoes, H. K., and DeLuca, H. F. (1990) *Tetrahedron Lett.* **31,** 1823–1824
17. Hedlund, T. E., Duke, R. C., and Miller, G. J. (1999) *Prostate* **41,** 154–165
18. Agadir, A., Lazzaro, G., Zheng, Y., Zhang, X.-K., and Mehta, R. (1999) *Carcinogenesis* **20,** 577–582
19. Wu, Q., Li, Y., Liu, R., Agadir, A., Lee, M. O., Liu, Y., and Zhang, X. (1997) *EMBO J.* **16,** 1658–1669
20. El-Deiry, W. S., Tokino, T., Velculescu, V. E., Levy, D. B., Parsons, R., Trent, J. M., Lin, D., Mercer, W. E., Kinzler, K. W., and Vogelstein, B. (1993) *Cell* **75,** 817–825
21. Aladjem, M., Spike, B., Rodewald, L., Hope, T., Klemm, M., Jaenisch, R., and Wahl, G. (1998) *Curr. Biol.* **8,** 145–155
22. Prost, S., Bellamy, C. O., Clarke, A. R., Wyllie, A. H., and Harrison, D. J. (1998) *FEBS Lett.* **425,** 499–504
23. Dame, M. C., Pierce, E. A., Prahl, J. M., Hayes, C. E., and DeLuca, H. F. (1986) *Biochemistry* **25,** 4523–4534
24. Takayama, S., Kochel, K., Irie, S., Inazawa, J., Abe, T., Sato, T., Druck, T., Huebner, K., and Reed, J. C. (1996) *Genomics* **35,** 494–498
25. Packham, G., Brimmell, M., and Cleveland, J. L. (1997) *Biochem. J.* **328,** 807–813
26. Takayama, S., Bimston, D. N., Matsuzawa, S., Freeman, B. C., Aime-Sempe, C., Xie, Z., Morimoto, R. J., and Reed, J. C. (1997) *EMBO J.* **16,** 4887–4896
27. Cohen, M., Padarathsingh, M., and Hendrix, M. (2000) *Am. J. Pathol.* **156,** 355–358
28. Zeiner, M., Niyaz, Y., and Gehring, U. (1999) *Proc. Natl. Acad. Sci. U. S. A.* **96,** 10194–10199
29. Schräder, M., Bendik, I., Becker-André, M., and Carlberg, C. (1993) *J. Biol. Chem.* **268,** 17830–17836
30. Glass, C. K. (2000) in *Introduction to Molecular & Cellular Research,* pp. 83–96, CMRC Endocrine Society Meeting, March 2000, San Diego, CA
31. Rochel, N., Wurtz, J. M., Mitschler, A., Klaholz, B., and Moras, D. (2000) *Mol. Cell* **5,** 173–179
32. Graumann, K., and Jungbauer, A. (2000) *Biochem. J.* **345,** 627–636
33. Koshiyama, M., Konishi, I., Nanbu, K., Nanbu, Y., Mandai, M., Komatsu, T., Yamamoto, S., Mori, T., and Fujii, S. (1995) *J. Clin. Endocrinol. Metab.* **80,** 1106–1112
34. Landel, C. C., Kushner, P. J., and Greene, G. L. (1994) *Mol. Endocrinol.* **8,** 1407–1419
35. Srinivasan, G., Patel, N. T., and Thompson, E. B. (1994) *Mol. Endocrinol.* **8,** 189–196
36. Stuart, J. K., Myszka, D. G., Joss, L., Mitchell, R. S., McDonald, S. M., Takayama, S., Xie, Z., Reed, J. C., and Ely, K. R. (1998) *J. Biol. Chem.* **273,** 22506–22514
37. Lüders, J., Demand, J., and Höhfeld, J. (2000) *J. Biol. Chem.* **275,** 4613–4617
38. Landis, S. H., Murray, T., Bolden, S., and Wingo, P. A. (1999) *Cancer J. Clin.* **49,** 8–31

Structural analysis of BAG1 cochaperone and its interactions with Hsc70 heat shock protein

Klára Briknarová[1,2], Shinichi Takayama[1,2], Lars Brive[1], Marnie L. Havert[1], Deborah A. Knee[1], Jesus Velasco[1], Sachiko Homma[1], Edelmira Cabezas[1], Joan Stuart[1], David W. Hoyt[3], Arnold C. Satterthwait[1], Miguel Llinás[4], John C. Reed[1] and Kathryn R. Ely[1]

[1]The Burnham Institute, La Jolla, California 92037, USA. [2]These two authors contributed equally to this work. [3]EMSL, Pacific Northwest National Laboratory, Richland, Washington 99352, USA. [4]Department of Chemistry, Carnegie Mellon University, Pittsburgh, Pennsylvania 15213, USA.

BAG-family proteins share a conserved protein interaction region, called the 'BAG domain', which binds and regulates Hsp70/Hsc70 molecular chaperones. This family of cochaperones functionally regulates signal transducing proteins and transcription factors important for cell stress responses, apoptosis, proliferation, cell migration and hormone action. Aberrant overexpression of the founding member of this family, BAG1, occurs in human cancers. In this study, a structure-based approach was used to identify interacting residues in a BAG1–Hsc70 complex. An Hsc70-binding fragment of BAG1 was shown by multidimensional NMR methods to consist of an antiparallel three-helix bundle. NMR chemical shift experiments marked surface residues on the second (α2) and third (α3) helices in the BAG domain that are involved in chaperone binding. Structural predictions were confirmed by site-directed mutagenesis of these residues, resulting in loss of binding of BAG1 to Hsc70 *in vitro* and in cells. Molecular docking of BAG1 to Hsc70 and mutagenesis of Hsc70 marked the molecular surface of the ATPase domain necessary for interaction with BAG1. The results provide a structural basis for understanding the mechanism by which BAG proteins link molecular chaperones and cell signaling pathways.

Both *in vitro* and *in vivo*[1–3], the BAG domain of BAG1 suppresses refolding of peptide substrates by the molecular chaperone Hsc70. This suppression apparently uncouples ATP-hydrolysis from peptide release[4] and acts as an antagonist of the cochaperone protein Hsc70 interacting protein[2,5] (Hip). BAG-family proteins are conserved throughout evolution, with homologs[5] found in humans, mice, *Drosophila, Caenorhabditis elegans, Schizosaccharomyces pombe, Saccharomyces cerevisiae* and plants. The human members of this family include BAG1, BAG2, BAG3 (CAIR-1/Bis), BAG4 (SODD), BAG5 and BAG6 (BAT3/Scythe)[5–10]. In addition to the BAG domain near the C-terminal end of the molecules, BAG proteins also contain diverse N-terminal regions that target cellular locations and interact with other proteins involved in numerous cellular processes[11,12]. It is speculated that BAG proteins serve as bridging molecules that recruit Hsc70 to specific target proteins, thus creating a novel mechanism to alter cell signaling by conformational change rather than post-translational modification[5–8,10].

Structure of BAG domain

NMR experiments indicate that the C-terminal region of BAG1 is highly helical (Fig. 1*a*), consistent with the results of circular dichroism (CD) analysis and secondary structure prediction[13].

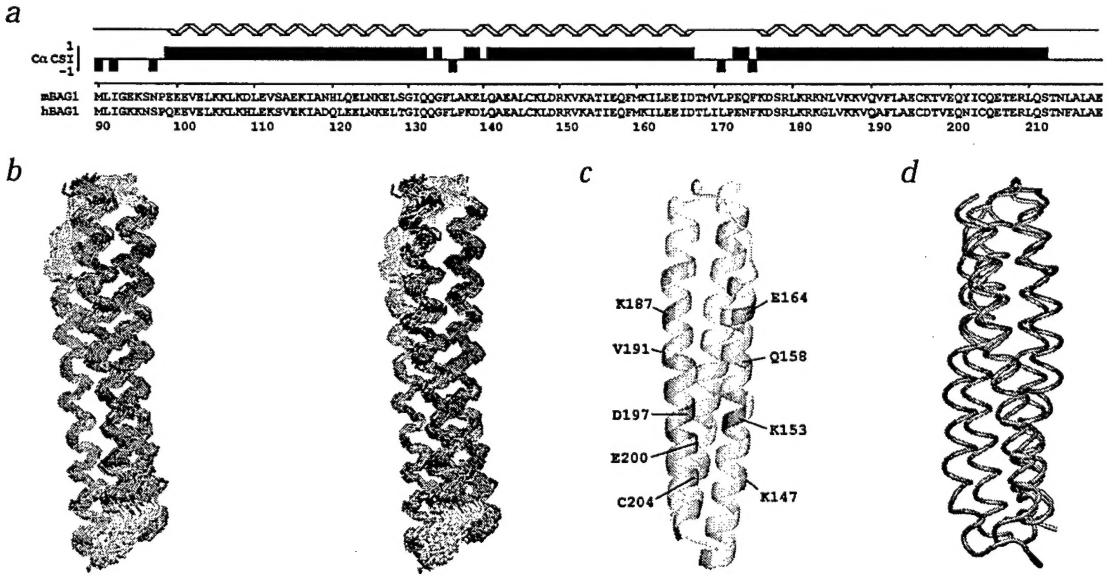

Fig. 1 C-terminal region of BAG1 is a three-helix bundle. ***a***, Cα chemical shift index[33] (CSI) of residues 90–219 of murine BAG1 (mBAG1). The sequence of the murine BAG1 fragment used in this study is indicated to scale below the CSI data and aligned with human BAG1L. The α-helices are defined schematically at the top of the figure. ***b***, Stereo image of superimposed backbone traces of a family of 25 final structures of BAG1 residues 99–210. The first helix (α1) is colored blue, the second one (α2) green and the third one (α3) orange; the connecting loops are white. The images were generated with the program MOLMOL[34]. ***c***, Ribbon representation of BAG1 residues 99–210 colored according to ^{1}H- and ^{15}N-chemical shift changes of the individual residues upon binding of Hsc70 peptide (Asn 256–Cys 267). The color intensity is proportional to the change. Gray indicates residues for which no data are available. Some of the residues with the most pronounced changes are labeled. The model depicted here is rotated 180° relative to the orientation in (*b*). ***d***, Comparison of BAG1 with syntaxin (view as in (*a*)). Tube models of the cα atoms of residues 101–212 of BAG1 (orange) and residues 27–146 of syntaxin (blue; PBD code 1BR0)[23] are superimposed. Note the similar configuration of helices in these two antiparallel three-helix bundles.

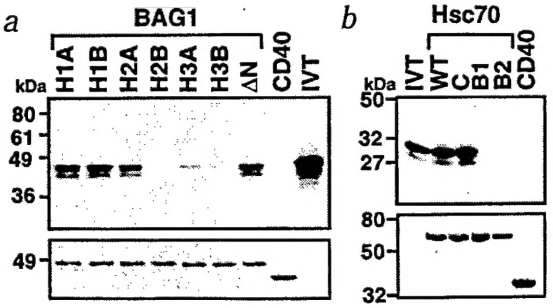

Fig. 2 Mutational analysis of BAG1 binding to Hsc70. ***a***, GST fusion proteins representing wild type BAG1 (WT; residues 90–219) or mutants were tested. Mutants were made by substituting Ala for surface residues in the central region of the elongated BAG1 molecule at residues on adjacent turns of each α-helix. The mutations were: H1A (E115A, K116A, N119A); H1B (E123A, K126A); H2A (D149A, R150A); H2B (E157A, K161A); H3A (Q190A); and H3B (D197A, Q201A). Proteins were immobilized on glutathione-Sepharose beads and tested for *in vitro* binding to *in vitro* translated (IVT) ^{35}S-L-Met-labeled Hsc70 ATPase domain (residues 67–377). GST-CD40 (cytoplasmic domain) was included as a negative control. Samples were analyzed by SDS-PAGE and autoradiography to detect bound Hsc70-ATPase (upper panel) and with Coomassie blue staining to verify loading of equivalent amounts of GST-fusion proteins (lower panel). IVT ^{35}S-Hsc70-ATPase was also loaded directly in the gel for comparisons of the amount of input *versus* bound Hsc70 ATPase. ***b***, GST-fusion proteins representing wild type Hsc70 (WT; residues 1–377) or mutant Hsc70 molecules with substitutions at sites predicted to bind BAG1 were tested. The mutations were: B1 (R258A, R262A), B2 (E283A, D285A) and C (E318A, R322A). The proteins were immobilized on glutathione-Sepharose beads and mixed with *in vitro* translated ^{35}S-L-Met-labeled mouse BAG1. The assay to detect bound BAG1 was performed and monitored as described for (*a*).

The structure of the BAG1 fragment studied here comprises three distinct helical regions — α1 (residues Glu 99–Gln 132), α2 (residues Lys 138–Asp 167) and α3 (residues Lys 176–Leu 210) — arranged in an antiparallel bundle (Fig. 1). Sequence similarities and secondary structure predictions[5,10] suggest that most BAG family proteins may contain a similar three-helix structure.

Interactions of BAG1 with Hsc70

We predicted regions of direct contact between BAG1 and the ATPase domain (residues 1–377) of Hsc70 (ref. 13) based on homology with a complex of GrpE and the ATPase domain of DnaK (the bacterial counterpart of Hsc70)[14]. To test this model experimentally, synthetic peptides representing two helices (residues Ala 54–Pro 63 and Asn 256–Cys 267), which flank the predicted binding crevice in Hsc70, were used in NMR-monitored titrations of BAG1. The latter peptide, Asn 256–Cys 267, induced pronounced chemical shift changes in the central region of α2 and α3 of BAG1 (Fig. 1*c*). These results demonstrated that residues interacting with Hsc70 lie on adjacent turns of α2 and α3 and are located on the same face of the conserved BAG domain.

Sites for mutagenesis in BAG1 were selected based on the results of these chemical shift experiments and used to evaluate the role of residues at predicted interacting surfaces between the BAG domain and Hsc70. In contrast to wild type protein, mutant BAG molecules with Ala substituted at residues Glu 157 and Lys 161 in α2 and Gln 190, Asp 197 and Gln 201 in α3 failed to bind Hsc70 ATPase domain in yeast two hybrid (data not shown) and *in vitro* binding assays (Fig. 2). These mutant molecules retained wild type folding patterns, as verified by CD (data not shown). Consistent with the model, mutant proteins with Ala substituted in the central region of α1 at residues Glu 115, Lys 116, Asn 119 or Lys 126 retained the ability to bind to Hsc70. The contact surfaces suggested by mutagenesis correlate well with those predicted by the chemical shifts (Fig. 1*c*). Thus, a region of BAG1 that is essential for binding to the ATPase domain of Hsc70 has been defined.

To test the predicted molecular surface of the ATPase domain of Hsc70 contacting BAG1, the BAG domain was docked interactively to the atomic model of Hsc70 (ref. 15). Our previous studies defined the minimal BAG1-binding region (residues 186–377) of Hsc70 (ref. 1). This region lacks the N-terminal lobe of the bi-lobed ATPase domain. Docking strategies optimized geometric and electrostatic charge complementarity of the central part of the electronegative BAG domain with the C-terminal lobe of the ATPase domain. Residues on the surface of the ATPase domain oriented to contact critical residues in the BAG domain were selected as sites for Ala substitution mutagenesis, including Arg 258, Arg 262, Glu 283 and Asp 285. Unlike the wild type ATPase domain, all of these mutants failed to bind BAG1 when tested in yeast two hybrid (data not shown) and *in vitro* binding assays (Fig. 2). In contrast, substitution of Ala for residues Glu 318 and Arg 322 on the opposite face of this lobe did not inhibit interaction with BAG1. These results define a surface region on Hsc70 that is the site for binding BAG1. This surface differs from that predicted by homology modeling[13] because the contact surface involves only one lobe of the ATPase domain.

The BAG1 and Hsc70 recognition surfaces predicted by these studies are shown in Fig. 3. The interacting region in Hsc70 is located on one face of the C-terminal lobe adjacent to a deep crevice in the bi-lobed ATPase domain. ATP binds at the bottom of this crevice[15,16]. Members of the Hsc70/Hsp70 heat shock family interact with linear peptide folding intermediates. This interaction is mediated by cycles of ATP binding and hydrolysis followed by ADP/ATP exchange and peptide release. The prokaryotic homologue of BAG1, GrpE, binds to both lobes of

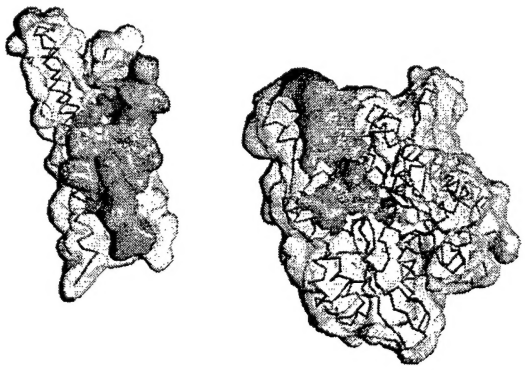

Fig. 3 Contact regions of the BAG1–Hsc70 ATPase complex. The proteins are represented by red Cα traces and transparent surfaces of BAG1 on the left and Hsc70 ATPase domain[15] on the right. An ADP molecule that binds in the cleft between the two lobes of the ATPase domain is shown in red as van der Waal's spheres. The complex has been 'opened up' by a 180° rotation of BAG1 to reveal the contact surfaces predicted from mutagenesis and molecular docking. The sites of mutation that abolish binding are colored yellow and adjacent contact sites suggested from molecular docking are colored cyan. This image was produced with the program SPOCK[35].

Fig. 4 BAG domain is necessary for transactivation of AR by BAG1L. Mutant BAG1L proteins containing Ala substitutions within the BAG domain that ablated Hsc70 binding *in vitro* and a BAG1L truncation mutant lacking α3 of the BAG domain (ΔC) were tested. Mutant proteins are H2B (E157A, K161A in α2) and H3B (D197A, Q201A in α3). (These sites are numbered 283, 287, 323 and 327 in human BAG1L). Cos-7 cells were transfected with fixed amounts of pSG5-AR, pLCI, pCMV-βGal and increasing amounts of pcDNA3-BAG1L, wild type and mutants. Cell extracts were prepared and assayed for CAT and β-galactosidase activity at 40 h after transfection. Data are expressed as fold transactivation relative to cells transfected with reporter gene alone (mean ± S.E.; n = 2).

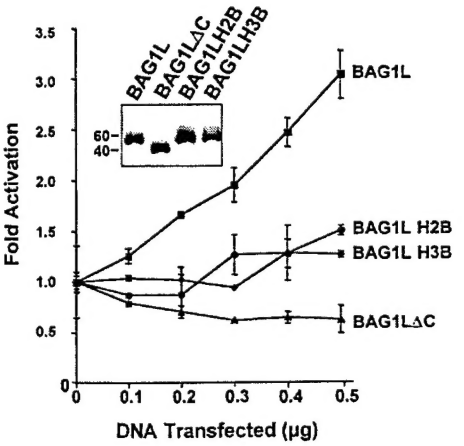

the Hsp70 homolog DnaK ATPase domain[14,17] and stimulates dissociation of ADP from DnaK by inducing a conformational change in the nucleotide-binding cleft, including the N-terminal lobe of the domain[14]. BAG1 is also known to promote dissociation of ADP[2], but the mechanism may differ and remains to be elucidated. In contrast to GrpE, our results suggest that contact with the N-terminal lobe of the ATPase domain may not be critical for binding of BAG1.

Analysis of the BAG1–Hsc70 contacts *in vivo*

The significance of the structural analyses was tested in intact cells, comparing the bioactivity of wild type and mutant BAG1 proteins. At least four isoforms of BAG1 are produced in many cells, including BAG1 and a longer isoform BAG1L. The unique N-terminal region of BAG1L contains both SV40 large T-like and nucleoplasmin-like candidate nuclear localization signals, which target BAG1L to the nucleus[5]. BAG1L has been shown to form complexes with and coactivate steroid hormone receptors[18–22], such as androgen receptor[11] (AR), in a manner requiring the BAG domain-containing C-terminal region of BAG1. We therefore engineered the same mutations described above for BAG1 into plasmids encoding the BAG1L protein and tested them for the ability to enhance the transcriptional activity of AR. As shown in Fig. 4, wild type BAG1L caused a concentration-dependent increase in AR-mediated transactivation of a reporter gene promoter containing androgen response elements (AREs)[11]. However, mutant BAG1L proteins containing the same Ala substitutions within the BAG domain that ablated Hsc70 binding demonstrated diminished capacity to affect AR transactivation in these assays. Immunoblot analysis confirmed that the differences in activity of wild type and mutant BAG1L proteins were not attributable to differences in levels of expression. We conclude therefore that the contact residues required for interaction of BAG1 with Hsc70 are critical for the function of this protein in cells.

Table 1 Structural statistics for BAG1

Ensemble	
R.m.s. deviation from experimental restraints[1]	
NOE distance restraints (Å)	0.030 ± 0.001
Dihedral angle restraints (°)	0.42 ± 0.03
R.m.s. deviation from idealized geometry	
Bonds (Å)	0.0031 ±0 .0002
Angles (°)	0.46 ± 0.01
Impropers (°)	0.36 ± 0.01
R.m.s. deviation from mean coordinates[2]	
Backbone atoms (N, Cα, C) (Å)	1.1 ± 0.4
Heavy atoms (Å)	1.6 ± 0.3
Ramachandran plot[2]	
Most favored regions (%)	94.2
Additional allowed regions (%)	4.4
Generously allowed regions (%)	1.0
Disallowed regions (%)	0.4

[1]No NOE distance and dihedral angle restraint was violated by more than 0.5 Å or 5°, respectively, in any of the structures.
[2]Residues 99–210; mean coordinates were obtained by averaging coordinates of the 25 calculated structures, which were first superposed using backbone atoms (N, Cα, C) of residues 99–210.

Structural similarity of BAG1 and syntaxin

BAG-family members bind to a variety of intracellular proteins and regulate diverse cellular processes including cell division, survival and migration. Members of this family link cell signaling to molecular chaperones, altering cellular pathways by changing protein conformation. Using the BAG1 structure, the database of known three-dimensional structures was searched with the program DALI[23] for similar folding patterns. A striking similarity (see Fig. 1*d*) was noted with the syntaxin protein[24,25]. Syntaxins are members of a large family of related proteins that are key components in protein trafficking. The N-terminal region of syntaxin is an independently folded antiparallel three-helix bundle that participates in protein–protein interactions. A hydrophobic groove between helices 2 and 3 on the surface of syntaxin lined by conserved residues can accommodate interactions with another helix in a distal portion of the molecule. This helix is 'swapped' when the molecule associates with SNARE complexes at the plasma membrane[25]. The structural similarities with BAG1 suggest that BAG domains may participate in similar protein–protein interactions, adapting to molecular exchange of α-helices. Future studies may reveal molecular interfaces in BAG-binding proteins that are complementary with BAG domains, and which may modulate Hsc70/BAG1 interactions.

Note added in proof: While this manuscript was under review, a study of the BAG1-interacting surface of Hsc70 ATPase domain using peptide libraries was reported[26]. Also, the crystal structure of BAG1 in complex with nucleotide-free Hsc70 ATPase domain was published[27]. BAG1 residues that interact with the ATPase domain in the crystal structure are located on α2 and α3, as suggested by chemical shift experiments in the present study. The contact surfaces colored here in Fig. 3 include most of the residues seen at the interface in the crystal structure, with the exception of residues in the N-terminal lobe of the ATPase domain. For direct comparison with the crystal structure, the reader should add 55 to the BAG1 sequence number used in our NMR study.

Methods

NMR spectroscopy. A recombinant fragment containing residues 90–219 of murine BAG1 was purified essentially as described for a longer construct[13]. NMR samples contained 1–2 mM ^{15}N-, ^{13}C/^{15}N- or ^{2}H/^{15}N-labeled protein in 10 mM potassium phosphate buffer, pH 7.2, 25 mM KCl, 1 mM DTT and 1 mM EDTA in 90% H_2O/10% D_2O. Spectra were acquired at 37 °C on a Bruker 500MHz and Varian 500, 600 and 750 MHz spectrometers. The data were processed and analyzed with Felix 98.0 (Molecular Simulations, Inc.). ^{1}H, ^{15}N and ^{13}C assignments were established based on CBCA(CO)NH, HNCACB, HNCO, CBCACOHA, C(CO)NH, H(CCO)NH, HCCH-TOCSY (HB)CB(CGCD)HD, ^{13}C/^{15}N-edited NOESY, 4D ^{15}N-edited NOESY and HNCACB optimized for Asn and Gln NH_2 groups. Distance restraints were obtained from 3D ^{15}N-edited NOESY and 3D ^{13}C/^{15}N-edited NOESY. ϕ and ψ dihedral angle restraints were generated with TALOS[28]. Structures were calculated with the torsion angle dynamics simulated annealing protocol implemented in CNS 1.0 (ref. 29) using restraints for 1,567 interproton distances (98 long range, $5 \leq |i-j|$, 267 medium range, $2 \leq |i-j| \leq 4$, 363 sequential and 839 intraresidual), 168 hydrogen bond distances, and 88 ϕ and 86 ψ dihedral angles. Statistics for 25 final structures are summarized in Table 1.

Chemical shift experiments and computer modeling. Helix-nucleated peptides representing helical regions of the ATPase domain of human Hsc70 predicted to bind to BAG1 were synthesized using a protocol described in ref. 30. Helix-nucleation was introduced to stabilize the helical nature of the synthetic peptides, corresponding with the known conformation in the protein[15,16]. The CD spectra for the nucleated peptides were consistent with enhanced helicity[30] relative to control linear peptides. ^{1}H-^{15}N HSQC spectra were recorded for ^{15}N-labeled BAG1 solutions containing varying concentrations of peptide. Most pronounced resonance shifts of BAG1 amides were noted and mapped onto the structure. To model the binding surfaces in a BAG1–Hsc70 complex, docking of BAG1 to Hsc70 ATPase domain (PDB accession number 1NGA)[15] was performed manually to visually optimize geometric fit and intermolecular distance between contact residues identified from the HSQC experiments and surface residues on the ATPase domain. Docking was directed to contact regions predicted from homology modeling[13].

Plasmids. Mutations in BAG1 were generated by two-step PCR-based mutagenesis using a full length murine BAG1 cDNA (SN 245–9) (ref. 31) as template. Products were purified by QiaQuick gel extraction kit (Qiagen), subcloned into the TOPO TA vector (Invitrogen) and sequenced. The fragments were subcloned into either pGEX4T-1 for expression as mutant GST-fusion proteins or into pJG4-5 for yeast two-hybrid assays. Mutations in Hsc70 were made by the same methods, using a cDNA encoding the ATPase domain[1].

Protein interaction assays. For yeast two hybrid assays[32], the yeast EGY48 strain was cotransformed with pJG4-5 plasmids encoding wild type or mutant BAG1/B42 transactivation domain fusion proteins, pGilda plasmids encoding Hsc70 ATPase/LexA DNA-binding domain fusion proteins and a β-galactosidase reporter gene (pSH18-34 or pRB1840).

For *in vitro* binding assays, DH5α cells were transformed with pGEX4T-1 plasmids encoding wild type or mutant GST-BAG1 fusion proteins. After induction at room temperature with 0.1 mM IPTG, cells were lysed by sonication, and expressed proteins were isolated from lysates by affinity purification on glutathione-Sepharose (Pharmacia). *In vitro* translated ^{35}S-methionine labeled Hsc70 ATPase domain[1] (1 μl) was mixed with 5 μg immobilized mutant GST-BAG1 fusion proteins, along with negative controls. Alternatively, GST-Hsc70 ATPase domain was produced and immobilized on glutathione-Sepharose and then mixed with *in vitro*-translated ^{35}S-BAG1 or negative control proteins. After 1 h incubation at 4 °C, beads were washed extensively and then subjected to SDS-PAGE electrophoresis to detect bound protein.

Reporter gene assays. Cos-7 cells (3×10^4 cells/well in 12-well plates) were transfected as described[11] with fixed amounts of 0.06 μg of pSG5-AR, 0.5 μg of pLCI, 0.04 μg of pCMV-βGal and increasing amounts of pcDNA3-BAG1L, wild type and mutant plasmids. Total DNA was maintained at 1.1 μg by the addition of empty plasmid. After 30 hrs, cells were stimulated with 1 nM R1881 for 10 h. Cell extracts were prepared and assayed for CAT and β-galactosidase activity at 40 h after transfection, expressing data as a ratio of CAT:β-galactosidase.

Coordinates. The coordinates have been deposited in the Protein Data Bank with accession code 1I6Z.

Acknowledgments

This research was performed in part at the Environmental Molecular Sciences Laboratory (a national scientific user facility sponsored by the U.S. DOE Office of Biological and Environmental Research) located at Pacific Northwest National Laboratory, operated by Battelle for the DOE. The authors are grateful to the staff at the HFMR facility at EMSL for useful discussions. We also thank K. Baker for protein purification and characterization, X. Jia for assistance with the Varian 500 MHz spectrometer and P. Crescenti for manuscript preparation. This work was funded by the National Institutes of Health NCI, NIHLB, USAMRDC Breast Cancer Program, the University of California Breast Cancer Research Program, the State of California Cancer Research Program, the Susan G. Komen Breast Cancer Foundation, the Human Frontier Science Program and CaPCURE.

Correspondence should be addressed to K.R.E. *email: ely@burnham.org*

Received 30 November, 2000; accepted 2 March, 2001.

1. Takayama, S. *et al. EMBO J.* **16**, 4887–4896 (1997).
2. Höhfeld, J. & Jentsch, S. *EMBO J.* **16**, 6209–6216 (1997).
3. Nollen, E.A.A., Brunsting, J.F., Song, J., Kampinga, H.H. & Morimoto, R.I. *Mol. Cell. Biol.* **20**, 1083–1088 (2000).
4. Bimston, D. *et al. EMBO J.* **17**, 6871–6878 (1998).
5. Takayama, S., Zhihua, X. & Reed, J.C. *J. Biol. Chem.* **274**, 781–786 (1999).
6. Doong, H. *et al. Oncogene* **19**, 4385–4395 (2000).
7. Lee, J. H. *et al. Oncogene* **18**, 6183–6190 (1999).
8. Jiang, Y., Woronicz, J. D., Liu, W. & Goeddel, D.V. *Science* **283**, 543–546 (1999).
9. Thress, K., Song, J., Morimoto, R.I. & Kornbluth, L. *EMBO J.* **20**,1033–1041 (2001).
10. Tschopp, J, Martinon, F. & Hofmann, K. *Curr. Biol. R* **9**, 381–384 (1999).
11. Froesch, B.A., Takayama, S. & Reed, J.C. *J. Biol. Chem.* **273**, 11660–11666 (1998).
12. Crocoll, A., Schneikert, J., Hubner, S., Martin, E. & Cato, A. C. *Kidney Int.* **57**, 1265–1269 (2000).
13. Stuart, J.K. *et al. J. Biol. Chem.* **273**, 22506–22514 (1998).
14. Harrison, C.J., Hayer-Hartl, M., Di Liberto, M., Hartl, F.-U. & Kuriyan, J. *Science* **276**, 431–435 (1997).
15. Flaherty, K.M., Wilbanks, S.M., DeLuca-Flaherty, C. & McKay, D.B. *J. Biol. Chem.* **269**, 12899–12907 (1994).
16. Flaherty, K.M., DeLuca-Flaherty, C. & McKay, D.B. *Nature* **346**, 623–628 (1990).
17. Liberrek, K., Marszalek, J., Ang, D., Georgopoulos, C. & Zylicz, M. *Proc. Natl. Acad. Sci. USA* **88**, 2874–2878 (1991).
18. Zeiner, M. & Gehring, U. *Proc. Natl. Acad. Sci. USA* **92**, 11465–11469 (1995).
19. Liu, R. *et al. J. Biol. Chem.* **273**, 16985–16992 (1998).
20. Schneikert, J., Hübner, S., Martin, E. & Cato, A.C.B. *J. Cell Biol.* **146**, 929–940 (1999).
21. Knee, D.A., Froesch, B.A., Nuber, U., Takayama, S. & Reed, J.C. *J. Biol. Chem.* **in the press** (2001).
22. Schneikert, J. *et al. EMBO J.* **19**, 6508–6516 (2000).
23. Holm, L. & Sander, C. *J. Mol. Biol.* **233**, 123–138 (1993).
24. Fernandez, I. *et al. Cell* **94**, 841–849 (1998).
25. Misura, K.M.S., Scheller, R.H. & Weis, W.I. *Nature* **404**, 355–362 (2000).
26. Petersen, G., Hahn, C. & Gehring. *J. Biol. Chem.* **in the press** (2001).
27. Sondermann, H. *et al. Science* **291**, 1553–1557 (2001).
28. Cornilescu, G., Delaglio, F. & Bax, A. *J. Biomol. NMR* **13**, 289–302 (1999).
29. Brünger, A.T. *et al. Acta. Crystallogr. D* **54**, 905–921 (1998).
30. Cabezas, E. & Satterthwait, A.C. *J. Am. Chem. Soc.* **121**, 3862–3875 (1999).
31. Takayama, S. *et al. Cell* **80**, 279–284 (1995).
32. Golemis, E.A., Gyuris, J. & Brent, R. In *Current protocols in molecular biology* (eds, Asbubel, F.M. & Struhl, K. J.) 1–17 (Wiley & Sons, Inc. New York; 1994).
33. Wishart, D.S. & Sykes B.D. *J. Biomol. NMR* **4**, 171–180 (1994).
34. Koradi, R., Billeter, M. & Wüthrich, K. *J. Mol. Graph.* **14**, 51–55 (1996).
35. Christopher, J.A. *The structural properties observation and calculation kit* (The Center for Macromolecular Design, Texas A&M University, College Station, Texas; 1998).